EDFB/IBP-76/8
ORNL/NSF/EATC-27

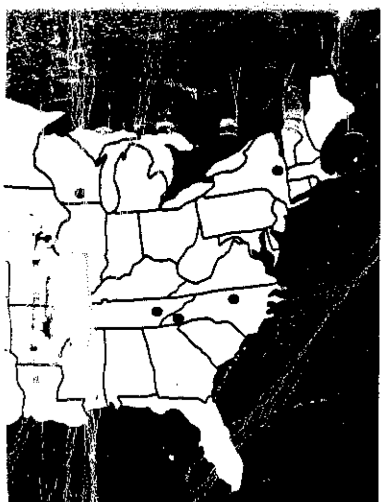

Eastern Deciduous Forest Biome
Analysis of Ecosystems

IBP

TEHM:

A Terrestrial Ecosystem Hydrology Model

D. D. Huff - R. J. Luxmoore - J. B. Mankin - C. L. Begovich

Environmental Sciences Division Publication No. 1019

OAK RIDGE NATIONAL LABORATORY
OPERATED BY UNION CARBIDE CORPORATION FOR THE ENERGY RESEARCH AND DEVELOPMENT ADMINISTRATION

Printed in the United States of America. Available from
National Technical Information Service
U.S. Department of Commerce
5285 Port Royal Road, Springfield, Virginia 22161
Price: Printed Copy $7.50; Microfiche $3.00

EDFB/IBP-76/8
ORNL/NSF/EATC-27

Contract No. W-7405-eng-26

TEHM: A Terrestrial Ecosystem Hydrology Model

D. D. Huff, R. J. Luxmoore, J. B. Mankin,
and C. L. Begovich

ENVIRONMENTAL SCIENCES DIVISION
Publication No. 1019

Research supported in part by the Eastern Deciduous Forest Biome, US-IBP, funded by the National Science Foundation under Interagency Agreement AG-199, DEB76-00761, and in part by the National Science Foundation - RANN under Interagency Agreement No. AEN 72-01243A03 with the Energy Research and Development Administration-Oak Ridge National Laboratory.

Date Published: April 1977

OAK RIDGE NATIONAL LABORATORY
Oak Ridge, Tennessee 37830
operated by
UNION CARBIDE CORPORATION
for the
ENERGY RESEARCH AND DEVELOPMENT ADMINISTRATION

ACKNOWLEDGEMENTS

The work presented in this report rests upon and in some instances explicitly includes the efforts of all those who have contributed to the Stanford Watershed Model, especially Norman Crawford and Ray Linsley. In addition, the work of R. A. Goldstein, via the model PROSPER, has been drawn upon heavily in the production of the TEHM. Others, most notably L. W. Swift, Jr. and W. T. Swank of Coweeta Hydrologic Laboratory, U.S. Forest Service, and G. S. Henderson and W. F. Harris of the Environment Sciences Division at ORNL have contributed time, ideas, and data that played an essential role in the development of the TEHM. M. R. Patterson, D. E. Fields, R. J. Raridon, J. K. Munro, R. D. Ellison, J. T. Holdeman, and J. Stolzey of the Computer Sciences Division of UCCND made significant contributions in translating the ideas into an efficient code as it evolved. To all of the people named above, and many others too numerous to name explicitly, who have taken part in the evolution of the TEHM, the authors of this report wish to express their gratitude for making the undertaking possible.

Research was supported in part by the Eastern Deciduous Forest Biome, US-IBP, funded by the National Science Foundation under Interagency Agreement AG-199, DEB76-00761 with the Energy Research and Development Administration - Oak Ridge National Laboratory and in part by the RANN Environmental Aspects of Trace Contaminants Program under National Science Foundation Interagency Agreement AEN 72-01243A03 with the Energy Research and Development Administration.

ABSTRACT

HUFF, D. D., R. J. LUXMOORE, J. B. MANKIN, and C. L. BEGOVICH. 1977. TEHM: A terrestrial ecosystem hydrology model. EDFB/IBP-76/8, ORNL/NSF/EATC-27. Oak Ridge National Laboratory, Oak Ridge, Tennessee. 147 pp.

The terrestrial ecosystem hydrology model (TEHM) combines mechanistic models for climatic and hydrologic processes with vegetation properties to explicitly simulate interception and throughfall; infiltration; root zone evaporation, transpiration, and drainage; plant and soil water potential; unsaturated and saturated subsurface flow; surface runoff; and open channel flow. It is also possible to use the TEHM with models for forest stand biomass dynamics and chemistry and exchange of heavy metals to study the transport and fate of trace contaminants at a watershed scale.

Walker Branch Watershed has been used as an example to illustrate development of the required input parameters and variables that are necessary to execute the TEHM. In all cases, emphasis has been placed on objective, physically based methods. When simulations of interception loss, soil moisture content, and base flow and storm flow are compared with observation, the overall adequacy of the model may be assessed.

For user convenience, the documentation includes a complete discussion of input formats, example data input sets, output summaries, and a microfische listing of the complete source deck and program output. As presented, the TEHM provides an operational tool and a model structure and data management capabilities that will be useful for future hydrologic simulation work. From that viewpoint, the TEHM represents an important step forward in establishment of an objective framework for the study of terrestrial ecosystems.

TABLE OF CONTENTS

Page

ACKNOWLEDGEMENTS iii

ABSTRACT v

INTRODUCTION 1

THEORY AND STRUCTURE OF THE TEHM 2
- Precipitation Data 2
- Climatic Variables 5
  - Dew Point Temperature 5
  - Wind Speed 6
  - Air Temperature 8
  - Solar Radiation 8
    - Temporal distribution of daily short-wave radiation 10
  - Net Long Wave Radiation 14
- Hydrologic Process Submodels 17
  - Interception and Throughfall 17
  - Infiltration 20
  - Root Zone Evaporation, Transpiration, and Drainage 24
  - Subsurface Flow 33
    - Source area runoff 34
    - Soil water transmission zones 36
    - Groundwater storage and flow 38
  - Total Streamflow 40

APPLICATION OF THE TERRESTRIAL ECOSYSTEM HYDROLOGY MODEL 40
- An Overview of Basin Simulation 40
  - Atmosphere Module 40
  - Landscape Module 41
- Walker Branch Watershed Case Study 41
  - Basin Description 41
- Data Set Preparation 41

Page

Precipitation and Deposition Data and Parameters . . . 44
Climatic data 44
Parameters that Characterize Soils 47
Storm Runoff Parameters and Variables 52
Groundwater Flow Parameters and Variables 56
Parameters and Variables that Characterize Vegetation 61
Root Variables and Parameters 65
The Channel Flow Module 70

OPERATION OF THE TEHM COMPUTER PROGRAM 74
Introduction 74
Scaling Factors 74
Precipitation Data Input 76
Formats 76
Example Listing of a Precipitation Data Set 80
Climatic Data and Basin Parameter Input 85
Formats 85
Example Listing of a Data Set for Terrestrial Segments 107
Simulation of Open Channel Flow 114
Formats and Example 114

SUMMARY OF SIMULATION RESULTS 120
Scope 120
Monthly and Annual Segment Water Balance Summaries 120
End of the Year Soil Moisture Storages 126
Throughfall Estimates 126
Soil Moisture 126
Streamflow Simulation 126
Future Plans 129

BIBLIOGRAPHY 133

APPENDIX 138

LIST OF TABLES

Table		Page
1	Comparison of field observations of throughfall with computed estimate	22
2	Summary of land slope distributions within Walker Branch Watershed	42
3	Data requirements for precipitation and wetfall data management programs	45
4	Variables required to characterize watershed climate	46
5	A summary of soils properties that are required for simulation	47
6	Average thickness of upper soil horizons at Walker Branch Watershed	48
7	Measured properties that specify hydrologic behavior of soil on Walker Branch Watershed	50
8	Simulated Cumulative Infiltration Capacity-Walker Branch Watershed	51
9	The empirical constants that characterize the water content versus hydraulic conductivity curve for Walker Branch Watershed	55
10	Relation between watershed cover and Manning's *n* (roughness coefficient)	57
11	A summary of runoff parameters needed for simulation	62
12	A summary of parameters that characterize vegetation	69
13	Subjective indication of the sensitivity of PROSPER parameters to the monthly water balance, midday plant water status and daily evapotranspiration and drainage rate	71
14	Length and effective upstream and downstream elevations of the East and West Forks of Walker Branch Watershed	72
15	A summary of parameters that characterize the channel system	73
16	An example of precipitation data input	81
17	The choices available for supplying input data to the TEHM	87
18	An example of climatic data and basin parameter input	108
19	Example input data set for channel flow simulation for Walker Branch Watershed	119
20	Variables plotted in PROSPER, CERES, and DRYADS	149

LIST OF FIGURES

Figure		Page
1	A schematic diagram of hydrologic processes	3
2	Assumed lapse rate as a function of time of day	4
3	Assumed air temperature distribution function	9
4	Fractional cloudiness as a function of the ratio of observed to potential radiation	16
5	Schematic representation of the interception loss submodel	18
6	The annual cycle of interception storage	19
7	Comparison of the TEHM interception submodel results with those from Helvey and Patric regression equations .	21
8	Example use of the TCA method for estimating infiltration .	23
9	Schematic diagram of PROSPER: A model of atmosphere-soil-plant water flow	25
10	Schematic diagram of electric circuit analogy to the soil-plant-water flow system	27
11	Schematic diagram of partitioned soil-water and plant- and root-soil flow systems.	29
12	Illustration of the conceptual subsurface flow model . . .	35
13	Assumed relationship between average surface soils drainage rate and fraction of basin contributing to storm runoff (variable source area fraction)	37
14	Topographic map of Walker Branch Watershed, showing locations of hydrologic data collection devices	43
15	Soil hydraulic properties for Fullerton average B 22t soils at Walker Branch Watershed	53
16	Soil hydraulic properties for Bodine average B2t soils at Walker Branch Watershed.	54
17	Hydrograph analysis for period January 10-24, 1974 at Walker Branch Watershed..	58
18	Hydrograph analysis for period March 19-28, 1974 at Walker Branch Watershed	59
19	Hydrograph analysis for period May 12-22, 1974 at Walker Branch Watershed	60
20	The seasonal pattern of leaf area index development for yellow poplar at Oak Ridge, Tennessee	63
21	The average annual depth distribution of lateral roots less than 5 mm in diameter for <u>Liriodendron</u> forest . . .	66
22	Approximate relationship between soil depth and the fraction of root cross-section per unit soil cross-section area	68
23	An example of the summary of calculations made by PROSPER for each month (November 1973)	121
24	An example of the summary of monthly water balance terms for a vertical column through a segment	122
25	An example of the monthly and annual water budget tabulation for a segment	124
26	An example of the printed summary of soil moisture storage values at the end of a year	127

Figure Page

27 Simulated and observed moisture content in surficial soils of Walker Branch Watershed 128

28 Simulated and observed monthly storm flow for the West Fork of Walker Branch Watershed 130

29 Simulated and observed monthly base flow for the West Fork of Walker Branch Watershed 131

30 Simulated and observed monthly total flow for the West Fork of Walker Branch Watershed 132

INTRODUCTION

A trend in hydrologic simulation modeling over the past decade has been toward inclusion of greater detailed representation of hydrologic processes and associated abiotic and biotic land-water interactions. This trend has been stimulated by federal legislation such as the National Environmental Policy Act, as amended in 1972 (PL92-500), which requires careful investigation of the environmental impact of any projects that will significantly affect the quality of the human environment.

One of the earliest attempts at combining hydrologic processes and the transport of abiotic materials in a simulation model was the work of Huff (1968). He developed a simulation model of the hydrologic transport of radioactive aerosols from fallout. That work combined the Stanford Watershed Model (Crawford and Linsley, 1966) and a consideration of the environmental chemistry of trace amounts of ^{90}Sr and ^{137}Cs to yield a predictive model for concentrations in streamflow. That work also laid the foundation for the Wisconsin Hydrologic Transport Model, described by Patterson et al. (1974).

The work described in the following pages is a further extension of the Wisconsin Hydrologic Transport Model. The goal of the work has been to provide more direct coupling of the hydrologic cycle and watershed biota, and a more physically based representation of watershed components. This has been accomplished by combining a modified version of a model of atmosphere-soil-plant water flow (PROSPER) (Goldstein et al., 1974) with the comprehensive Wisconsin model. In the process of merging the two models, some significant changes have been made in both models; nonetheless this report draws heavily upon the existing documentation for both of them to describe the combined model.

The combined model forms an integral part of a unified transport model package. The atmospheric transport model (Mills and Reeves, 1973), a model of soil chemical exchange of heavy metals (Begovich and Jackson, 1975), a plant-growth model (Dixon et al., 1976) and a mineral uptake model (Luxmoore et al., 1976b) are all designed to link together with the watershed model (TEHM) to form the unified transport model.

In preparing documentation for the TEHM, which is the key linkage between the components of the unified transport model, three major topics have been described. They are:

(1) The theory and structure of the TEHM. This section presents detailed discussions of the foundations and structure of the algorithms that represent processes in the model. The objective of this section is to provide enough information to allow a user to modify any part of the code with a minimum investment of time spent understanding the program.

(2) Application of the TEHM. This section gives the problems faced by the user of the code when applying it. Guidelines for operation of the TEHM, including lists of the variables and parameters to be specified, together with suggestions for making such estimates, are given. The section also includes format guides and a sample input set.

(3) Summary of results. This section highlights the type of data available in the output, and provides guides to understanding the printed results and how they are interrelated.

It will be apparent that there are significant differences in the level of detail one encounters in the various sections of this report. Those processes where information is abundant have been modeled in the fullest detail warranted. Other processes are represented by very simple and empirical relations, which may cause the reader to wonder why there is such an uneven level of detail in the TEHM. The basic reason is a philosophy that the model represents a current state of knowledge, organized in a structure that can be improved as new information becomes available. Our goal is to present as complete a description of various processes as practical. This is done in the firm belief that others will find parts of the model that will be useful for other applications, and will want process representations that stand alone. We are aware that following our philosophy results in detail in some parts of the TEHM that does not improve model accuracy that is limited by other, more gross representations.

THEORY AND STRUCTURE OF THE TEHM

The hydrologic processes represented in the terrestrial ecosystem hydrology model (TEHM) are shown schematically in Fig. 1. Each of the rectangular boxes in the figure indicates an identifiable model component. In the following sections, the underlying concept and equations for each component are described.

Precipitation Data

Hourly observed precipitation data are used as one of the primary inputs for each watershed sub-unit (or segment) that is simulated. The model assumes that the precipitation is representative for the segment. Precipitation input is multiplied by a constant factor, so that adjustment of point values to larger areas or different locations is possible.

Snowfall conditions are determined using estimated surface air temperature and an assumed lapse rate. The lapse rate function is shown in Fig. 2. The temperature at 750 ft above the segment surface is computed using:

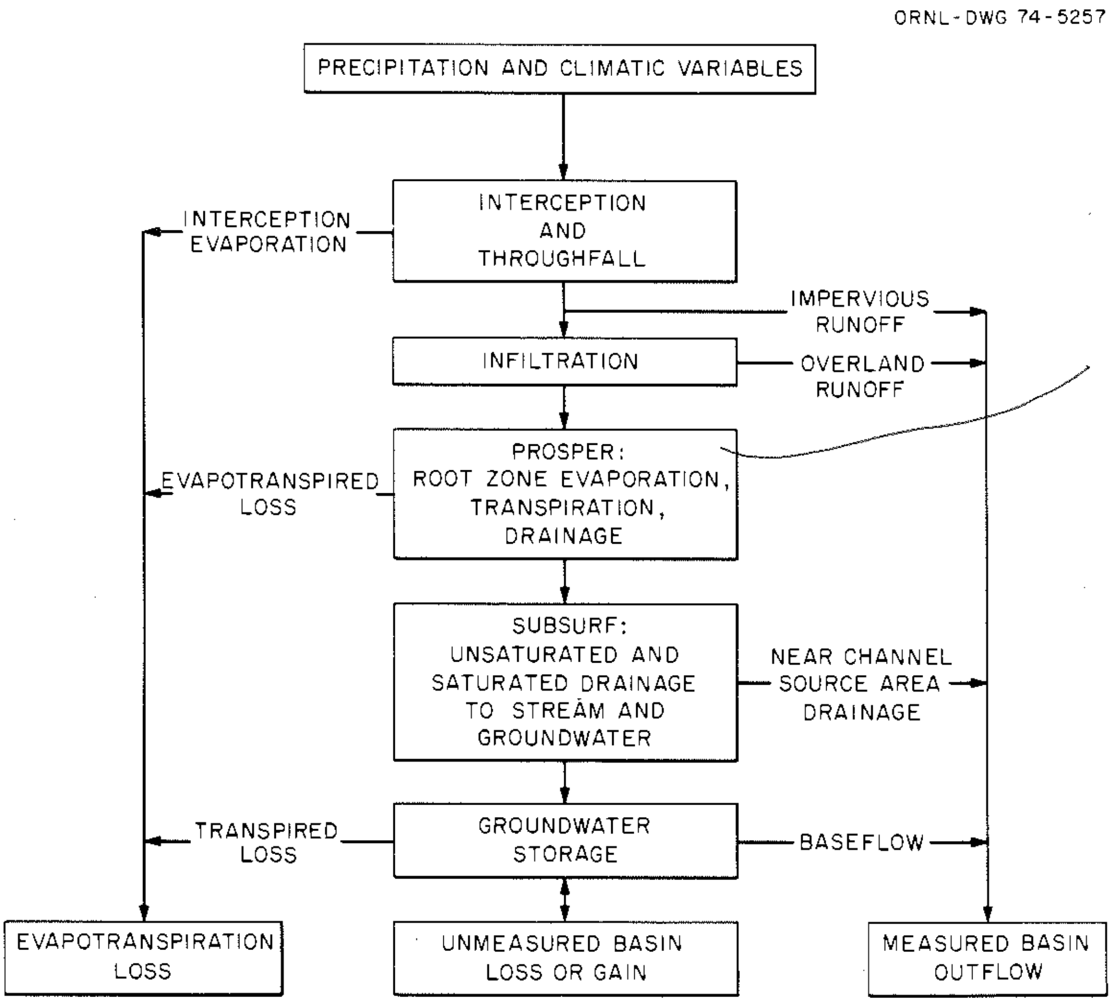

Fig. 1. A schematic diagram of hydrologic processes.

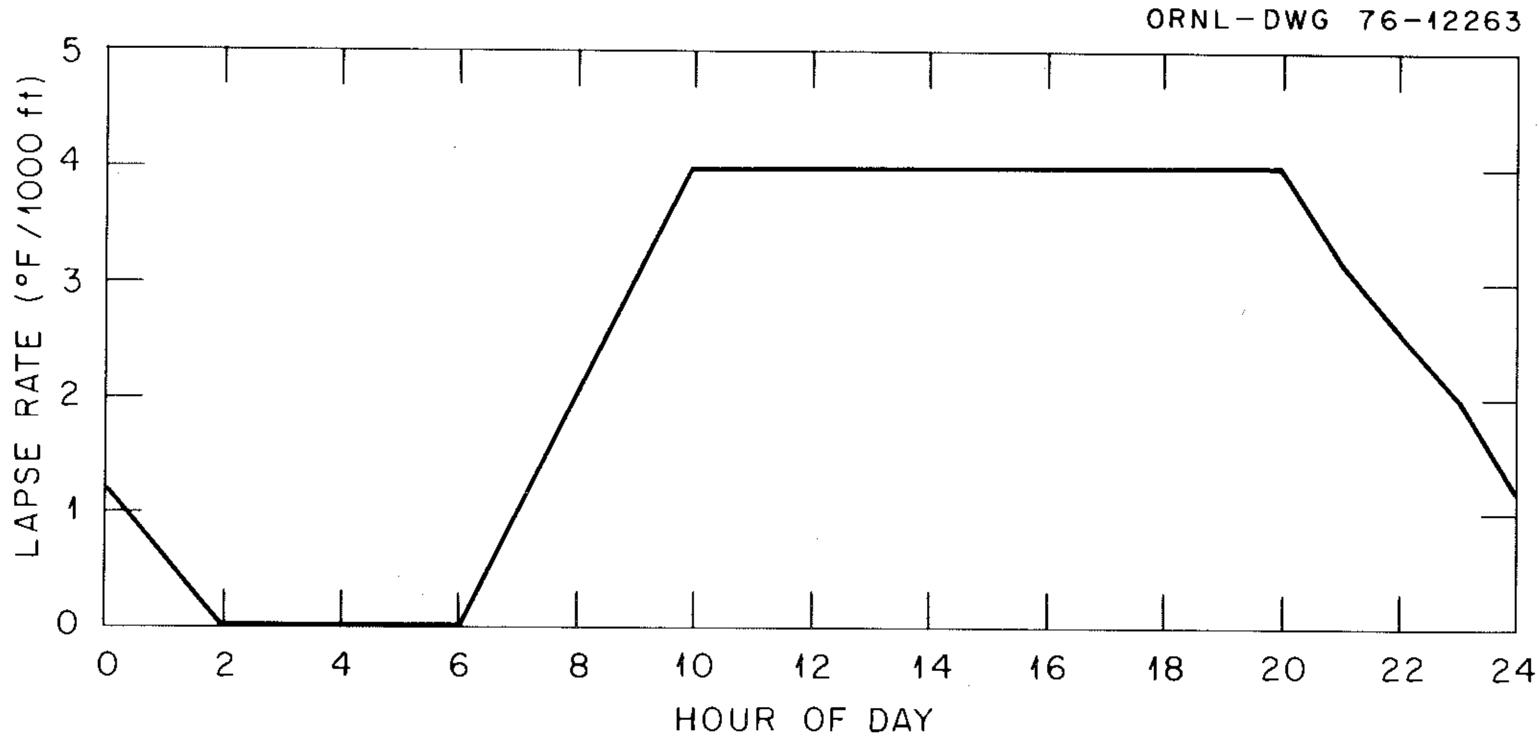

Fig. 2. Assumed lapse rate as a function of time of day.

$$T_{750}(t) = T_S(t) - 0.75\ L(t,P) \quad , \qquad (1)$$

where

$T_{750}(t)$ = air temperature at 750 ft above segment at hour t,
$T_S(t)$ = air temperature at the segment surface at hour t, and
$L(t,P)$ = the assumed lapse rate at hour t and precipitation rate P.

If the calculated air temperature at 750 ft above the segment is less than 32°F, snow is assumed to be falling.

Climatic Variables

In addition to hourly precipitation data, hydrologic simulation for a watershed segment requires the following climatic data:

(1) average daily dew point temperature,
(2) average daily wind speed,
(3) daily maximum and minimum air temperature, and
(4) daily total solar radiation.

Each of the climatic variables listed above is used in the estimation of evaporation and transpiration losses from the watershed segment, and enters into energy balance computations for snowpack accumulation and melt. The use of each variable and the manipulations performed on raw data are described below.

Dew point temperature

Dew point temperature is used by the model to estimate the actual water vapor pressure of the air mass over the basin segment. It is assumed that a single value of vapor pressure is representative of conditions for any given day. The relation between dew point temperature and actual vapor pressure is:

$$e_a = (2.1706 \times 10^8)\ e^{(-7482.6/(T_d+398.36))} \quad , \qquad (2)$$

where

e_a = actual vapor pressure (mb),
e = base of natural logarithm, and
T_d = dew point temperature (°F).

The above equation has been adapted from the work of Lamoreux (1962). In many cases, relative humidity data are collected and must be converted into estimated dew point temperature. The recommended method for the conversion is based on the assumption that maximum air temperature and minimum relative humidity occur simultaneously. Such an assumption eliminates the necessity of observation time corrections between independent air temperature and humidity records. The procedure used to derive dew point temperature is:

(1) Compute saturation vapor pressure with the equation:

$$e_s = (2.1706 \times 10^8)\ e^{(-7482.6/(Ta+398.36))} \quad , \qquad (3)$$

where

e_s = saturation vapor pressure (mb),
e = base of natural logarithm, and
Ta = air temperature (°F)

(2) Compute dew point temperature from the equation:

$$T_{dew} = \{7.4826 \times 10^3/\ln\ [2.1706 \times 10^8/(RHxe_s/100)]\} - 398.36 \quad , \ (4)$$

where

T_{dew} = dew point temperature °F,
ln = natural logarithm,
RH = relative humidity (%), and
e_s = saturation vapor pressure (mb).

The calculation method described above can lead to an estimated dew point temperature that exceeds the minimum daytime temperature. Although this implies supersaturation of the atmosphere, internal tests in the TEHM select the higher of the ambient air or dew point temperatures to estimate actual vapor pressure. A computer program that implements the procedure described above is given in the Appendices.

Wind Speed

Wind speed information is used in the calculation of vapor transport away from the evapotranspiration surface, and for snowpack energy exchange with the atmosphere.

Since wind speed is a function of height and surface roughness conditions, it is necessary to supply some information regarding the location and exposure of the recording anemometer to allow estimation of the wind movement within the forest canopy. The method used is to extrapolate observed wind speed to a height above canopy level, then estimate a wind speed profile down into the canopy.

For a well-exposed anemometer, a logarithmic velocity profile is assumed to be suitable for extrapolating speeds to 100 ft above ground surface. The equation used is:

$$\frac{U_i}{U_X} = \frac{\ln[i-D)/Z_o]}{\ln[X-D)/Z_o]} \quad , \qquad (5)$$

where

U_i = wind speed at elevation i,
D = zero plane displacement level,
Z_o = surface roughness length, and
X = anemometer height.

In the absence of better information, one may assume that Z_o may be estimated as one-twentieth the height of the prevailing roughness elements at the anemometer site (Byers, 1969). The zero plane displacement refers to the elevation above the surface where the logarithmic velocity profile reaches zero. It has been assumed to be two-thirds of the prevailing roughness height, and is generally negligible compared to the anemometer height.

Extrapolation of the wind speed profile down into the canopy employs two functions, based upon the work of Murphy and Knoerr (1970). The logarithmic function described above is used to determine wind speed above and at the top of the canopy (with adjustments for D and Z_o), then an exponential function of the form:

$$U_i = U_1 * C^{a(Z_i - C)} \quad , \qquad (6)$$

where

U_1 = velocity at the top of the canopy,
a = velocity profile extinction coefficient,
Z_i = stand height of layer i, and
C = total stand height,

and

$a \cong 0.0015\ cm^{-1}$ as an estimate based upon the work of Shinn (1969) is used to estimate wind speed within the canopy.

The equation can be integrated to estimate the average wind speed in an overstory layer of thickness ΔZ (from canopy top to bottom limbs) to yield:

$$\overline{U} = \frac{U_i\ (1 - e^{-a\Delta Z})}{aZ} \quad . \qquad (7)$$

It is expected that the parameter (a) will be a function of leaf area index, and will vary seasonally. For applications to Walker Branch Watershed, it has been estimated that $a = 0.0013\ cm^{-1}$ during the growing season, and $a = 0.0006\ cm^{-1}$ during dormant season conditions. These estimates were derived by comparing observed wind speeds at the reference site and in the canopy for a few cases. The thickness of the canopy layer was taken as 1200 cm (Curlin and Nelson, 1968).

Thus, using the equations presented above or empirical correlations between anemometer readings at the permanent site and wind movement in the canopy of the basin segment under study, one can derive a correction factor to be applied to the basic wind data set. As discussed later, model results are relatively insensitive to wind speed.

Air Temperature

Temperature data are required for a number of computations during simulation. The basic input calls for daily maximum and minimum air temperature. Two manipulations may be performed on the data within the TEHM. Depending upon observation time, the maximum temperature reported for a given date may have occurred on the preceding day (e.g., when observations are taken with maximum and minimum recording thermometers and reported as of 8 a.m. on a given day). Adjustments for observation time are controlled by input, as explained in the section on input data. Once the maximum and minimum temperatures have been established, a smooth curve is fitted between successive values to provide estimated hourly air temperature. Figure 3 illustrates the shape of the temperature curve (see listing of ANUMON, array TEMPF for the explicit values). In using the function, it is assumed that the minimum daily temperature always occurs at 6 a.m., and the daily maximum always occurs at 4 p.m. Formats to be used for temperature data input are described on pages 57-58 in the WHTM User's Manual (Patterson et al., 1974).

Solar Radiation

Solar radiation data are most often available as daily totals at a meteorological station with a different exposure than the site to which they are to be applied. To make such values acceptable for use in TEHM

ORNL-DWG 76-12262

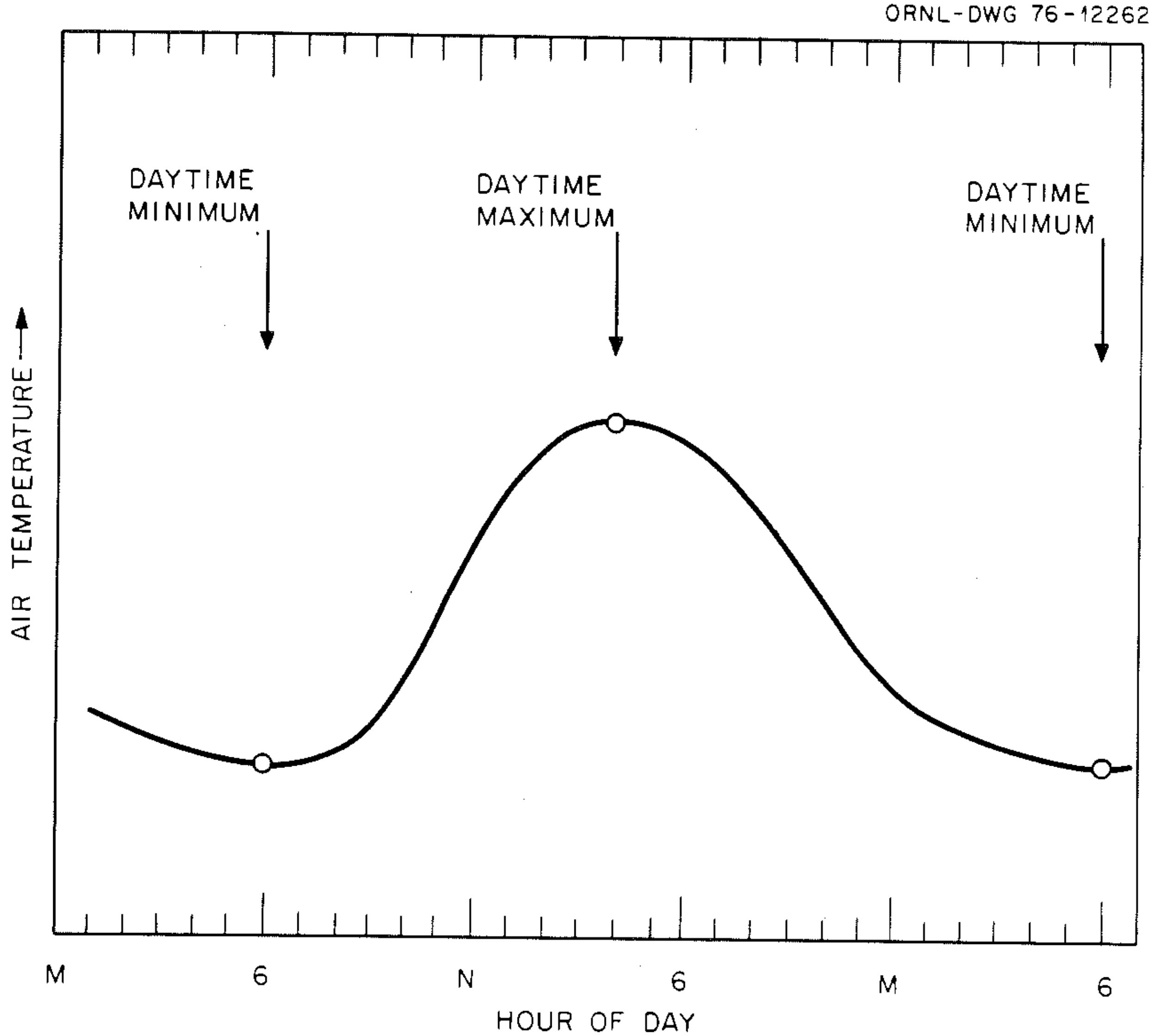

Fig. 3. Assumed air temperature distribution function.

simulation computations, daily observations must be adjusted for the slope and azimuth of the receiving surface and also distributed into hourly increments through each day. The basis of radiation adjustments for slope and azimuth of a watershed or sub-basin is the equivalent slope theory (Lee, 1963), which allows one to define an equivalent latitude and longitude on the earth where a horizontal surface is parallel to the slope at the study site, and thus has the same angular relationship to the solar beam. With standard relationships, one may then compute the potential radiation on a horizontal surface at the equivalent slope location, and equate it to the potential radiation on the basin slope. Finally, one calculates the potential radiation on a horizontal surface at the study site and uses the ratio of potential radiation on the slope to that on the horizontal plane to adjust observed daily radiation to the slope and azimuth of the study site. The computations are all included in the TEHM, thus readers not interested in the details of the equations used may wish to skip to the next section.

Temporal distribution of daily short-wave radiation

The temporal distribution of daily radiation into hourly increments is based on the use of the solar altitude equation. The intensity of solar radiation at a point on a horizontal plane tangent to the earth's surface is directly proportional to the sine of the solar altitude angle during the day. Hence the time integral of the sine of the solar altitude angle is proportional to the amount of energy received for any interval between sunrise and sunset. The ratio of the integral for a given hour to the solar day total thus represents the fraction of the daily radiation that is assigned to that hourly increment. In the absence of cloud cover data, we assume a uniform cloud cover for each hour of a given day.

Details of the methods used for adjusting solar radiation data are briefly described below.

Slope and aspect adjustments. The equation for the equivalent latitude of a slope (LA_{eq}) is:

$$LA_{eq} = \arcsin(\cos S * (\sin(\phi) + (\sin S * \cos\phi * \cos Z)), \qquad (8)$$

where

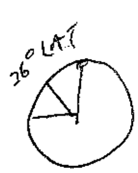

S = the positive angle between the plane of the slope and the horizontal plane,
ϕ = the true latitude of the slope (degrees), and
Z = the positive angle measured clockwise from north to the direction of the steepest downhill slope (azimuth).

(note: The implemented program deals with only the northern hemisphere).

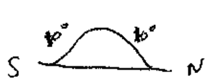

The difference in longitude or time shift between the actual and equivalent slope (ΔLO) is given as:

$$\Delta LO = \arctan [\sin S * \sin Z/(\cos S * \cos \phi - \sin S * \sin \phi * \cos Z)] , \quad (9)$$

where S, ϕ, and Z are as defined above.

The potential daily radiation on a horizontal surface depends upon the solar declination and the time between sunrise and sunset, in addition to the site location. The declination of the sun is the angle between the earth's equator and the latitude at which the sun is directly overhead at solar noon. The equation for the declination is:

$$D = \arcsin \{0.39785 * \sin [4.869 + 0.0172 * t + 0.03345 * \sin (6.2241 + 0.0172 * t)]\} , \quad (10)$$

where

t = Julian date, where January 1 = 1 and December 31 = 365 or 366, and all angles are expressed in radians.

The declination ranges between +23.5° on June 21 and -23.5° on December 21.

Day length for a horizontal plane at a given location is calculated in terms of an "hour angle" between solar noon and sunrise or sunset. If each 24-hr day is represented by 360°, one hour is equivalent to 15° or $\pi/12$ radians. The hour angle between solar noon and sunset (τ) on a horizontal surface at the equivalent location is given by

$$\tau = \arccos [-\tan (LA_{eq}) * \tan D] , \quad (11)$$

where

τ = hour angle between solar noon and sunset,
LA_{eq} = latitude for the equivalent slope, and
D = declination of the sun.

Adjustment for the time difference between the true and equivalent slope coordinates translates the hour angles for sunrise and sunset to the longitude of the actual site. Thus:

$$\tau_r^e = -\tau - \Delta LO \text{ and}$$

$$\tau_s^e = \tau - \Delta LO \quad , \qquad (12)$$

where

τ_r^e = hour angle of sunrise, and
τ_s^e = hour angle of sunset for the equivalent slope adjusted to the solar time at the true slope site.

Similarly the hour angles for sunrise (τ_r^a) and sunset (τ_s^a) on a horizontal surface at the actual site can be determined by replacing LA_{eq} with the site latitude ϕ in the hour angle equation. The times of sunrise (τ_r) and sunset (τ_s) on the actual slope are taken to be the lesser (absolute value) of τ_r^e and τ_r^a and of τ_s^e and τ_s^a, respectively.

The above calculations must be checked for extreme conditions of no sunrise or sunset and for double days with two sunrises and two sunsets. These extreme cases can occur on some slopes that face toward the poles.

One additional factor is needed to calculate potential radiation at a point. It is the solar constant, adjusted for the eccentricity of the earth's orbit. The eccentricity describes the varying earth-sun distance and accounts for the unequal length of the seasons, and is given by

$$E = 1.0 - 0.0167 * \cos [(t - 3) * 0.0172] \quad , \qquad (13)$$

where the angle is expressed in radians, and t is Julian date. The solar constant for one hour (R1), adjusted for eccentricity, is given as

$$R1 = (60. * 1.95)/E^2 \quad , \qquad (14)$$

where the solar constant above the earth's atmosphere is 1.95 cal cm^{-2} $min.^{-1}$ (Drummond, 1968).

The potential daily radiation on the true slope (R_{ps}) may be calculated from the equivalent latitude (LA_{eq}) as follows:

$$R_{ps} = R1 * \{\sin D * \sin (LA_{eq}) * (\tau_s - \tau_r) + \cos D * \cos (LA_{eq}) * [\sin (\tau_s + \Delta LO) - \sin (\tau_r + \Delta LO)]\} * 3.82 \quad . \qquad (15)$$

The potential daily radiation on a horizontal plane (R_{ph}) at the latitude of the slope (ϕ) can be obtained by using ϕ in place of LA_{eq} and using τ_r^a and τ_s^a for the times of sunrise and sunset.

The ratio of potential radiation on the slope to that on a horizontal plane is used to modify the observed radiation to obtain a radiation estimate for the slope. The estimated actual radiation on the slope is thus:

$$R_e = R_{obs} * \frac{R_{ps}}{R_{ph}} \quad , \tag{16}$$

where

R_{obs} = observed solar radiation (measured on horizontal surface exposed to cloud cover similar to that for the slope),
R_{ps} = potential radiation for the slope, and
R_{ph} = potential radiation on a horizontal surface at the slope site.

A final adjustment to estimated radiation on the slope (R_e) is used to convert it to a map area basis (R_m) using the slope inclination (S)

$$R_m = R_e/\cos S \quad . \tag{17}$$

All these adjustments reduce to unity and have no effect if the slope is a horizontal surface (i.e., if S = 0.0).

Temporal distribution of daily short-wave radiation. There are two basic operations used to distribute total daily solar radiation into hourly increments. First, solar time is adjusted to coincide with local standard time. Then the amount of radiation received on the slope is partitioned among the hours of the day to correspond to local standard time. No adjustments are made for daylight savings time or irregularities in time-zone boundaries because we think they are unwarranted for our purposes.

The adjustment of solar time to local time has two components. First is the proximity to the central longitude of the local time zone, which is usually at the nearest integer multiple of 15°. Because each hour is associated with 15° of longitude, the difference between the site longitude and the local standard time longitude corresponds to one-fifteenth of a decimal hour per degree. If the site is west of the standard longitude, the time difference is added because solar noon will occur later. Thus, the time correction for location within the local time zone is

$$\Delta \text{ Clock Time} = (L - L_s)/15 \quad ,$$

where

L = the true slope longitude (degrees),
L_s = the local standard time longitude (degrees), and
Δ Clock Time is given in minutes.

Second is a correction between noon and clock-time noon to account for the irregular rotation of the earth. The adjustment for the irregular rotation of the earth is based on the equation of time, which is the difference between true solar right ascension (α):

$$\alpha = \arctan \{0.91745 * \tan [4.86891 + 0.017202 * t + 0.033446 * \sin (6.22411 + 0.017202 * t)]\} \quad ; \qquad (19)$$

and mean solar right ascension (β):

$$\beta = 0.017202 * t - 1.41430 \quad , \qquad (20)$$

where all angles are expressed in radians. If β is greater than $\pi/2$, it is reduced by π radians. These functions of Julian date (t) are empirical and result in adjustments that range from -14 to +16 clock minutes per day during the year. When the two corrections are summed, they may be added to clock-time noon to obtain the local standard time for solar noon. Then it is possible to relate solar radiation directly to local clock time.

The partitioning of daily insolation into hourly increments is done by evaluation of the integrated form of the solar altitude versus time equation for each hour before and after solar noon. The solar altitude durations for each hour of the day are totaled and the ratio of the particular hourly solar altitude duration to the total daily duration is applied to the daily radiation on the slope to give the hourly proportion of radiation. The integrated form of the solar altitude equation was described earlier as part of the equation used to calculate potential radiation on a slope (R_{ps}).

Net Long Wave Radiation

The inclusion of the long-wave radiation balance in the surface energy balance is an option and can be excluded if desired. A logical variable called RNØN is described in the section called 5 LANPAR in the input data set. It is included when one wishes to be particularly concerned with the vegetation energy balance (e.g., when primary productivity is to be estimated).

The net loss of radiant energy of a surface is the difference between the long-wave radiation emitted by the atmosphere and the radiation emitted by the surface itself. The long-wave radiation from the atmosphere depends upon the relative volumes and temperatures of emitting agents in the atmosphere such as water vapor, carbon dioxide, and liquid water.

An empirical relationship suggested by DeVries (1955) has been adapted and implemented (as function RNLONG) to estimate the net long-wave radiation balance for vegetation. The relation is:

$$H_{lo}^{net} = \varepsilon * \sigma * \left[T_{ea}^{4} - T_{ai}^{4} * g(P_w, m) \right] , \qquad (21)$$

where $g(P_w, m) = \left[(a + b * P_w^{1/2}) * (1 - Vm) \right] + Vm,$

H_{lo}^{net} = net long wave radiation ($cal \cdot cm^{-2} \cdot min^{-1}$) ,

ε = emmissivity (use 0.95 for vegetation) ,

$\sigma = 1.35 * 10^{-12}\ cal \cdot cm^{-2} \cdot sec^{-1} \cdot {}^{o}K^{-4}$ (Boltzman constant) ,

T_{ea} = surface temperature of vegetation (°K) ,

T_{ai} = air temperature at standard observation height (°K) ,

a = constant ≈ 0.44 ,

b = constant ≈ 0.61 ($mbar^{-1/2}$) ,

P_w = vapor pressure at standard observation height (mbar) ,

m = fractional cloudiness, and

V = a cloud height parameter described below.

In implementing this equation, assumptions must be made for several of the parameters and variables used. Emissivity was assumed to equal 0.95 because vegetation has radiation properties of a grey body (van Wijk and Scholte Ubing, 1963). The air temperature and vapor pressure at standard observation height are input data to the model and the surface temperature of the vegetation is calculated by assuming it is a linear function of air temperature and hourly incoming short wave radiation. The assumed relationship is:

$$T_{ea} = T_{ai} + [0.045 * (HRSOL)] - 0.5 , \qquad (22)$$

where

T_{ea} = vegetation surface temperature (°C) ,
T_{ai} = air temperature at standard observation height (°C), and
HRSOL = hourly incoming solar radiation, (cal cm^{-2} hr^{-1}).

At low radiation periods (early morning, late afternoon), leaf temperature is lower than air temperature, whereas during the main part of the day, leaf temperature will be one to two degrees higher than air temperature.

Brunt (1932) suggested the empirical relationship ($a + bPw^{\frac{1}{2}}$) as an adjustment factor for water vapor. The constants a and b are from data tabulated by van Wijk and Scholte Ubing (1963), chosen to represent the southeastern part of the United States.

The two cloud parameters, m and V, are determined by simple intuitive relationships, based on incoming solar radiation. The fractional cloudiness (m) has a range from 0 to 1.0 and is defined as an inverse function of the ratio (PERMAX) as shown in Fig. 4 below:

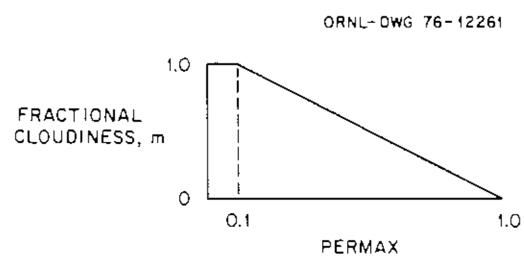

Fig. 4. Fractional cloudiness as a function of the ratio of observed to potential radiation.

PERMAX is the ratio of observed daily short wave radiation (RASØL) to the expected maximum radiation for each date (RADMAX). RADMAX is scaled to seasonal changes in incoming solar radiation by three parameters chosen to represent the southeastern United States:

$$RADMAX = RMEAN + RDEV * SIN[2. * \pi * (TDATE-81.)/365] \quad , \qquad (23)$$

where

RMEAN = 550 cal cm^{-2} day^{-1},
RDEV = 250 cal cm^{-2} day^{-1}, and
TDATE = Julian date.

The cloud height parameter (V) ranges from 0.0 for very high or no clouds to 0.9 for low (stratus) clouds (van Wijk and Scholte Ubing, pg. 97, 1963). Taking advantage of the fact that low clouds usually are associated with complete cloud cover and high clouds with little or no fractional cloudiness, we let V = 0.9*m.

Hydrologic Process Submodels

Interception and Throughfall

Precipitation on a forest canopy is adjusted for interception and evaporation losses using a coupled variable interception storage capacity and combined energy balance and mass transport evaporation method. Figure 5 is a schematic representation of the interception loss submodel. The interception storage capacity varies seasonally in the same fashion as leaf biomass. Figure 6 illustrates an example of the annual cycle of interception storage capacity for the Oak Ridge area, and also presents the regression equations developed by Helvey and Patric (1965) for estimating throughfall in a mixed hardwood forest. Although these regression equations are not used in the TEHM, they are useful for purposes of comparison. In Fig. 6, P represents total rainfall and n is the number of storms. Each time more than 6 hr elapses between measurable precipitation, a new storm begins. Evaporation loss is estimated in the TEHM using the relationship presented by Goldstein _et al_, (1974).

$$Fv = \left[\frac{(R_N - G)\Delta}{\sigma C_p \rho} + \frac{\overset{\star}{\rho 2} - \rho 2}{r_a}\right] \Bigg/ \left[1 + \frac{Lv\Delta}{\sigma C_p \rho}\right] , \qquad (24)$$

where

Fv = vapor flux away from the interception surface,
R_N = net radiation (solar plus long wave) absorbed by the canopy surface per unit time,
G = amount of heat energy transferred from the canopy surface to the soil per unit time,
Δ = slope of the saturation vapor pressure vs temperature curv at ambient canopy temperature,
σ = ratio of convection area to evapotranspiration area,
Cp = specific heat of air at constant pressure,
ρ = density of air,
$\rho 2$ = actual vapor pressure of atmosphere above the canopy,
$\overset{\star}{\rho 2}$ = saturation vapor pressure of atmosphere above the canopy,
r_a = atmospheric resistance to transfer of water between the canopy and air above the canopy,
r_a = $3.3\,(\ell)^{0.3}/\sqrt{v}$, where ℓ is a characteristic average leaf length in the canopy, and v is wind speed, and
L_v = latent heat of vaporization for water.

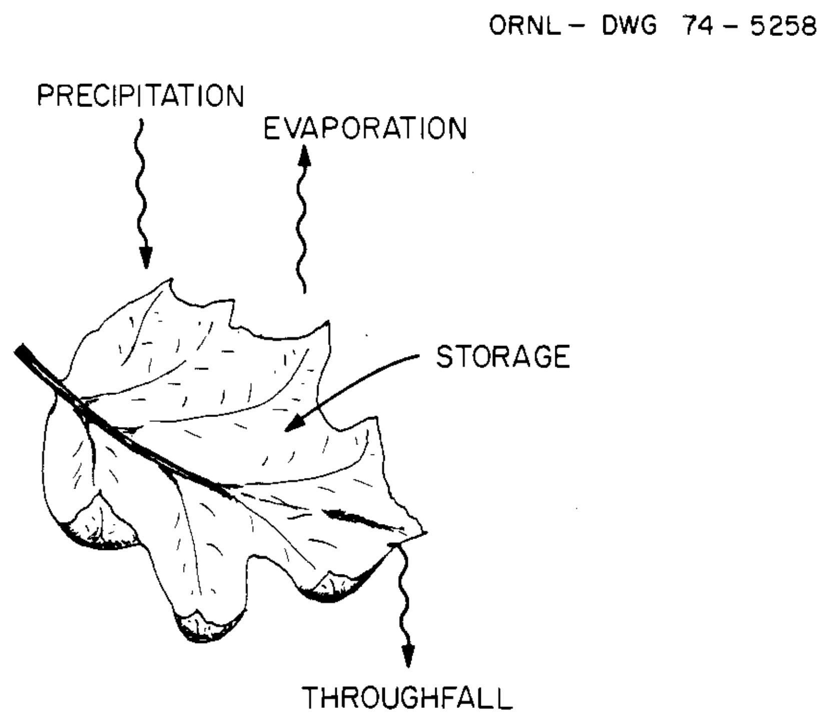

EVAPORATIVE LOSS = *f* (TEMPERATURE, RADIATION, HUMIDITY, WIND)
STORAGE = *f* (SEASONAL CANOPY DEVELOPMENT)
THROUGHFALL = PRECIPITATION − EVAPORATION

Fig. 5. Schematic representation of the interception loss submodel.

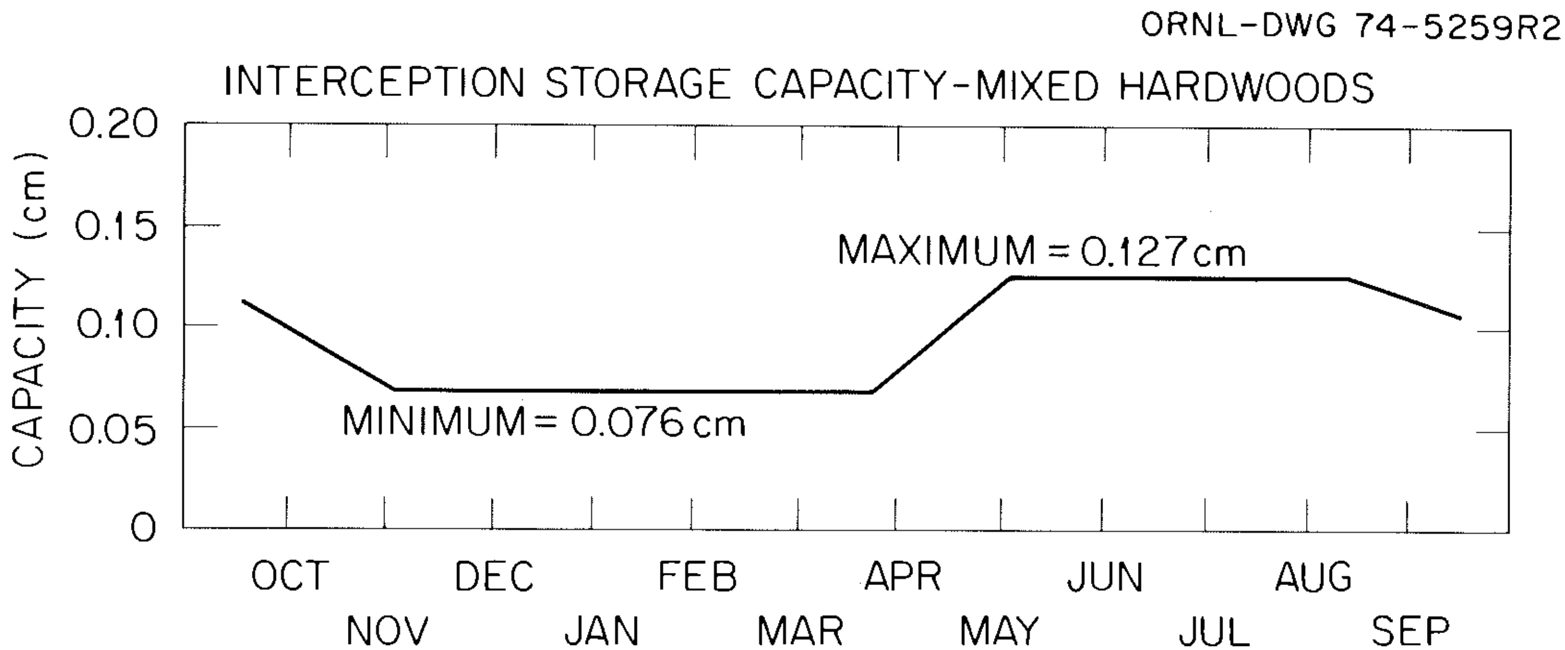

ESTIMATION OF INTERCEPTION BY REGRESSION EQUATIONS (cm)

(PATRICK AND HELVEY)

DORMANT SEASON: $I = (0.059 * \Sigma P) + 0.05 * n$

GROWING SEASON: $I = (0.083 * \Sigma P) + 0.091 * n$

Fig. 6. The annual cycle of interception storage.

Figure 7 compares integrated interception loss computed using the TEHM submodel at hourly time intervals with corresponding values derived from the Helvey and Patric regression equations for Walker Branch Watershed (WBW) during water year 1970. Table 1 compares the two methods with throughfall field data from WBW for 1971. Throughfall is approximately equal to the difference between precipitation and interception, since stemflow is approximately offset by litter interception and evaporation. Based upon the excellent agreement between independent methods, the interception component has been judged adequate for use in the TEHM.

Infiltration

The method used for estimating infiltration rates of throughfall in the TEHM is the time compression approximation recently described by Reeves and Miller (1975). The method uses a cumulative infiltration curve for the soil in question, and compares actual cumulative infiltration to the maximum cumulative infiltration possible for a specified interval. At each point during a rainfall event, the initial conditions depend upon the cumulative infiltration up to that time. If, during the next interval, cumulative rainfall exceeds cumulative infiltration, surface runoff is calculated. Otherwise, the input is added to accumulated infiltration, and a new initial condition is established for the next interval. Figure 8 illustrates a simple example that begins at actual time T_0 (top axis), when the infiltration capacity of the soil is represented by the point (I_0, E_0). During the actual time span T_0 to T_1, the amount of water supplied exceeds the infiltration capacity, so runoff is produced $[M_1-(I_1-I_0)]$ and the maximum amount of infiltration possible occurs. In this case, the equivalent time (the amount of time required to infiltrate a given amount at the maximum rate) increases the same amount as the actual time. However, in the interval from T_1 to T_2, the supply rate is lower than the maximum infiltration possible, so all water infiltrates in that period. The increase in equivalent time is less than that for actual time, and is defined by the curve for the interval considered. Miller and Reeves (1975) found that the time compression approximation method may slightly underestimate total infiltration (up to 20% for the cases they studied) when erratic rainfall occurs (e.g., downpour, then drizzle, then downpour). They suggest that this fault may be overcome by applying a small correction factor to bring seasonal or annual infiltration totals into agreement with observations. No attempt has been made to provide for such adjustment in the TEHM. Furthermore, we assume that if the elapsed time between infiltration events does not exceed 24 hr, any new event begins with the ending equivalent time and cumulative infiltration from the preceding event. After 24 hr, the soil is assumed to recover completely, and the equivalent time is set to zero. As more information becomes available, we anticipate establishing an approximate relation between soil moisture conditions and the equivalent time variable.

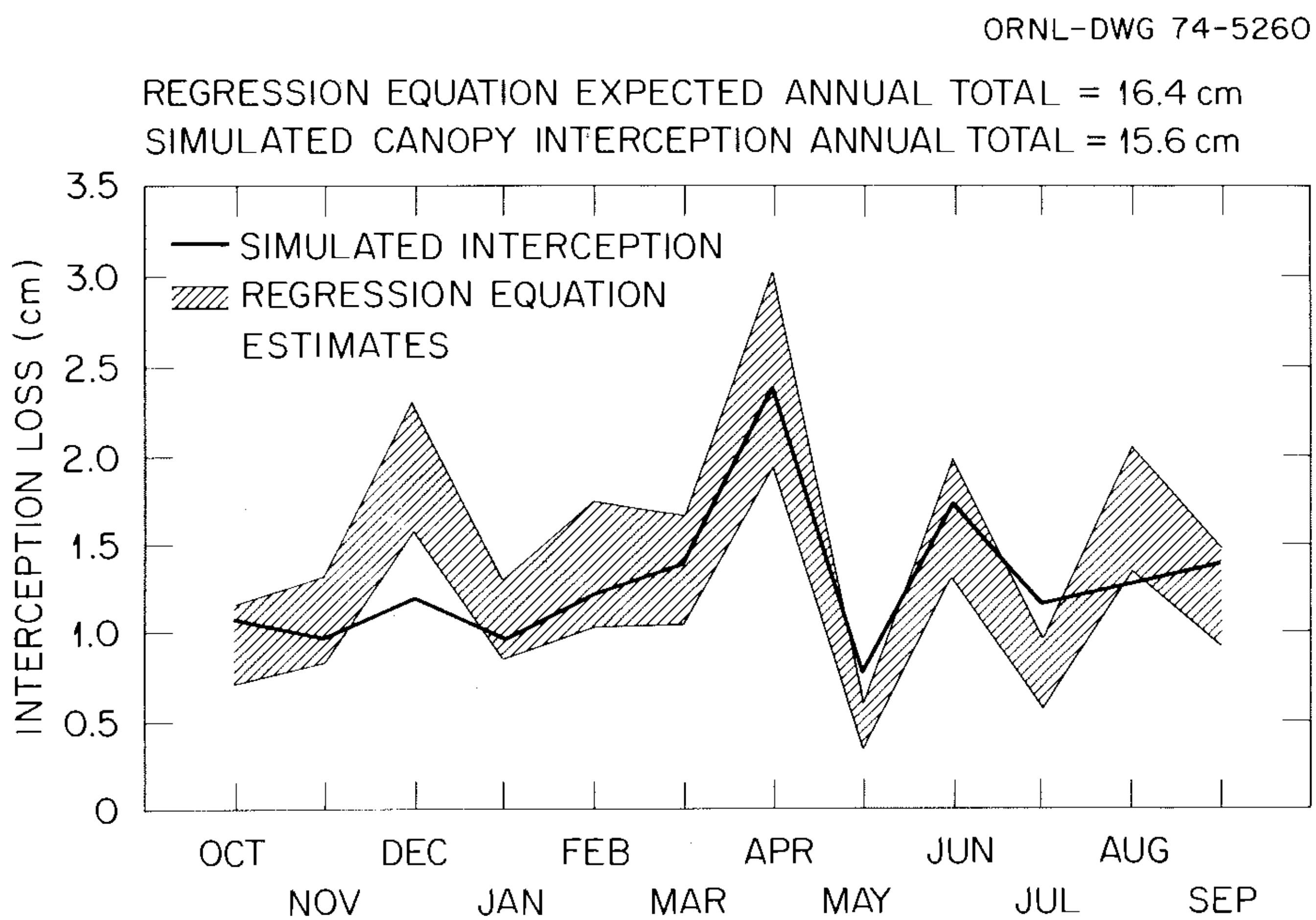

Fig. 7. Comparison of the TEHM interception submodel results with those from Helvey and Patric regression equations.

Table 1. Comparison of field observations of throughfall[a] with computed estimates

Period	Precipitation (cm)	Observed[b] throughfall (cm)	Estimated[c] throughfall (cm)	Simulated[d] throughfall (cm)
May 18 to June 10	5.5	4.2	4.8	4.8
June 10 to July 8	8.2	5.7	6.4	5.9
July 8 to July 28	16.4	14.8	14.0	14.8
July 28 to September 17[e]	15.1	12.7	12.6	12.6
Total period	45.2	37.4	37.6	38.1

[a] Ooes not include stemflow.

[b] Oata provided by G. S. Henderson, Oak Ridge National Laboratory, 1974.

[c] $T = (0.901 \times \Sigma P_i) - (0.079 \times i)$cm; $i = 1, \ldots, n$
Adapted from Helvey and Patrick, *Water Resour. Res.*, 1(2), 1965.

[d] Simulated using simple canopy storage model.

[e] Sampling period assumed to end at noon.

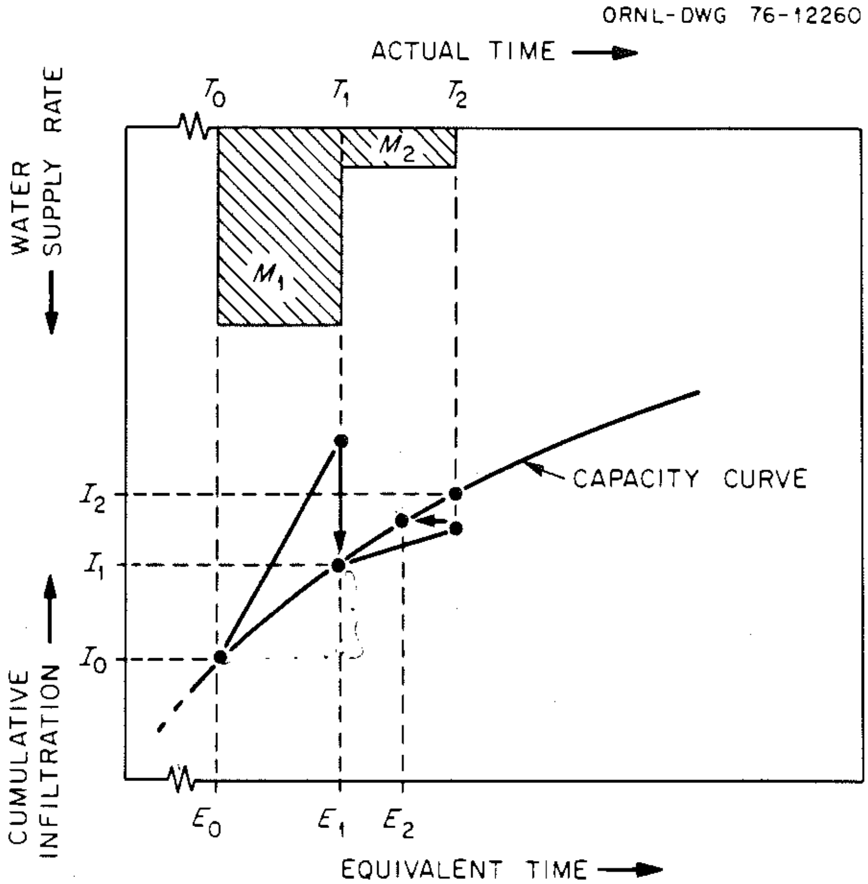

Actual Time Period	Water Supplied	Potential Infiltration	Actual Infiltration	Surface Runoff Amount	Ending Equivalent Time
T_0 to T_1	M_1	$I_1 - I_0$	$I_1 - I_0$	$M_1-(I_1-I_0)$	E_1
T_1 to T_2	M_2	$I_2 - I_1$	M_2	none	E_2

Fig. 8. Schematic example of the time compression analysis (TCA) method for estimating infiltration.

Root Zone Evaporation, Transpiration, and Drainage

The basis for simulating root zone moisture dynamics in the TEHM is the model PROSPER, described by Goldstein et al. (1974) and Swift et al. (1975). The model is presented schematically in Fig. 9. Briefly, the operation of the model is as follows:

(1) Infiltration, which is calculated using the TCA method (Miller and Reeves, 1975), enters the first soil layer.
(2) Evapotranspiration is calculated using an iterative method and the vertical redistribution flow of soil moisture is also computed.
(3) The new soil moisture content of each layer is calculated by algebraically summing the infiltration, redistribution, and evapotranspiration flows. Excess moisture in a layer generates lateral flow.
(4) Drainage is calculated from the conductivity of the deepest soil layer, thus completing one cycle of computations. The next cycle begins again at step 1.

Interception, throughfall, and infiltration computations were described earlier, and together form the basis for computing moisture input to the top soil layer. The calculation of evapotranspiration and soil water redistribution is based upon the assumption that the flux of liquid water to the evapotranspiration surface is equal to the vapor flux away from it.

The vapor flux from the evapotranspiration surface is calculated by the equation:

$$F_V = \frac{\dfrac{[f(A)+1]\,[R_N-G]\Delta}{[\sigma f(A)+1]\,\rho C_p} + [f(A)+1]\,\dfrac{(\rho 2^{*}-\rho 2)}{r_a}}{\dfrac{r_a + r_x}{r_a} + \dfrac{[f(A)+1]\,L_V\Delta}{[\sigma\, f(A)+1]\,\rho\, C_p}}, \qquad (25)$$

where

F_V = vapor flux away from the evapotranspiration surface,
r_x = resistance of the evapotranspiration surface to the release of water vapor,
A = actual leaf area index,
$f(A) = k\,A/(1 + A/A_0)$ = effective leaf area index,
k, A_0 = canopy scale factors, and the remaining terms have the same definition as in Eq. (24) presented earlier. Equation (25) is the modification of the relation found in Goldstein et al. (1974) that is given by Swift et al. (1975). The relation f(A) was developed to account for periods of canopy development or other periods when the

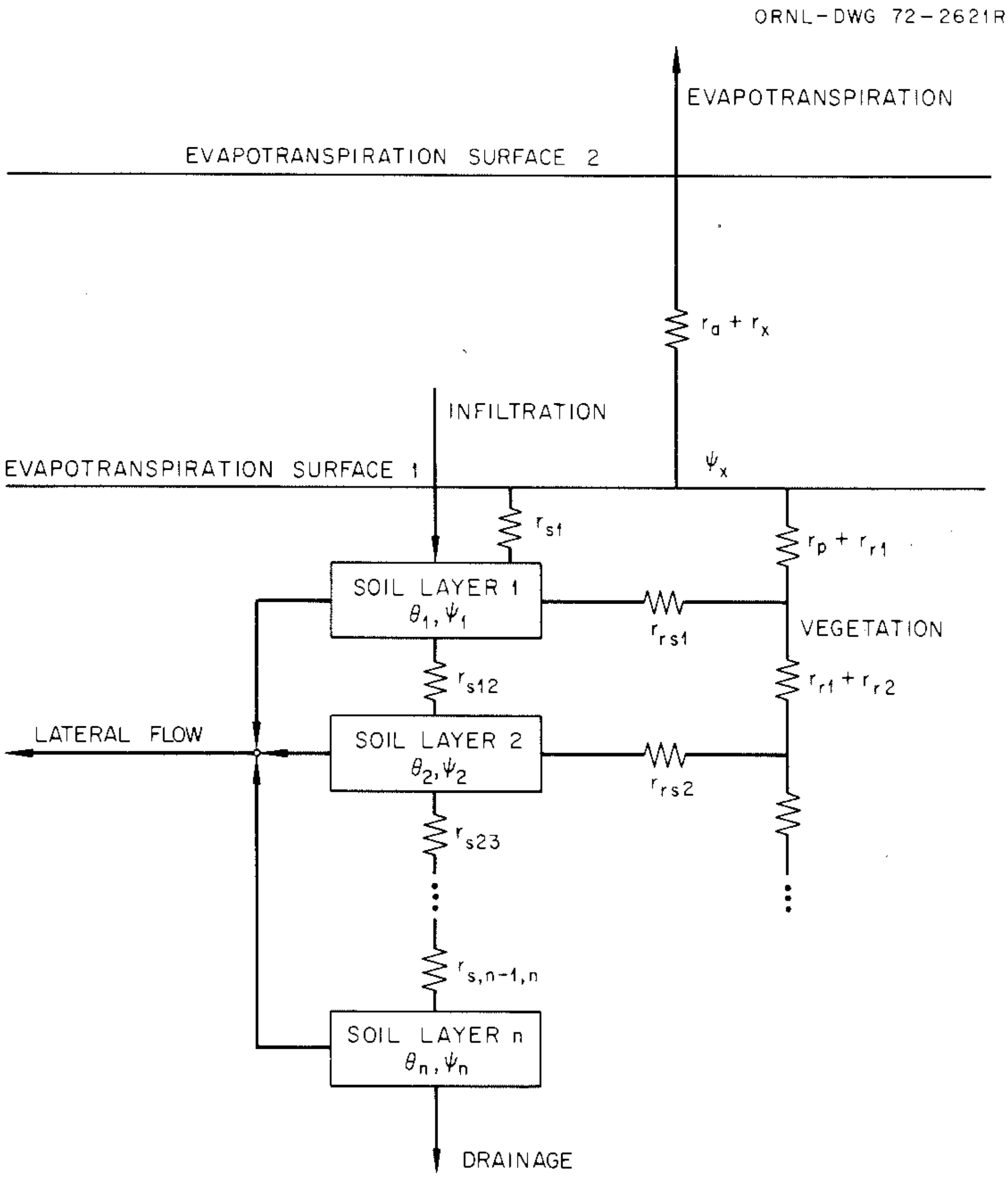

Fig. 9. Schematic diagram of PROSPER: A model of atmosphere-soil-plant water flow.

canopy has incomplete development. (The user who is not interested in details of the computation should skip to the next section.)

The other terms in Eq. (25), except for r_x, are either constants or functions of the environmental conditions. In the TEHM r_x, which is the resistance of the ET surface to the release of water vapor, is hypothesized to be of the form

$$\bar{r}_x = r_o + (r_c - r_o)\, e^{h(\Psi_c - \Psi_o)} \qquad 0 \leq \Psi_o \leq \Psi_c$$
$$r_x = r_c \qquad \Psi_o > \Psi_c\ , \tag{26}$$

where

r_o = minimum evapotranspiration surface resistance,
r_c = maximum evapotranspiration surface resistance,
Ψ_o = evapotranspiration surface water potential,
Ψ_c = surface water potential at which the surface resistance becomes a maximum, and
h = an exponent which determines how rapidly the resistance reaches its maximum value.

Thus, the vapor flux from the evapotranspiration surface is a nonlinear function of the surface water potential (Ψ_o).

The liquid water flux to the evapotranspiration surface is estimated through use of the electrical circuit analogy to the soil-plant-water flow system shown in Fig. 10. The calculations are done using standard techniques for solving electrical circuit problems. The symbols used in Fig. 10 are:

n = an arbitrary integer that signifies the number of soil layers,
Ψ_k = soil water potential for the k^{th} soil layer, $1 \leq k \leq n$,
$\underline{\Psi}_o$ = evapotranspiration surface water potential,
$\bar{\Psi}_k$ = water potential within the plant at the k^{th} soil layer. (These terms are eliminated mathematically, so they are never calculated.),
i_1^k ($1 \leq k \leq n$) = the water flow between soil layers (when k = 1, it represents the water evaporated from the surface of soil layer 1),
i_2^k ($1 \leq k \leq n$) = water flowing in the root system in the k^{th} soil layer (when k = 1, it is the water flowing in the aboveground portion of the plant ,
i_3^k, $1 \leq k \leq n-1$, = the water flowing across the soil-root interface in the k^{th} soil layer,
r_1^k, $1 \leq k \leq n$ = resistance to flow of water between soil layers (when k = 1, it is the resistance to flow across the soil at interface),
r_2^k, $1 \leq k \leq n$ = resistance to flow of water within the root system

ORNL-DWG 76-12259

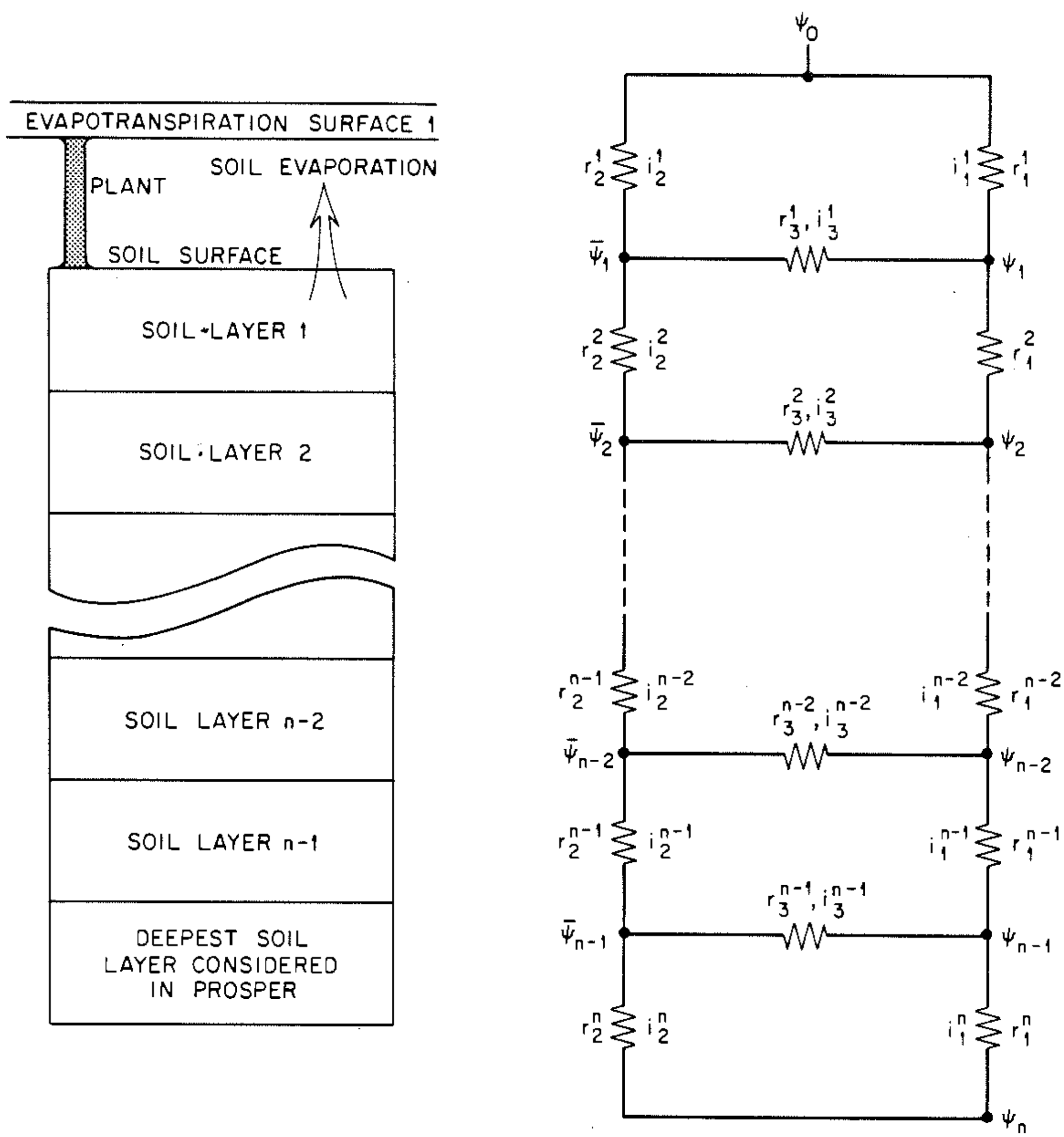

Fig. 10. Schematic diagram of electric circuit analogy to the soil-plant-water flow system.

between the k^{th} and the $(k-1)^{th}$ soil layers (when $k = 1$, r_2^k is the resistance to flow of water in the above ground portion of the plant).

r_3^k, $1 \le k \le n-1$, = resistance to flow of water across the soil-root interface in the k^{th} soil layer.

It is convenient in the calculations to use conductance instead of resistance; e.g., $g_2^k = 1/r_2{}^k$, which is more amenable to computer-based calculations when resistance is infinite so that zero flow (and conductance) is implied.

It is also convenient to partition the soil-water-plant system shown in Fig. 10 into a soil-water flow system (Fig. 11b) and a plant and soil-root interface system (Fig. 11c) to simplify the calculations. The equations are coupled later to represent the integrated system. Figure 11b is a schematic circuit diagram of the soil-water flow system, which may be represented by the following equations:

$$i_1^k = g_1^k\,(\Psi_k - \Psi_{k-1}),\quad k = 1,2,---,n \quad . \qquad (27)$$

Because the soil-water contents of each layer are known at any point in time, the water potentials and the soil conductivities of each soil layer can be determined.

The TEHM uses the method of Green and Corey (1971) as implemented and described by Luxmoore (1973) to estimate soil conductivity where experimental data on the relationship between water content and unsaturated conductivity are unavailable. The basis of the method is the pore-interaction model of Marshall (1958), and uses the equation of Green and Corey (1971):

$$K(\Theta)_i = \frac{K_s}{K_{sc}} \cdot \frac{30\,\gamma^2}{\rho\, g\, \eta} \cdot \frac{\varepsilon^P}{n^2} \sum_{j=1}^{m} [(2_j + 1 - 2i)\, h_j^{-2}] \ , \qquad (28)$$

$$i = 1,2,---m$$

where

$K(\Theta)_i$ = the calculated conductivity for a specified water content or pressure (cm min-1),

Θ = the water content ($cm^3\ cm^{-3}$),

i = the last water content class on the wet end (e.g., i = 1 identifies the pore class corresponding to the saturated water content, and i = m identifies the pore class corresponding to the lowest water content for which conductivity is calculated),

ORNL-DWG 76-12258

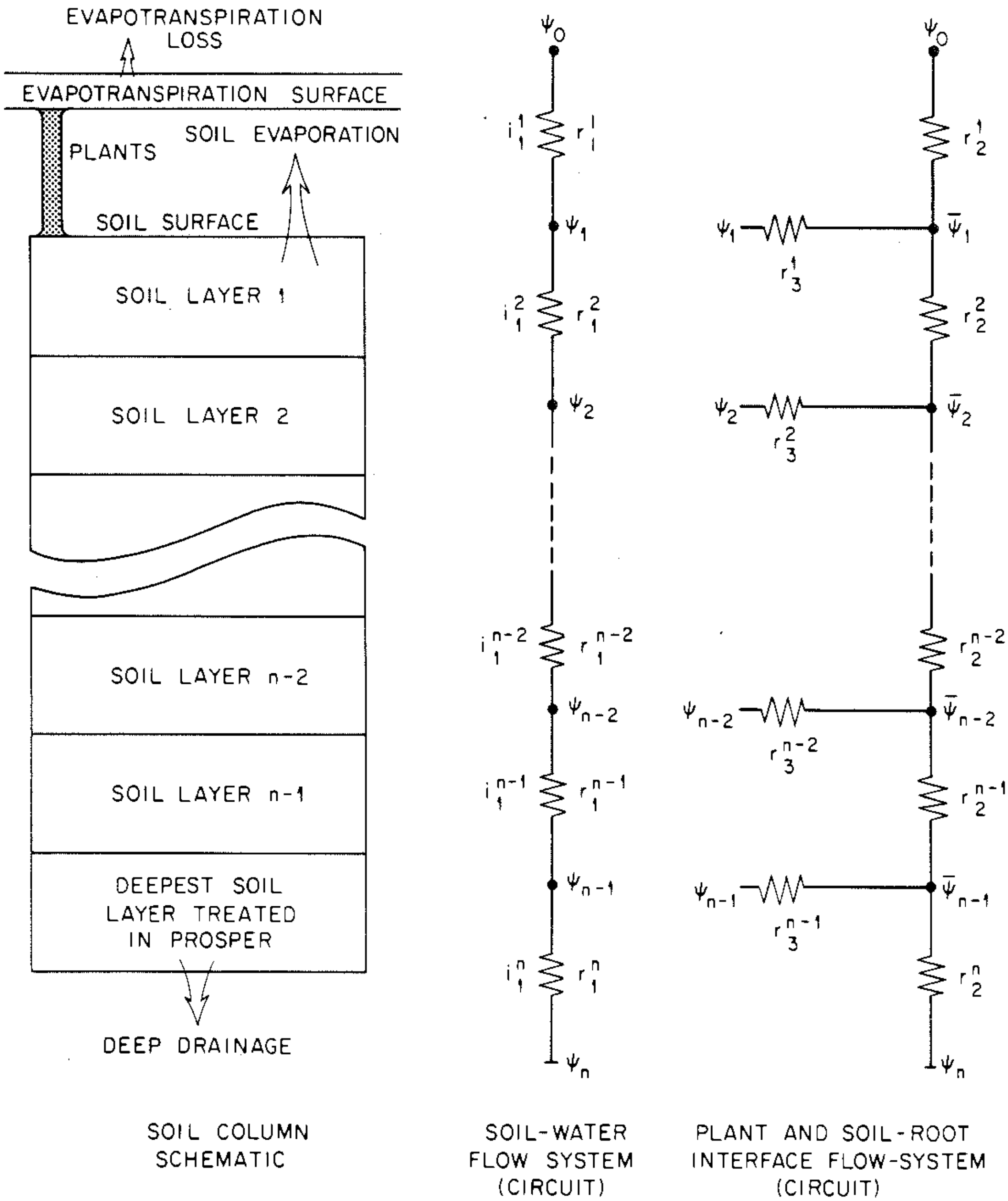

Fig. 11. Schematic diagram of partitioned soil-water and plant- and root-soil flow systems.

K_s/K_{sc} = the matching factor (measured saturated conductivity/calculated saturated conductivity),

γ = the surface tension of water (dynes cm^{-1}),

ρ = the density of water (g cm^{-3}),

g = the gravitational constant (cm sec^{-2}),

η = the viscosity of water (g cm^{-1} sec^{-1}),

ε = the porosity (cm^3 cm^{-3}), defined in various ways depending on the method of calculation,

P = a parameter that accounts for interaction of pore classes,

n = the total number of pore classes between $\Theta = 0$ and Θ_s, the saturated water content: $n \geq m$ (see text); n may or may not vary with Θ depending on the calculation method, and

h_j = the pressure for a given class of water-filled pores (cm of H_2O).

The user must supply a few corresponding measured values of water content and pressure. A specific example is provided later in this report. The model uses linear interpolation between points to estimate pressures associated with each water content pore class. A detailed explanation and evaluation of the method has been presented by Luxmoore (1973).

An alternative to the Green and Corey (1971) method for estimating hydraulic conductivity and soil water pressure has also been included in the TEHM. Any one of the following three equations may be selected to estimate hydraulic conductivity:

$$K(\Theta) = k_3 \, \Theta^{k_4} , \tag{29}$$

$$K(\Theta) = k_3 \cdot \exp \left[k_4(\Theta - k_2) \right] , \tag{30}$$

$$K(\Theta) = k_3 / \{1 + \exp \left[-k_4(\Theta - k_5) \right] \} , \tag{31}$$

where

$K(\Theta)$ = hydraulic conductivity at water content Θ,

Θ = fractional volumetric water content, and

k_i = empirical parameter constants for each equation, where i refers to the index number for the input of parameter values.

The option may be used when observed data are available for the $K(\Theta)$ versus Θ relation for the basin soils. In this case, a best-fit set of values is chosen for the equation that most closely represents data, and the user specifies the equation and values for parameters as model input.

Any one of the following four equations may be used to approximate the water content versus soil-water suction (pressure) relationship:

$$PSM = P_3\ (P_2 - \Theta)/\Theta^{P_4} \quad , \tag{32}$$

$$PSM = P_3\ (P_2 - \Theta)\ (P_5 - \Theta)/(P_2 + P_6 - \Theta) \cdot \Theta^{P_4} \quad , \tag{33}$$

$$PSM = P_3\ [(1/\Theta^{P_4}) + (P_5/\Theta)]\ (P_2 - \Theta)/(P_2 + P_6 - \Theta), \tag{34}$$

$$PSM = [P_3\ (P_2 - \Theta)^{P_5}]/\Theta^{P_4} \quad , \tag{35}$$

where

PSM = soil water pressure (cm of water),
Θ = fractional volumetric water content,
P_i = empirical parameter constants for each equation, where i refers to the index number for the input of parameter values.

The equations given above are only a few of those possible. They are included here as an example of the flexibility available when data exist for defining the relationships they express, rather than some preferred set of approaches. The motivation for their use is primarily computational speed and convenience.

When the flow of water between two layers is calculated using an approximation to Darcy's law, it is necessary to specify an appropriate hydraulic conductivity term, recognizing that each layer may have a different average value at any instant. We assume that the conductivity of the layer contributing water is most important. The averaging of the conductivities of two layers has been rejected because it led to unrealistically low flow rates between very wet and very dry layers. Thus, in the TEHM, the soil conductances are given as

$$g_1^1 = 2K_1/d_1 \quad , \text{ and}$$

$$g_1^k = \frac{K^*}{(d_k + d_{k-1})/2} \qquad k = 2, 3, \ldots, n \quad , \tag{36}$$

where

K^* = soil conductivity (e.g., by Green and Corey method) of layer k or k - 1, whichever has the highest total water potential, and
d_k = thickness of the k^{th} soil layer.

Thus, all quantities in Eq. (27) are known except Ψ_0. The determination of Ψ_0 will be discussed later.

Figure (11c) is the schematic diagram of the water flow system within the plant and across the soil-root interface. From this diagram one writes the following equations:

flux within the plant.

$$i_2^1 = g_2^1\,(\bar{\Psi}_1 - \Psi_o) \quad ,$$

$$i_2^k = g_2^k\,(\bar{\Psi}_k - \bar{\Psi}_{k-1}), \quad k = 2,3,\text{---}, n-1 \quad , \tag{37}$$

$$i_2^n = g_2^n\,(\bar{\Psi}_n - \bar{\Psi}_{n-1}) \quad .$$

If the k^{th} layer is below the rooting zone, we set $g_2^k = 0$. Also note that:

flux from soil to root

$$i_3^k = g_3^k\,(\Psi_k - \bar{\Psi}_k), \qquad k = 1,2,\text{---}, n-1, \tag{38}$$

conservation of mass

$$i_3^k + i_2^{k+1} - i_2^k = 0, \qquad k = 1,2,\text{---}, n-1 \;. \tag{39}$$

The unknown terms in Eqs. (37) and (38) are the i_2^k's, i_3^k's, $\bar{\Psi}_k$'s, and Ψ_o. Combining (37) and (38) to solve for $\bar{\Psi}_k$, then substituting for $\bar{\Psi}_k$ in (39) yields *in resistance form*:

$$-r_3^k\, i_2^{k+1} \;+\; (r_2^k + r_3^k + r_3^{k-1})\, i_2^k - r_3^{k-1}\, i_2^{k-1} = \Psi_k - \Psi_{k-1} \quad , \tag{40}$$

where i_2^{n+1}, g_3^o and $i_2^o = 0$.

This system of equations may be solved for the i_2^k's except for the unknown value of Ψ_o. Then Eq. (39) may be solved for i_3^k to determine the amount of transpiration flow from each soil layer.

The total transpiration flow is given by i_2^1 and the evaporation flow from the first soil layer is given by i_1^1. Therefore, the total evapotranspiration is given by

$$ET = i_1^1 + i_2^1 = F\ell \quad , \tag{41}$$

which are determined from Eqs. (27) and (40) except for the unknown surface water potential, Ψ_0.

We now have all the equations to solve the atmosphere-plant-soil-water flow system except that we do not know the evapotranspiration surface water potential, Ψ_0. To determine this variable the TEHM uses the following procedure:

(1) Choose an initial guess for Ψ_0. This is set as -1 bar initially and as the value at the previous time step in subsequent time periods.
(2) Solve (25) for the vapor flow from the evapotranspiration surface, F_v.
(3) Solve (27) and (40) for the liquid flow to the evapotranspiration surface, F_ℓ.
(4) Determine the difference, $\zeta = F_\ell - F_v$.
(5) Using the subroutine ABSICA (Westley and Watts 1970), choose a new value of Ψ_0.
(6) Repeat the procedure until $|\zeta| \leq \varepsilon$, where ε is an arbitrarily small positive number. The value of ε in the present version of the TEHM is 10^{-5}.
(7) Solve for the water flux from each soil layer using (38) and (27).
(8) Solve for the new value of soil moisture in each soil layer.
(9) Calculate the drainage and lateral flow. In this version, drainage is estimated by

$$\text{Drainage} = K_n$$

where K_n is the soil conductivity of the last soil layer. This estimate makes the tacit assumption that the gravitational potential dominates flow from the last soil layer. This is a tenuous assumption at best, but it is the best approximation that we feel we can make at the present time. Lateral flow occurs only when the receiving soil layer is saturated.
(10) Proceed to the next time step, and repeat the procedure.

Subsurface Flow

There are three objectives that the subsurface flow component of the simulation model is designed to satisfy. First, the studies of Hewlett (1961a), Betson and Marius (1969), Dickinson and Whiteley (1970), Dunne and Black (1970), Freeze (1972), Lee and Delleur (1972), Engman and Ragowski (1974), Ishaq (1975) and others have shown the advisability of integrating the variable source area concept into hydrologic models. The subsurface flow component of the TEHM explicitly represents a hypothesis that relates subsurface drainage rate and variable source area runoff.

Second, unsaturated drainage rates have been shown to be a significant portion of "dry weather" flow from steeply sloped, shallow soils (Hewlett, 1961b and Weyman, 1973). Thus another goal of the model is to represent unsaturated drainage rates as determined by soil moisture and soil hydraulic properties.

Finally, the third objective considered in the design of the subsurface flow model component was to require minimum complexity of field data and computational methods. This final goal requires a subjective trade-off between simplifying assumptions (which introduce error) and data requirements and computing time.

The conceptual subsurface flow model is illustrated in Fig. 12. There are three regions of interest: the root-zone, which is assumed to contain the source areas; the soil-water transmission zone, which may contain up to five layers; and the groundwater zone. In the root zone, the basic assumption is that the drainage rate between the first and second layers determines the rate of runoff from variable source areas (hence their size also). In the soil-water transmission zone, the drainage rate may be approximated by the hydraulic conductivity of the soil. In the groundwater zone, outflow is assumed to be directly proportional to the amount of groundwater present, and is partitioned between flow measured at the basin outlet as streamflow, and unmeasured seepage loss.

Source Area Runoff

Input to the source area component is assumed to be the amount of throughfall that infiltrates into the top root-zone layer, as calculated by TEHM. Thus, input depends upon soil hydraulic properties in the root zone, climate, the stage of canopy development, and antecedent moisture conditions as affected by evapotranspiration.

It is recognized that much of the variable source area response occurs at the soil surface in the field, whereas the model assumes that variable source area runoff must first pass through the top layer of the root zone. This assumption probably introduces an incorrect delay in the timing of storm runoff response. However, until more is learned about the actual behavior of variable source areas in the field, more detailed or complicated conceptual models are probably unwarranted. The conceptual model described here was chosen partially for ease of merging with PROSPER.

Drainage from source areas is assumed to enter the stream channel directly. The lower limit of source area extent represents the permanent part of source areas that are linked to the stream in the basin and will contribute subsurface drainage at all times. The response time of these permanent source areas during a storm is determined by the average thickness and hydraulic properties of the root zone layers. The hydraulic properties are determined from the information required for PROSPER simulations. Ideally, the relationship between soil-water content and

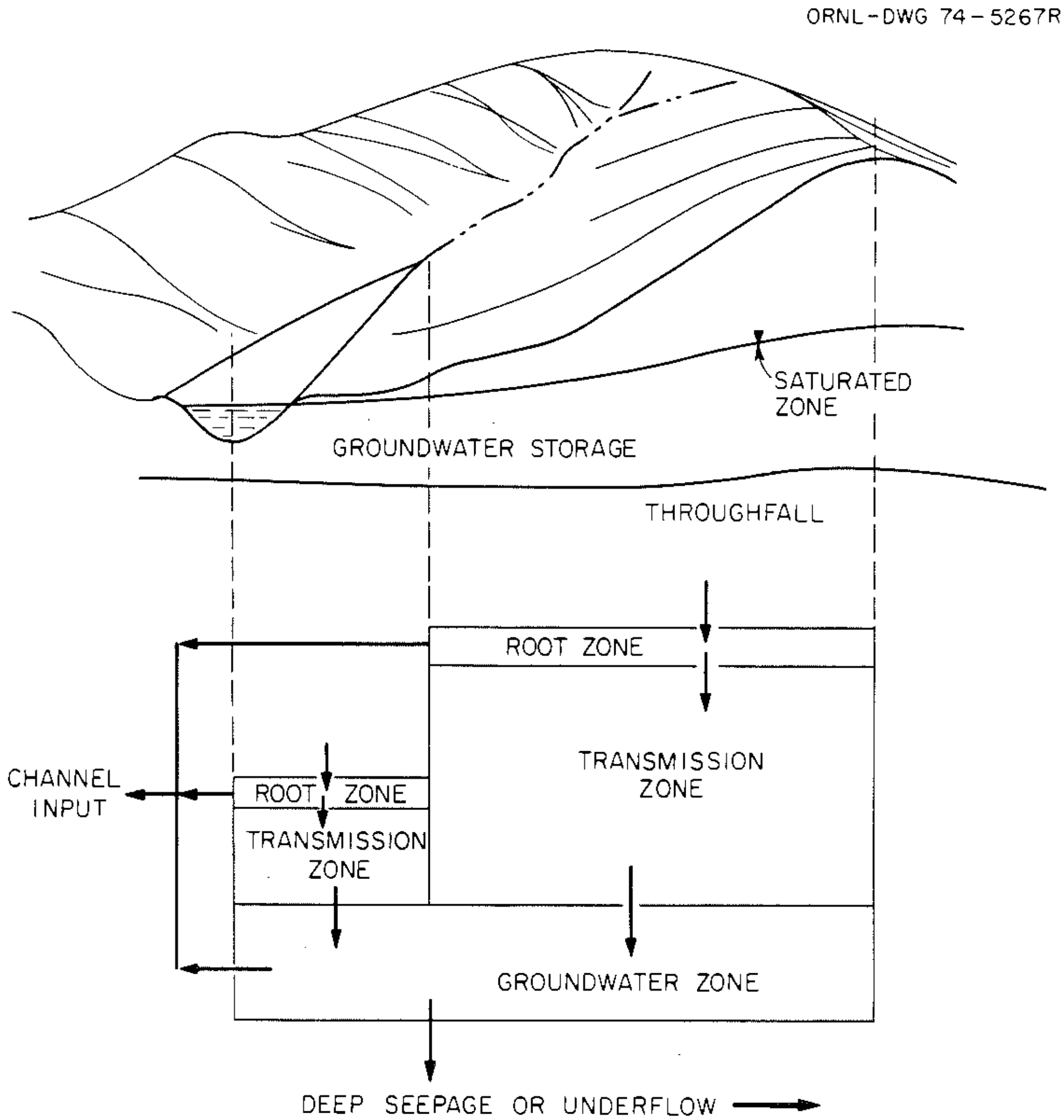

Fig. 12. Illustration of the conceptual subsurface flow model.

hydraulic conductivity will be determined directly through *in situ* soil column drainage experiments, following a method such as that of Cheng et al. (1975). Alternatively, the relationship may be approximated using the Green and Corey method, as described by Luxmoore (1973).

The variability of runoff response from variable source areas is made up of two components. First, the drainage rate of water between soil layers is assumed to be a nonlinear function of soil water content and input. As soil moisture increases, the runoff per unit source area is assumed to be directly proportional to the increase in soil water flux through the root zone. Secondly, the fraction of the basin segment that contains variable source areas has been assumed to increase as the drainage rate through the root-zone increases. Thus, the variable source areas expand as a function of root zone drainage. The form of the relationship used in the TEHM is shown in Fig. 13. When the root zone soil water flux rises above a threshold value, the fraction of source areas draining to the channel is assumed to increase linearly until a specified upper limit is reached. It is assumed that source area growth begins when the stream channel system starts to expand (e.g., when the length of flowing channel begins to increase in a first or second order basin). The drainage rate that corresponds to the discharge rate when channel expansion begins thus is assumed to mark the point where drainage from variable source areas begins to enter the channel directly. It should be noted that the variable source area contribution is independent of surface runoff caused by exceeding the infiltration capacity in the TEHM. Thus, in principal, both surface runoff and variable source area flow could be calculated.

Soil water transmission zones

The soil water transmission zones are characterized by a table or graph of the relationship between soil water content and hydraulic conductivity. The relationship must span the expected range of soil water contents found in the field. In the subsurface flow model, the relationship is approximated by

$$K(\Theta) = KS_i \, e^{a_i(\Theta-\Theta_s)} \qquad 1 \le i \le 3 \quad , \qquad (42)$$

where

$K(\Theta)$ = hydraulic conductivity at water content Θ,
KS_i = saturated conductivity parameter,
a_i = curve fitting parameter,
Θ = water content,
Θ_s = water content at saturation, and
i = number of portions of the curve necessary to approximate the (K vs Θ) relationship.

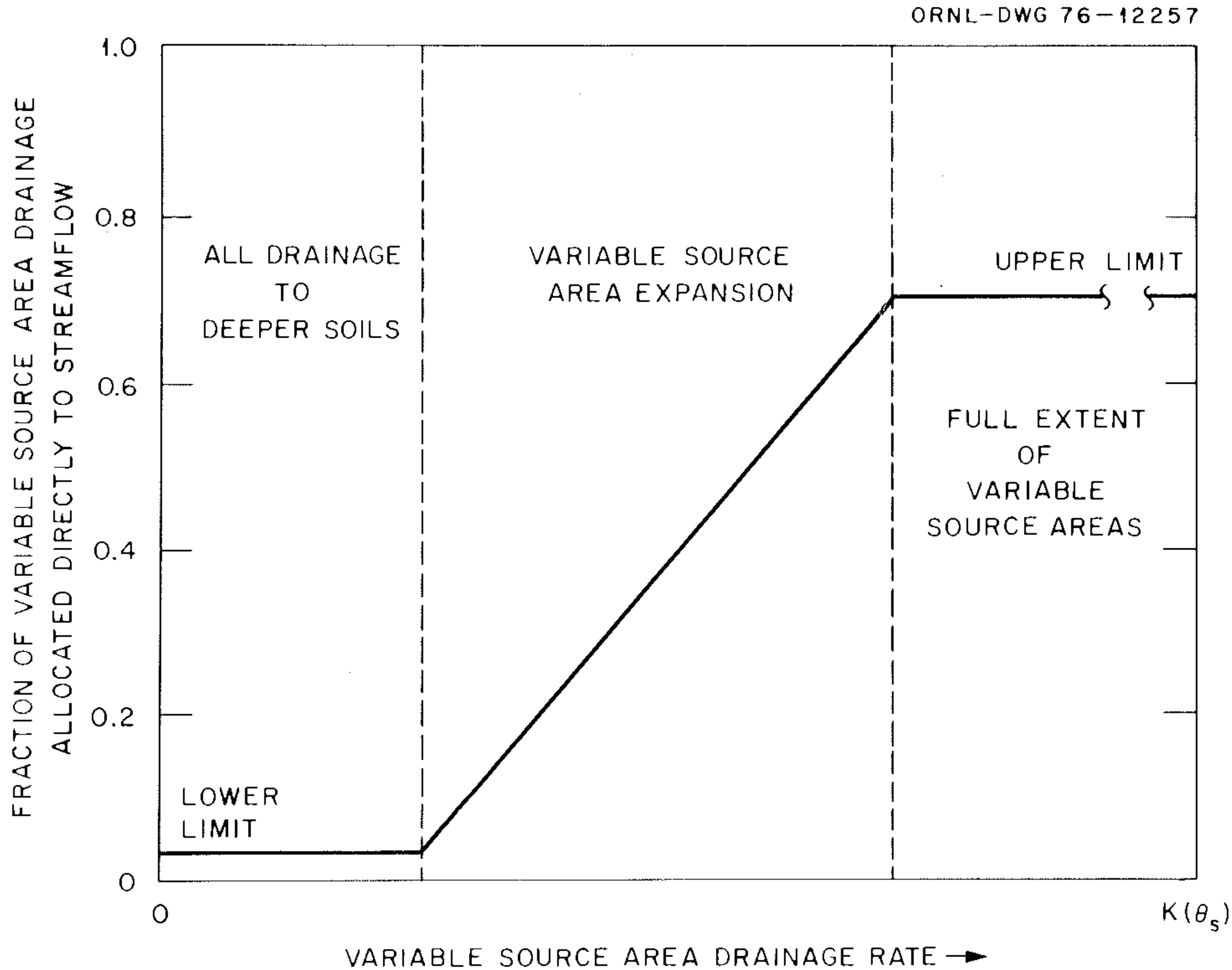

Fig. 13. Assumed relationship between average surface soils drainage rate and fraction of basin contributing to storm runoff (variable source area fraction).

Drainage is assumed to be dominated by gravitational flow, hence the drainage rate at any point in time is assumed to be numerically equal to the hydraulic conductivity, which is a nonlinear function of water content, and varies depending upon the moisture supply rate. For each transmission layer, a continuous water content variable is maintained for each component through numerical integration of the continuity equation:

$$\frac{\partial \Theta i}{\partial t} = I(t,p,\Theta_{i-1},C) - K(\Theta_i) \quad , \qquad (43)$$

where

Θ_i = water content of zone i,
t = time,
I = moisture input,
P = precipitation or throughfall,
Θ_{i-1} = water content of overlying soil,
C = climatic factors (e.g., solar radiation, temperature), and
$K(\Theta_i)$ = hydraulic conductivity of zone i, assumed equal to drainage rate.

Equation (43) is used to calculate water content, where the input term is the calculated drainage rate from the overlying layer, and drainage loss is the input for the next lower layer. The outflow from the bottom layer in the soil water transmission zone is used as input to the groundwater compartment of the model.

Groundwater storage and flow

The Darcy law for saturated flow may be represented as:

$$Q_g = K_s A \frac{\partial H}{\partial s} \quad , \qquad (44)$$

where

Q_g = groundwater flow rate through a cross-sectional area A of the aquifer,
K_s = saturated hydraulic conductivity, and
$\frac{\partial H}{\partial s}$ = the hydraulic gradient along the flow path.

We assume that the saturated conductivity remains constant and that the product of cross-sectional area and hydraulic gradient is directly proportional to the amount of groundwater in the aquifer. With those assumptions, Eq. (44) becomes:

$$Q_g = k\ S_g = -\frac{dS_g}{dt} \quad , \qquad (45)$$

where

S_g = amount of groundwater in the aquifer, and
k = constant.

From Eq. (45), it can be shown that

$$\frac{Q_g(t)}{Q_g(t_o)} = e^{-k(t-t_o)} \quad , \qquad (46)$$

where

$Qg(t)$ = groundwater flow at time t, and
e = base of natural logarithm.

When the time interval considered is one day, the ratio of flows in Eq. (46) is defined as the daily recession constant K_r, (Linsley et al., 1958):

$$K_r = \frac{Q_g(\text{day} + 1)}{Q_g(\text{day})} \quad . \qquad (47)$$

Thus the relationship between the storage constant k and the daily recession constant K_r is

$$k = \frac{-\ln K_r}{(t-t_o)} \quad , \qquad (48)$$

where

$(t - t_o)$ = a one-day (24-hr) time interval, and
K_r = the ratio of instantaneous dry weather flow rates that occur exactly one day apart.

In the WHTM (Patterson et al., 1974), the storage constant accounts for the time lag between infiltration of a pulse of water and its appearance as groundwater outflow. However, in the TEHM, the soil layers exert the major time-buffering effect, and the storage constant (k) is more appropriately related to the interflow recession constant, using Eq. (48).

When this approach is used, the groundwater storage constant (k) dominates baseflow response during and shortly after major storms. When dry weather conditions exist, groundwater outflow usually balances the unsaturated drainage input from the transmission zone. Thus the groundwater flow recession between storms is dominated by the hydraulic properties of the soil.

Total Streamflow

The total flow input to the channel system includes direct channel precipitation and impervious area runoff, runoff from permanent and variable source areas, and groundwater inflow. If groundwater is lost or gained via seepage between adjacent basins, the groundwater discharge term is multiplied by a user-determined constant. Total flow input is routed through the channel system, using a kinematic wave routing method based upon the Manning equation.

APPLICATION OF THE TERRESTRIAL ECOSYSTEM HYDROLOGY MODEL

An Overview of Basin Simulation

The methodology used for basin simulation in the TEHM is an outgrowth of that used in the Wisconsin Hydrologic Transport Model (WHTM; Patterson et al., 1974) and the earlier Stanford Watershed Model-IV (Crawford and Linsley, 1966). The documentations of those simulation model programs thus provide a comprehensive background for using the TEHM.

The general sequence in basin simulation progresses from atmosphere to landscape to the channel system. In the TEHM, each of these steps in the sequence is represented by a main program and several functions and sub-routines.

Atmosphere Module

The atmosphere module is called the PRECIP link, and has been fully described in the WHTM documentation (Patterson et al., 1974; Chapters II and III, pp. 21-46). It deals primarily with data for precipitation and wetfall deposition of dissolved and particulate materials. The function of the PRECIP link is to organize hourly precipitation and deposition data into labeled files that are accessible by the landscape link. It also establishes a master inventory file of data sets that have been created during model execution. The file is updated each time information is added prior to basin simulation, and the master file is also checked before basin simulation begins to ensure that the necessary data are on file. The PRECIP link (together with the main program) is always the first program component to be run when a basin is simulated. Because it has been fully documented in the WHTM User's Manual it is not discussed further here. However, abridged descriptions of input formats and data requirements have been included here for the convenience of the user.

Landscape Module

The major differences between the TEHM and the WHTM lie within the component that simulates the landscape hydrology of a basin. A comprehensive discussion of the theoretical basis of the processes contained in the landscape model was presented earlier. Here, we parallel that discussion with a step-by-step description of the development of the data set required for simulating runoff to the channel system. As a vehicle for explaining the data set development, we have used Walker Branch Watershed near Oak Ridge, Tennessee, as the example basin.

Walker Branch Watershed Case Study

Basin Description

Walker Branch Watershed is a 97.5-ha drainage area that comprises a 38.4-ha west fork and a 59.1-ha east fork, each with a weir and continuous stage height recorder at the drainage outlet (Fig. 14). The basin is located in the Ridge and Valley province of east Tennessee at 84°17' west longitude and 35°58' north latitude. The basin overstory is predominantly oak-hickory, although pine, yellow poplar, and chestnut oak are also present. The mean basal area of vegetation in the basin is 20.8 m^2 ha^{-1} (Grigal and Goldstein, 1971). Elevation ranges between 250 m and 345 m above mean sea level. Soils are predominantly of the Fullerton or Bodine series, are well-drained, and have high chert content and a high infiltration capacity. Data from Peters et al. (1970) show that the average slope is quite steep in the basin; Table 2 indicates that nearly half the basin contains slopes in excess of 30%, and the weighted-average slope is in excess of 23% for the whole basin.

Data Set Preparation

Preparation of a comprehensive data set for simulation with the TEHM requires four major sets of parameters and data:

(1) Precipitation and deposition data and parameters,
(2) Climatic data,
(3) Parameters to characterize soils and vegetation, and
(4) Parameters to characterize stream channels.

Table 2. Summary of land slope distributions within Walker Branch Watershed

Slope Summary:

Slope class (%)	Percent of area West Fork	Percent of area East Fork	Combined total
2-5	0.6	1.5	1.1
5-12	10.8	10.6	10.7
12-20	28.7	19.8	23.3
20-30	17.6	14.2	15.6
> 30	42.3	53.9	49.3
Average percent slope	23%	24%	23%

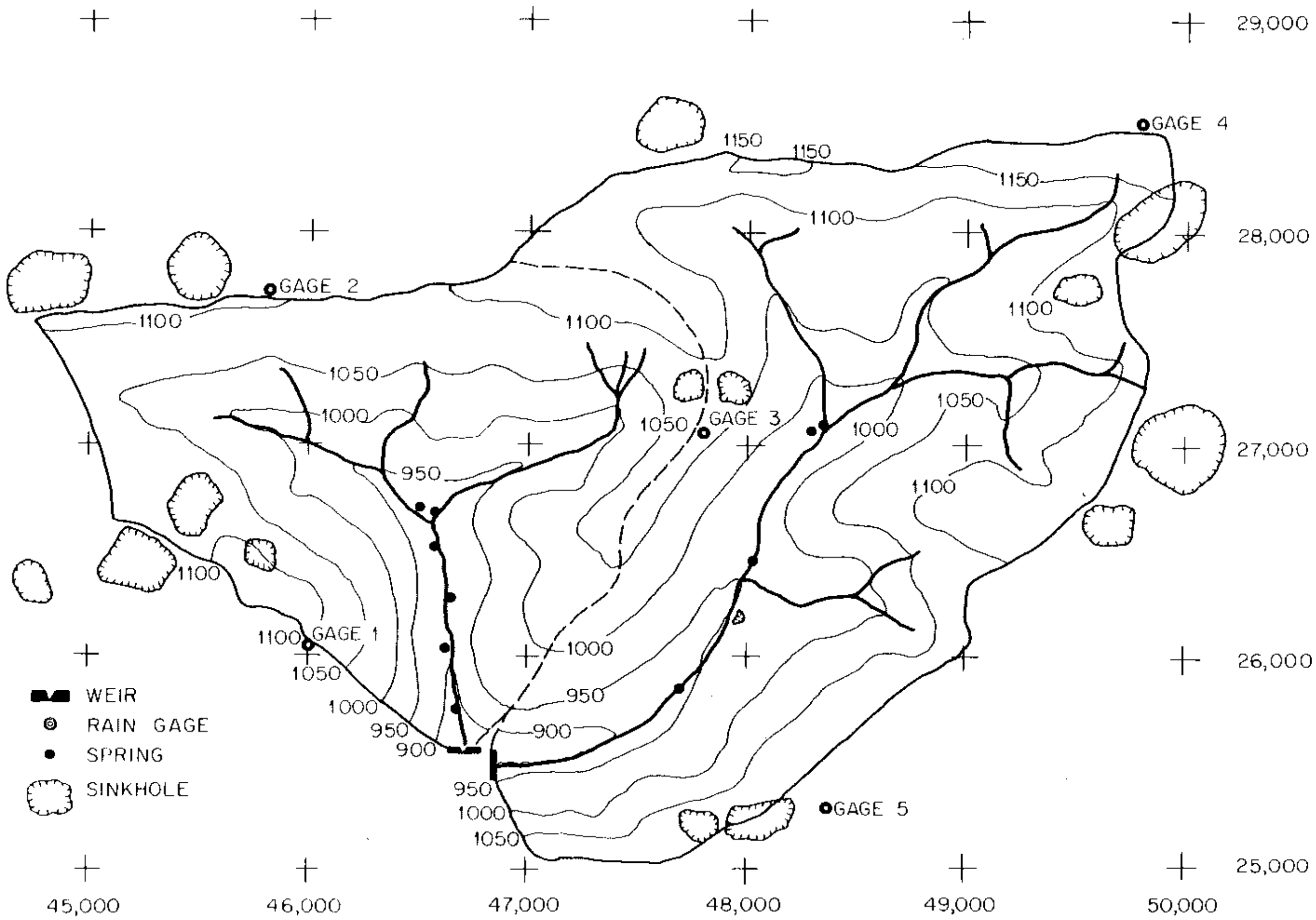

Fig. 14. Topographic map of Walker Branch Watershed, showing locations of hydrologic data collection devices.

Each major input component is described in detail in the remainder of this chapter, together with a summary listing of the required parameters and variables and an example of each that is applicable to Walker Branch Watershed. Copies of the data are available on punched cards at Oak Ridge National Laboratory.

Precipitation and Deposition Data and Parameters

The first step in basin simulation is to read and store precipitation and wetfall data for subsequent use, and to establish data inventory files, which are used and updated by other components of the TEHM. The input data include information on the location, Weather Bureau identification code, and type of each precipitation gauge that will be used in the simulation, as well as hourly or daily precipitation totals. The TEHM uses hourly precipitation data for simulations, and contains software to allow for the distribution of daily precipitation totals into hourly values. Time distribution is based on corresponding data from the recording raingage selected as most representative of the site in question. Detailed descriptions of all the options and associated data input variables and formats are included in the WHTM documentation (Patterson et al., 1974). For convenience, Chapter III contains documentation for routine application. The required input data and parameters for the precipitation and wetfall data management component are summarized in Table 3.

Climatic data

Climatic data that are used to simulate hydrologic behavior of Walker Branch Watershed have been obtained from the Oak Ridge, Tennessee, Weather Service Office of the National Oceanic and Atmospheric Administration. The data have all been compiled from hourly observations. The data that are required are daily maximum and minimum air temperature, average daily dew point temperature, average daily wind speed, and total daily solar radiation. The use of all of these variables in the TEHM has been discussed earlier, and in general, data may be used in the form reported by NOAA. Table 4 shows a description of the variables required to characterize the climate of a watershed segment to be simulated.

Proper use of observed wind speed data depends on the specification of its relationship to wind speed in the forest canopy. Wind speed in the canopy can be estimated using the methods outlined in the discussion of climatic variables. Based upon published data (NOAA, 1972), the average measured monthly wind speed at Oak Ridge is 180 cm sec^{-1} at an anemometer that is 30.5 m above ground level. For a canopy that is 2000 cm high, the estimated surface roughness length is 33.3 cm, and the zero plane displacement level is approximately 22.2 cm. Thus the average wind speed at the top of the canopy is estimated from (5) as

Table 3. Summary of required precipitation and wetfall data and variables

Data or variable[a]	Description
SPACES	Maximum number of raingages to be used to represent the watershed
YRS	Number of water years of data expected for the run
INNAME	Watershed name
WB	Weather Bureau precipitation station number (each gage)
NAME	Name of each raingage station
ELEV	Elevation of each raingage, feet above m.s.l.
LAT	Latitude (degrees, minutes, seconds) for each raingage
LONG	Longitude (degrees, minutes, seconds) for each raingage
GTYPE	Type of raingage at a site (recording or storage)
FRP	Values of hourly or daily precipitation totals

[a] This list comprises the minimum set of information that must be available to assemble and store precipitation data for a hydrologic simulation run. Deposition data are not required for the current TEHM model unless transport calculations are to be made.

Table 4. Variables needed to characterize a watershed segment climate

- Average atmospheric pressure (bars)
- Daily maximum and minimum air temperature (°F), and the time(s) that readings are taken
- Average daily dew point temperature (°F)
- Average daily wind speed (mph), and a description of the exposure of the anemometer (height, surrounding obstructions, etc.)
- Total daily solar radiation, the latitude and longitude of the observation station, the average slope of each watershed segment, the azimuth of each segment slope (degrees from North), and the latitude and longitude of each basin segment

$$U_i = (180) \ln [(2000-22.2)/33.3 \;/\; \ln (3048-22.2)/33.3]$$

$$= 165 \text{ cm sec}^{-1}$$

The average wind speed in the canopy is estimated from (7) as

$$\bar{U} = \frac{(165)\ (1-e^{-1.56})}{(.0013)\ (1200)} = 85 \text{ cm sec}^{-1}$$

for growing season conditions and 115 cm sec^{-1} for dormant season conditions. Thus the average canopy wind speed for all conditions is about 100 cm sec^{-1}. The drag coefficient for growing season conditions is 0.47, and for dormant season conditions it is 0.64.

Parameters that Characterize Soils

The underlying assumption of the TEHM is that a basin segment may be represented by an average soil and vegetation column for purposes of hydrologic simulation. Thus, to characterize the soils of a segment, it is necessary to specify the dimensions and properties of an average soil column. A summary of the required input is shown in Table 5 below:

Table 5
A summary of soils properties that are required for simulation

- The average thickness of the soil column, including thickness estimates for different soil horizons
- Relationships between soil water pressure, moisture content, and hydraulic conductivity for each layer identified
- A cumulative infiltration capacity curve

The logical place to begin is with the vertical profile. For Walker Branch, this poses a problem, because the thickness of the weathered mantle is highly variable. In fact, it apparently ranges from zero to more than 30 m and probably averages about 4.5 to 5.0 m (Henderson, pers. comm., 1976). For our studies, we have estimated that the representative soil depth is approximately 5 m. Probably the most important part of the soil profile for water relations contains the rooting zone and soil immediately below it. Fortunately, this is the portion of the soil profile most easily studied. For Walker Branch, Peters et al. (1970) have compiled extensive data on the physical properties of the soils found there. They have found that Fullerton and Bodine soils (Ultisols) together cover between 90 and 96% of the total basin area. Thus for our studies, we consider only these two soil types. Table 6 shows that on the average, the A-horizon is 40 cm

Table 6. Average thickness of upper soil horizons at Walker Branch Watershed (after peters *et al.*, 1970)

Horizon	Thickness (cm) Pit 1	Pit 3	Pit 4	Pit 8	Pit 10	Average
Fullerton cherty silt loam						
A	46 cm	48 cm	43 cm	36 cm	23 cm	39 ± 10 cm
B	>61 cm	>58 cm	>48 cm	>66 cm	>84 cm	>50 cm[a]
Bodine cherty silt loam						
A	51 cm	61 cm	46 cm	43 cm	48 cm	50 ± 7 cm
B	>41 cm	>43 cm	>61 cm	>64 cm	>56 cm	>43 cm[a]

[a] At the 0.67 confidence level.

thick and the B-horizon is >50 cm thick for Fullerton soils. For Bodine soils, the A-horizon is 50 cm thick and the B-horizon is >~45 cm thick on the average. For simulation purposes, we therefore assume that the average soil column has a vertical structure as shown below:

Soil	Soil Type: Fullerton	Soil Type: Bodine	
A-horizon	40 cm	50 cm	Rooting zone
B-horizon	50 cm	50 cm	layers
B-horizon	60 cm	50 cm	Mineral soil below the rooting zone
B-horizon	180 cm	180	Soil water transmission
B-horizon	180 cm	180	zone
	>510 cm	>510 cm	Saturated zone

The properties that are required to specify hydrologic behavior of soils include the porosity of the soil layers and a relationship between water content and soil water pressure for the different soil types present, in addition to a measured hydraulic conductivity value at a known water content. For Walker Branch soils, the pertinent data have been drawn from the report by Peters et al. (1970) and are summarized in Table 7.

In addition to specifying data that characterize the physical (hydraulic) properties of soils, a cumulative infiltration capacity curve is required. There are many suitable methods available for determining the cumulative infiltration capacity, including ring or sprinkling infiltrometer tests, or even theoretical calculations based upon the known physical properties of the soil. For Walker Branch, where the soils are very well drained, infiltration rates are seldom limiting, so we could have chosen to approximate the cumulative infiltration relationship as a simple linear function with a slope equal to the saturated hydraulic conductivity of the A-horizon soils. This would have the effect of assuming that all throughfall will infiltrate into the root zone. However, a finite-element Galerkin model for saturated-unsaturated porous media flow (Reeves and Duguid, 1975) has been used to simulate the cumulative infiltration capacity for Walker Branch soils. Table 8 represents the outcome of that simulation for Fullerton cherty silt loam. The initial soil moisture conditions were typical of those occurring during the month of April in any year.

Once it has entered into the root-zone, flow is governed by Darcy Law calculations and it is possible that the moisture supply will exceed the capacity of the root zone and deeper soils to accept it. In that case, the excess input is labeled as lateral flow and conveyed to the

Table 7. Measured properties that specify hydrologic behavior of soils on Walker Branch Watershed

Soil category	Property	Fullerton	Bodine
A-horizon	Sat'd conductivity	1440 cm/day	1440 cm/day
B-horizon	Sat'd conductivity	720 cm/day	1440 cm/day

	Water content (θ)			
	Fullerton		Bodine	
Soil water suction (cm)	A-horizon (cm^3/cm^3)	B-horizon (cm^3/cm^3)	A-horizon (cm^3/cm^3)	B-horizon (cm^3/cm^3)
15000	0.159	0.221	0.179	0.176
5000	0.182	0.238	0.187	0.184
1000	0.202	0.253	0.205	0.194
667	0.216	0.262	0.216	0.199
333	0.238	0.271	0.242	0.209
100[a]	0.267	0.308	0.279	0.228
25	0.305	0.334	0.329	0.257
5	0.334	0.358	0.364	0.284
0[b]	0.341	0.364	0.373	0.291

[a] Water content at 100 cm (H_2O) suction is assumed to equal field capacity.

[b] Water content at 0 pressure is assumed equal to layer porosity.

Table 8. Simulated cumulative infiltration capacity — Walker Branch Watershed

Total infiltration (cm)	Elapsed time (min)	Total infiltration (cm)	Elapsed time (min)	Total infiltration (cm)	Elapsed time (min)
0	0	0.25	0.15	0.50	0.83
0.75	1.75	1.00	2.74	2.00	6.83
4.00[a]	15.00	6.00	23.29	8.00	31.57
10.00	39.86	12.00	48.15	14.00	56.44
16.00	64.72	18.00	73.01	20.00	81.30
22.00	89.59	24.00	97.87	26.00	106.20
28.00	114.40	30.00	122.70	60.00	247.00

[a] Values after 12 min are all extrapolated at constant rate.

stream channel system. Thus there is redundancy in the infiltration calculations, and in the absence of infiltration data it is acceptable to approximate the infiltration capacity as a constant, high rate and allow subsequent calculations to deal with excess inputs to the soil.

Characterization of the soil water transmission zone requires knowledge of the relationship between water content and hydraulic conductivity. For our purposes, we use the relationship for drying soils, and neglect the hysteretic effects associated with wetting and drying cycles in the soil. The relationship is specified by fitting data to the expression

$$K(\theta) = Ae^{-B(\theta_s - \theta)},$$

where

$K(\theta)$ = the hydraulic conductivity at volumetric water content level θ (cm day^{-1}),
θ_s = the water content at saturation (cm^3 cm^{-3}), and
A and B = empirical constants.

For Walker Branch soils, Figs. 15 and 16 show plots of estimated θ versus $K(\theta)$ values, together with curves that have been fitted to the data. The values of the empirical constants for the various limbs of the curves are presented in Table 9.

Initial conditions of soil moisture are usually assumed to equal field capacity, which is operationally defined to be soil moisture at a desorption pressure of -100 cm (-.1 bar). These values generally do not represent an accurate assessment of soil moisture, so a preliminary simulation period of at least three months duration is used to obtain more representative values. The field capacity estimates for Walker Branch soils were noted in Table 7, together with assumed soil porosity (or θ_s).

Storm Runoff Parameters and Variables

The parameters that are associated with storm runoff to the stream channel in the TEHM are related to either overland flow or runoff from variable source areas. Overland flow parameters include the average length, slope, and hydraulic roughness of overland flow planes, and the fraction of basin area that is impervious and hydraulically connected to a channel that carries concentrated flow. The average length may be estimated as the quotient of the basin area and twice the total length of channels that convey concentrated flow during storms. Generally, the value ranges between 15 and 120 m. For Walker Branch, the value is estimated as 25 m on the basis of field observation. The average slope for Walker Branch is approximately 24% (or 0.24 m m^{-1}). The roughness

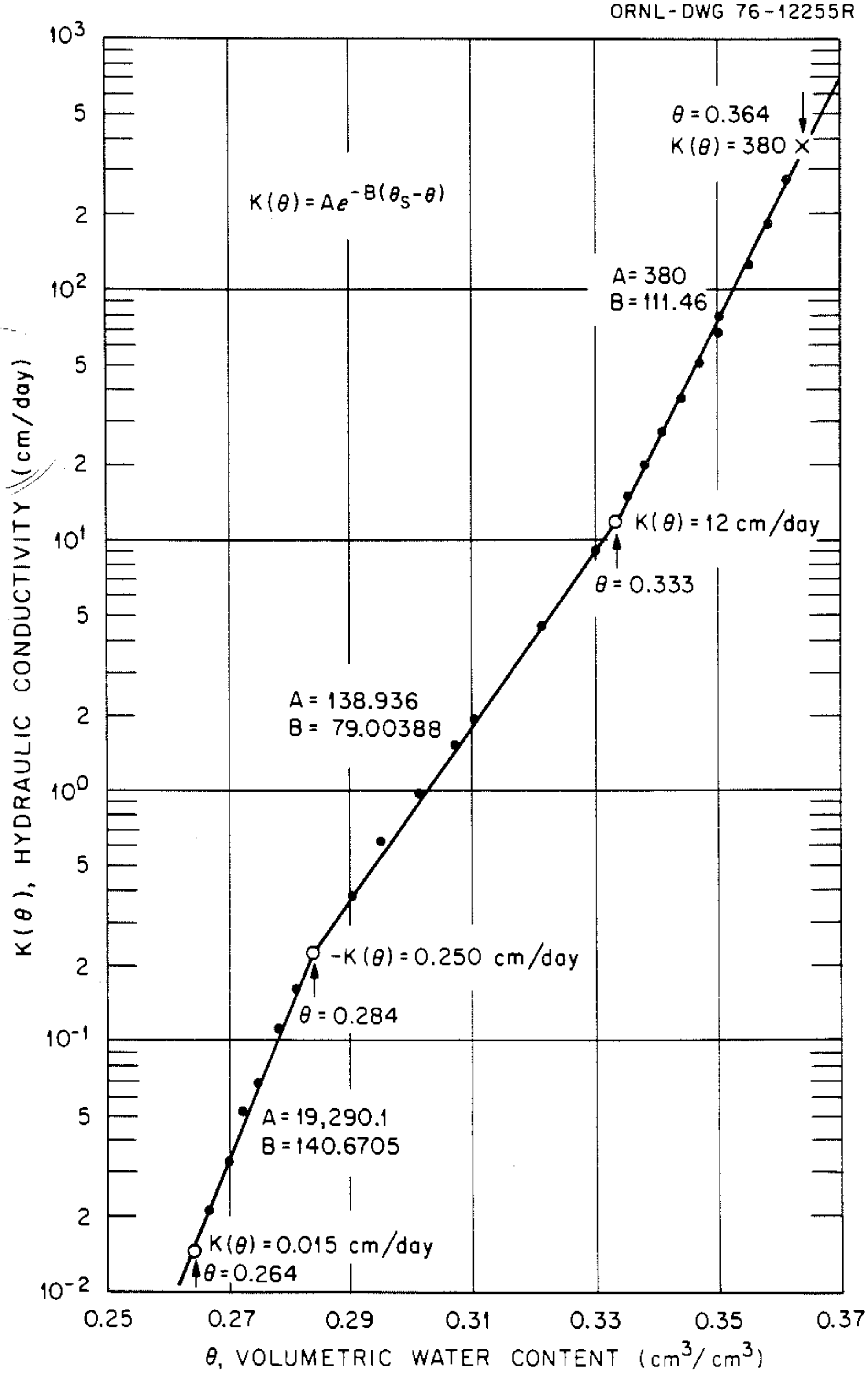

Fig. 15. Soil hydraulic properties for Fullerton average B 22t soils at Walker Branch Watershed.

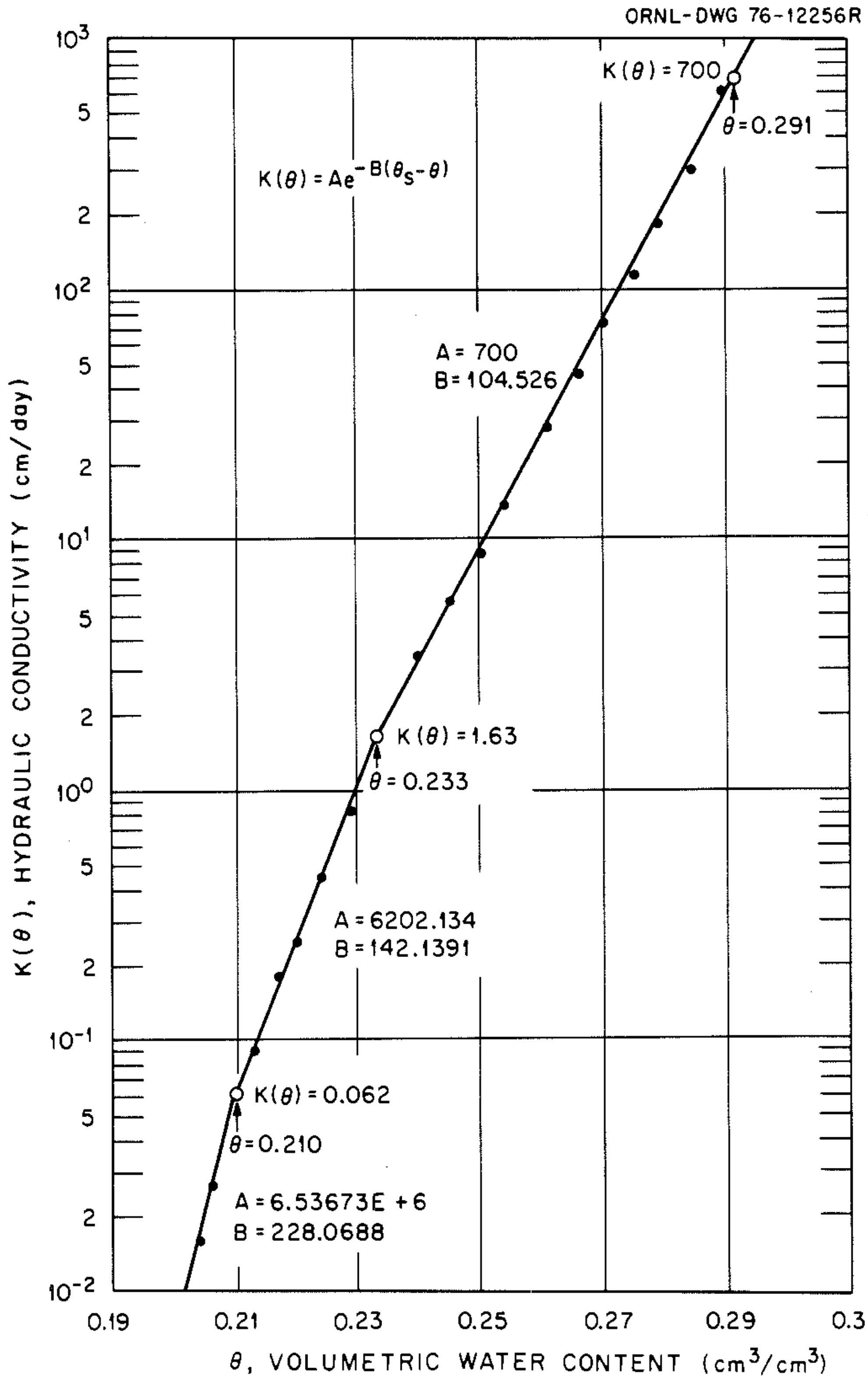

Fig. 16. Soil hydraulic properties for Bodine average B2t soils at Walker Branch Watershed.

Table 9. The empirical constants that characterize the water content versus hydraulic conductivity curve for Walker Branch Watershed

Soil type	Water content range (cm^3/cm^3)	A (cm/day)	B	Saturation water Content (θ_s)
Average	0 < 0.284	19,290.1	140.6705	0.364
Fullerton B22t	$0.284 \leq \theta$ 0.333	138.936	79.0039	0.364
	$0.333 < \theta \leq 0.364$	380.00	111.460	0.364
Average	$\theta < 0.210$	6,536,730	228.06875	0.291
Bodine B2t	$0.210 \leq \theta < 0.233$	6202.134	142.1391	0.291
	$0.233 \leq \theta \leq 0.291$	700.00	104.52587	0.291

coefficient has been estimated based upon the recommendations of Crawford and Linsley (1966) for relating watershed cover and Manning's n (roughness coefficient). Those values are reproduced in Table 10. For Walker Branch, the roughness coefficient for overland flow was estimated to be 0.40. The fraction of the basin that is impervious includes the stream channel and any rock outcrops or paved areas connected to a channel. For Walker Branch, this area is estimated to comprise about 1% of the total basin.

The parameters that characterize variable source areas are the lower and upper limits of their areal extent and the soil moisture conditions associated with those limits. The upper limit of areal extent for variable source areas may be estimated from the peak rainfall and associated runoff rates for major storms. For Walker Branch the maximum observed ratio of rainfall rate to runoff rate at peak flow is $\sim$0.7, which is assumed to represent the upper limit of source areas. We assume the lower limit is 0.01, and represents the portion of the basin covered by dry weather seeps and marshy areas. The moisture conditions associated with the initiation of source area growth have been assumed to be related to runoff or streamflow rate. Much of the channel system in Walker Branch experiences intermittent flow. Thus we assume that source areas will begin to grow at the same time that the length of flowing channel increases. For Walker Branch this usually corresponds to a soil drainage rate of about 1.5 cm day^{-1} or a soil moisture that corresponds to field capacity. The peak extent of source areas (corresponding to peak flow rates) occurs at a drainage rate of about 10 to 12 cm day^{-1} which occurs at a soil moisture that is approximately half-way between field capacity and saturation at Walker Branch.

Groundwater Flow Parameters and Variables

Groundwater flow is represented as outflow from a single storage compartment at a rate that is directly proportional to the amount of water present. Thus it is necessary to specify both a rate constant for outflow and an initial storage value for groundwater. Based upon the earlier discussion of subsurface flow calculations, a classical hydrograph separation method was used to find a value for the interflow recession coefficient. The method is illustrated in Figs. 17 to 19. The average value for the interflow recession coefficient determined graphically is 0.03 ± 0.01 hr^{-1}, which corresponds to a daily recession coefficient of about 0.5. The implication is that base flow will usually be approximately equal to soil water drainage after about 3 to 5 days for Walker Branch Watershed. Observed hydrographs appear to match this expected behavior well.

Once the groundwater storage constant has been determined, the initial value for groundwater storage may be found directly by dividing the initial baseflow rate by the storage constant. For the 1974 water year simulation, the initial baseflow rate was 0.21 cfs (or 0.0036

Table 10. Relation between watershed cover and Manning's n (roughness coefficient)

Type of cover	Manning's n (roughness coefficient)
Smooth asphalt	0.012
Asphalt or concrete paving	0.014
Packed clay	0.03
Light turf	0.20
Dense turf	0.35
Dense shrubs and forest litter	0.40

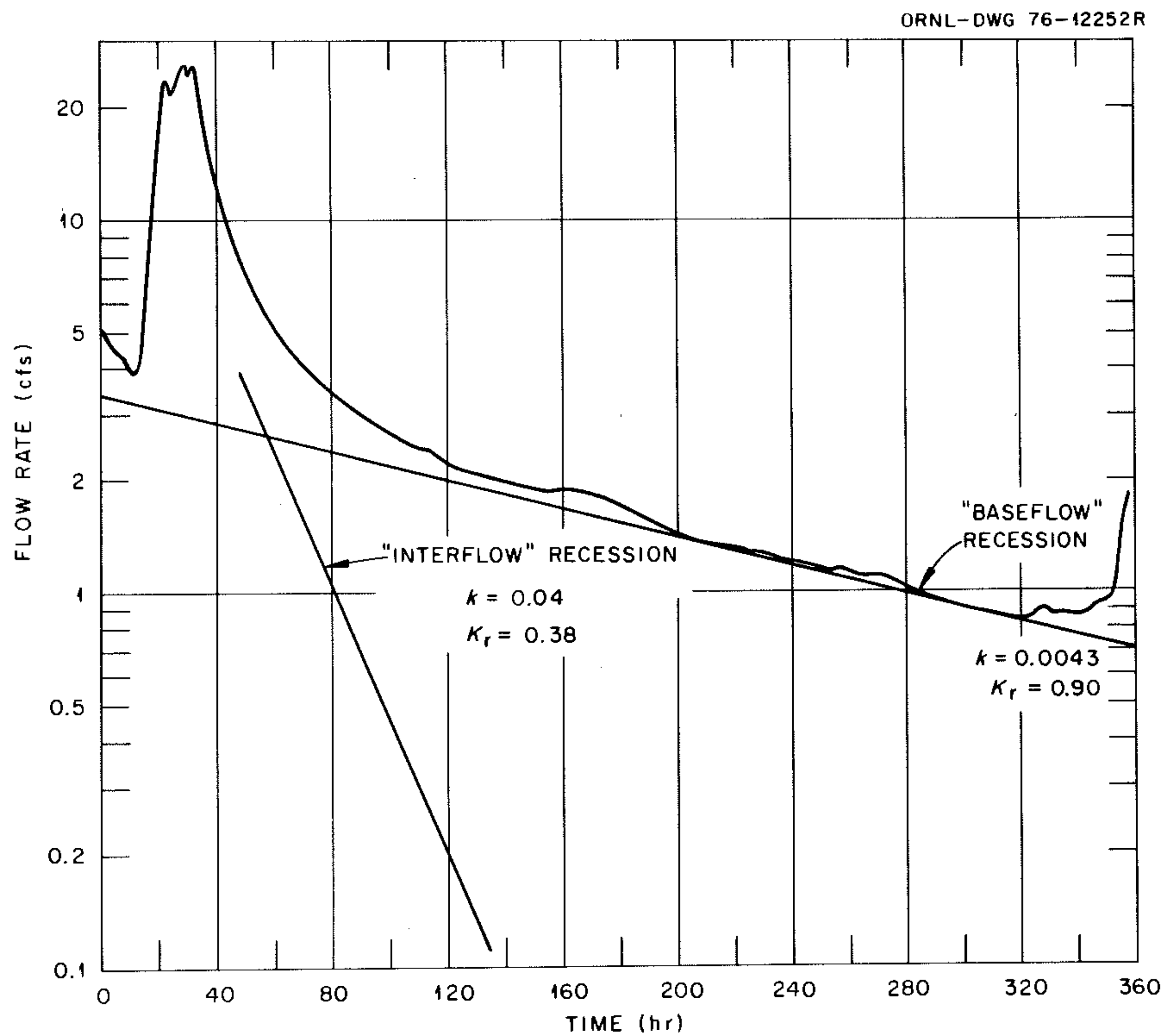

Fig. 17. Hydrograph analysis for period January 10-24, 1974 at Walker Branch Watershed.

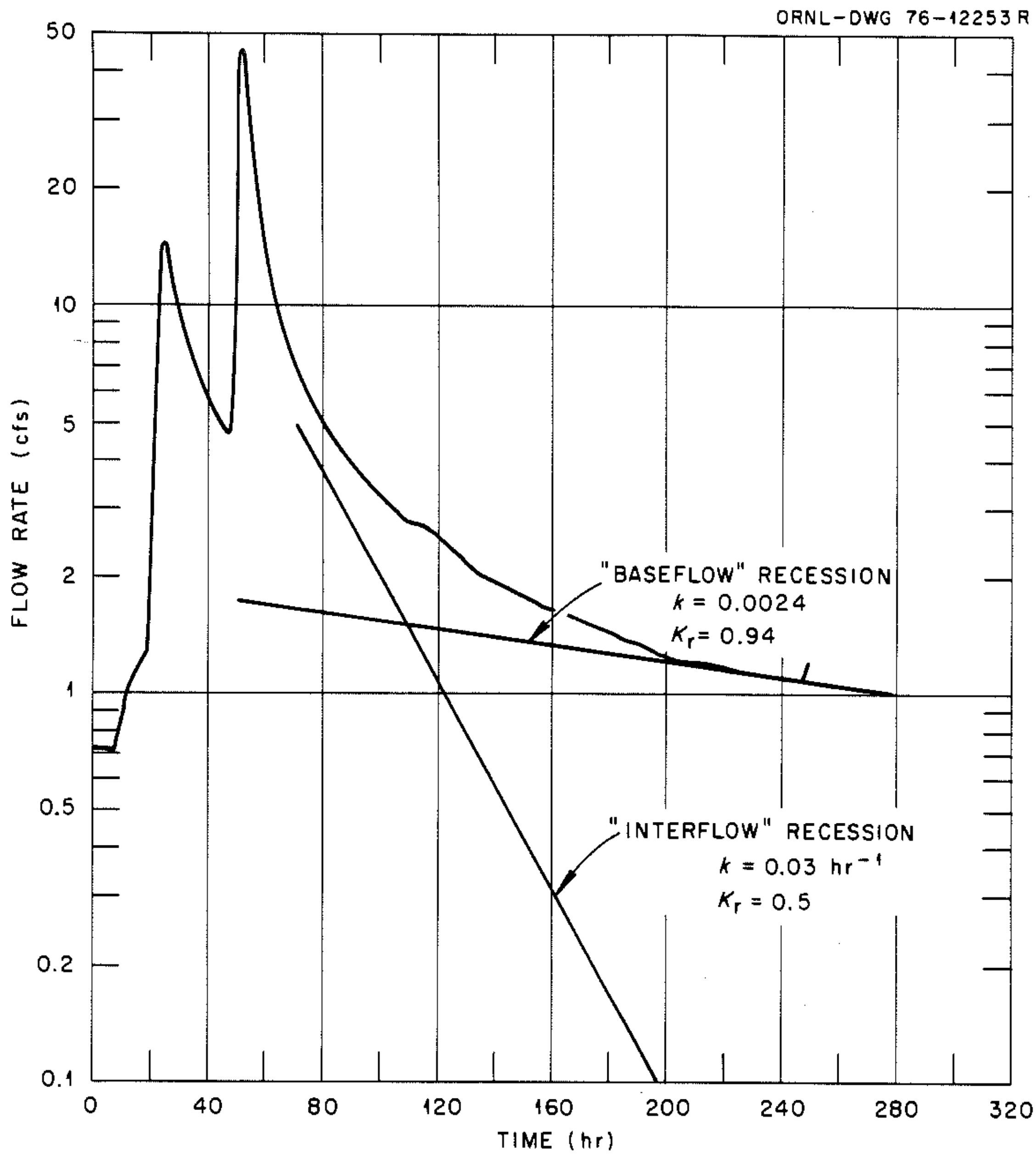

Fig. 18. Hydrograph analysis for period March 19-28, 1974 at Walker Branch Watershed.

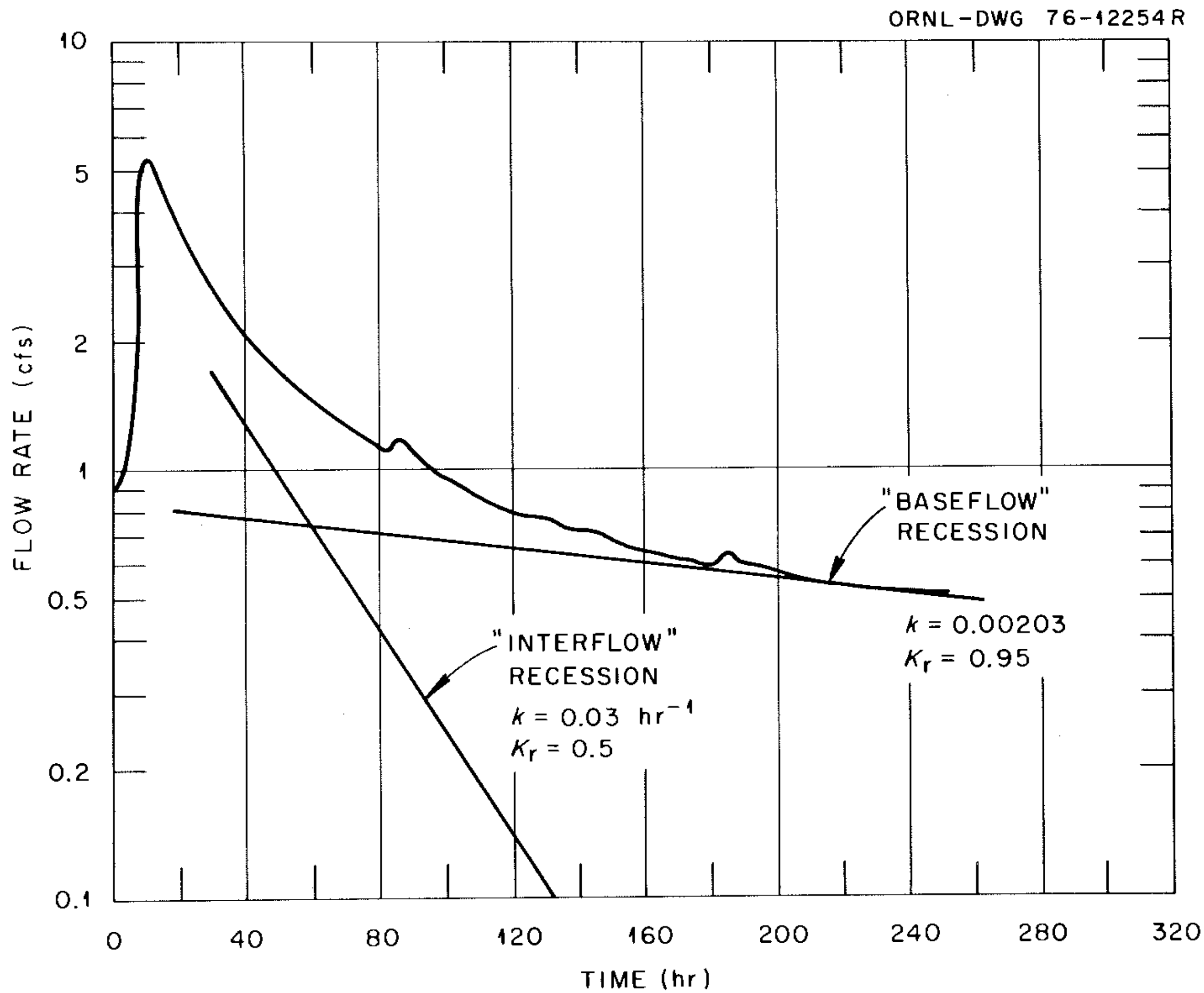

Fig. 19. Hydrograph analysis for period May 12-22, 1974 at Walker Branch Watershed.

cm hr^{-1}), which corresponds to an initial groundwater storage value of 0.12 cm.

Groundwater flow across watershed divides has been hypothesized for the East and West Forks of Walker Branch Watershed. Henderson et al. (1971), state that both topography and geologic structure are favorable for water movement from the East Fork to the West Fork basins. When the baseflow component of runoff is separated using the method described by Huff and Begovich (1976), the groundwater flow per unit area from the East Fork averages 30% lower than the value for the combined East and West Fork areas. On the West Fork, the groundwater flow per unit area is about 46% higher than the combined total. When one normalizes the apparent loss from the East Fork (i.e., computes the volume of flow loss) and compares it to the volume "gained" by the West Fork, the average annual groundwater loss from the East (1972-1974) is within 4% of the average annual groundwater gain to the West.

From preceding discussion, we estimate that the average fraction of groundwater loss across basin divides is +0.30 for the East Fork, and -0.46 for the West Fork. (The effect of a negative loss fraction in the TEHM is to yield a net groundwater input.)

Parameters and Variables that Characterize Vegetation

The parameters and variables that characterize watershed vegetation in the TEHM are associated either with the vegetation and associated canopy or the root-zone. The vegetation and related canopy properties that must be determined or estimated are the type of dominant vegetation (e.g., deciduous, coniferous, grassed), the resistance to water flow in vegetation, and the temporal distribution of albedo, leaf area index, and interception storage capacity. The root-zone properties that must be specified include measures of root density and cross-sectional area (spatial distributions) and soil water contents at the vegetation wilting point.

Walker Branch vegetation has been characterized as oak-hickory forest (deciduous). The average leaf length, which is related to boundary layer resistance (see Monteith, 1965 or Kreith, 1965), has been estimated as 10 cm from direct observation. The seasonal pattern of leaf area index (LAI) development for yellow poplar in the Oak Ridge area is shown in Fig. 20 (Burgess and O'Neill, 1975).

For simulation purposes, we have assumed that the temporal pattern and the magnitudes shown in the figure are representative of the mesic hardwoods on Walker Branch Watershed. From the data given in the figure, we estimate the following model input values:

Table 11. A summary of runoff parameters needed for simulation

Storm flow

- Hydraulic properties of an average overland flow plane length, slope, roughness, and impervious fraction
- Upper and lower area limits for variable source area together with associated drainage rates

Groundwater

- Rate constant that relates groundwater flow to basin storage (recession constant)
- Initial value estimate for groundwater storage
- Fraction of groundwater flow that is lost or gained across basin divides

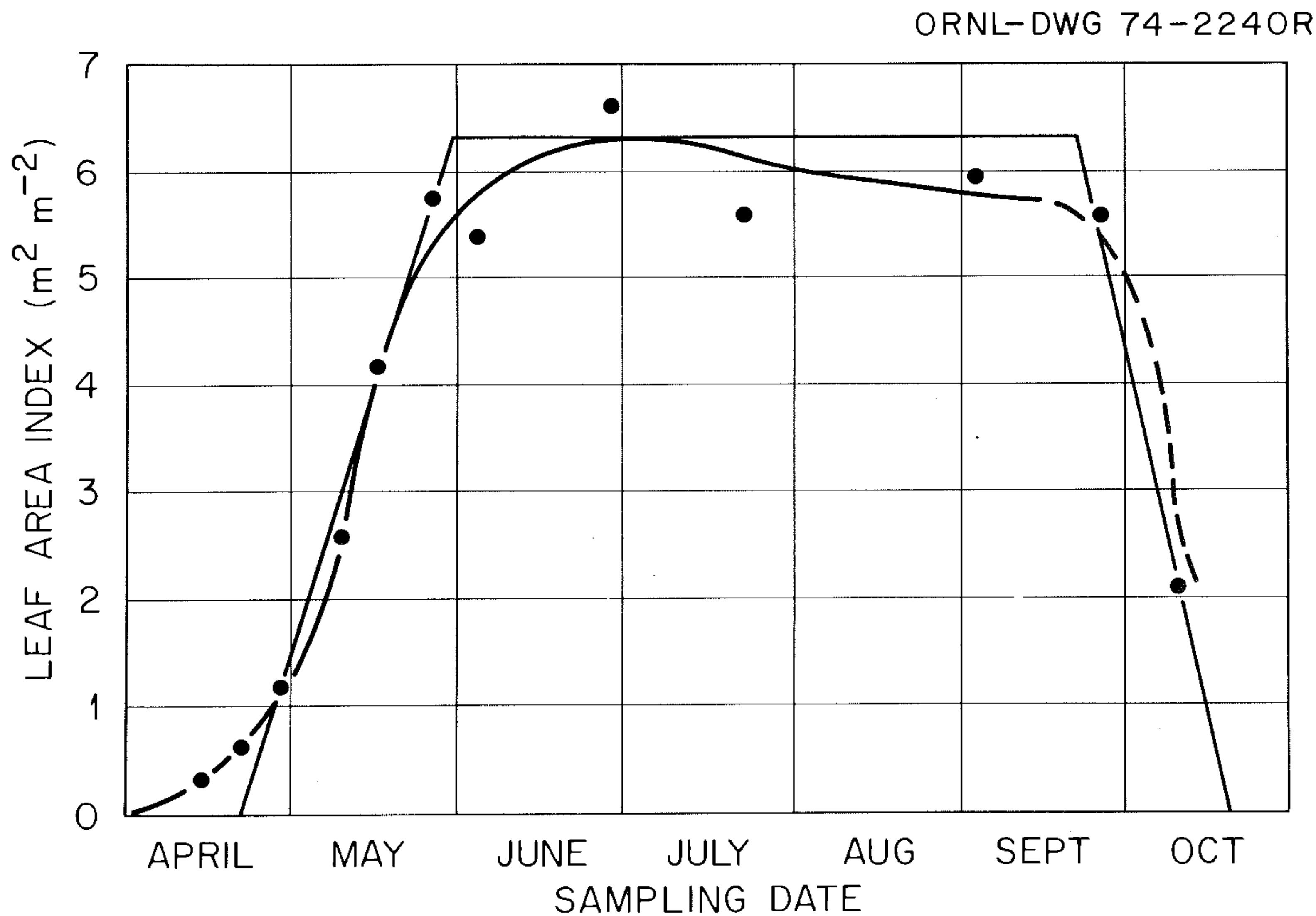

Fig. 20. The seasonal pattern of leaf area index development for yellow poplar at Oak Ridge, Tennessee.

Event	Julian day of year	Leaf area index
Leaf-out start	110	0.001
Full canopy	151	6.3
Leaf-fall start	262	6.3
Leaf-fall end	290	0.001

The albedo of the dominant oak-hickory canopy may be estimated from information presented by Swift et al., 1975. Their work gives estimates of 0.22 and 0.16 for summer and winter albedo respectively. We assume that albedo increases linearly from the winter to summer value during the period from leaf-out to full canopy development, and decreases linearly from the summer to the winter value during the period of leaf-fall.

The wilting point of the vegetation is assumed to occur when the soil water potential reaches -15 bars. Thus, the soil moisture content at the wilting point may be taken from the soil moisture versus soil water potential relationships estimated by the Green and Corey method (Luxmoore, 1973). A soil moisture value of 0.001 may be used if one wishes to assume that some transpiration will occur beyond the wilting point. For our application we chose water content values to correspond to a soil water potential of -15 bars for each soil layer in the root zone.

The interception storage capacity parameters used by the TEHM are the maximum and minimum values, and the temporal change of leaf-area index. The amount of rainfall that is intercepted is assumed to be a function of the total area index, which includes leaf area, branch and stem area, and bole area, and is also related to the condition of litter on the forest floor. Through experience, we have found that the values for interception storage in mixed hardwoods may be approximated as

$$S_i = 0.009 \times [LAI + 8] \quad , \qquad (43)$$

where S_i = interception storage (cm/cm^2), and

LAI = leaf area index (m^2/m^2).

Thus for Walker Branch Watershed, the estimated maximum and minimum interception storage parameters are 0.129 cm cm^{-2} and 0.072 cm cm^{-2} respectively. We assume that these values follow the same temporal pattern as the leaf area index function. Refined estimates of the interception storage parameters can be obtained either by calibration using throughfall observations from field study, or by comparisons with regression equations such as those presented by Helvey and Patric (1965). It should be noted that the estimated interception storage parameters given by Eq. (43) (above) are explicitly for the TEHM, which operates on hourly estimated time increments. The daily version of PROSPER requires approximately a two-fold increase in the values before comparable results are obtained.

Root Variables and Parameters

The average annual depth distribution of lateral roots less than 5 mm in diameter for *Liriodendron* forest is shown in Fig. 21 (Harris et al., 1973). The data represented by Fig. 21 suggest that about 90% of the root biomass is contained in the top 45 cm of soil, and that the remaining 10% is contained in the 45- to 90-cm layer. These findings agree well with those of Kochenderfer (1973) and Striffler (1957).

The cross-sectional area of roots per unit area of soil for forested areas has been derived from experimental data gathered at Walker Branch Watershed. The following results summarize the calculations that were made to estimate the average root cross-sectional area for an Oak-Hickory stand.

We assume all roots are the same length, thus the volume and weight are directly proportional to the cross-sectional area. The relative number of roots in a size class is estimated as the ratio of the fraction of weight in the size class (observed) to the estimated relative weight (or average cross-sectional area) of roots in the size class. The average cross-sectional area of all roots is estimated as the ratio of total relative area to total relative number of roots. The estimated mean cross-sectional area is thus 0.097 cm^2 for all roots, or a mean diameter of 3.5 mm. Direct measurement of mean diameter of roots for a single site where roots were excavated and measured was 1.6 mm for Walker Branch Watershed. For estimation purposes, we have chosen a mean diameter of 2.5 mm to represent average roots in an oak-hickory stand.

Kochenderfer (1972) and Striffler (1957) have presented data summarizing the average number of root endings per unit area. Those data are summarized below:

Average number of roots per 930 cm^2 - oak hickory forest sites

Soil depth

0.3 m	0.6 m	0.9 m	1.2 m	1.5 m
120±30	40±20	15±10	8±5	4±2

The fraction of root cross-section area to total soil area as a function of depth has been estimated from the data presented above,

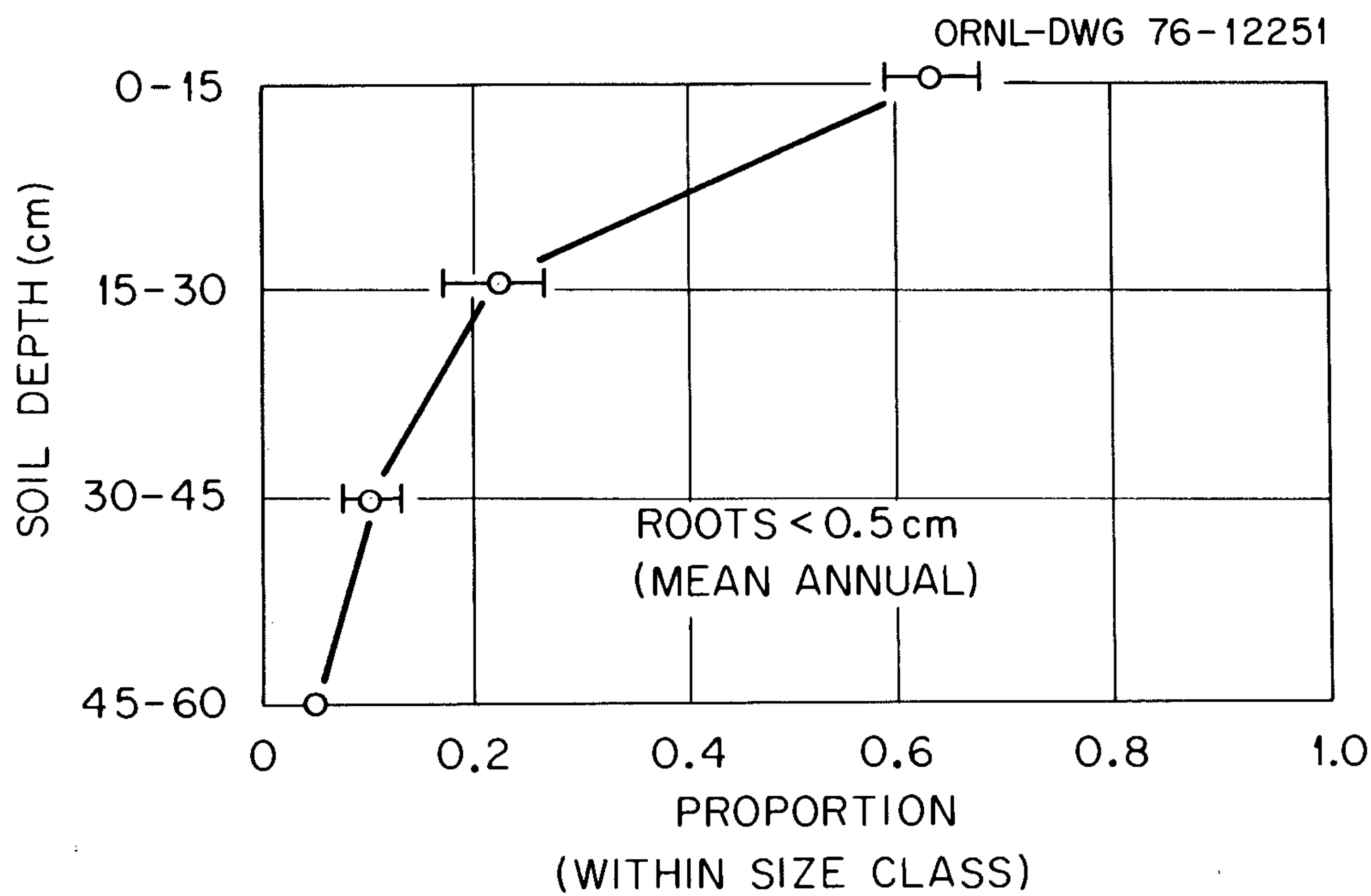

Fig. 21. The average annual depth distribution of lateral roots less than 5 mm in diameter for Liriodendron forest.

assuming a mean root diameter of 2.5 mm. The resulting relationship is shown in Fig. 22 and is presented as a guide for parameter estimation. When Fig. 22 is used as a guide for estimating the fractional cross-section area of roots, the values for Walker Branch Watershed are 0.004 and 0.0015 for the 0- to 45-cm and 45- to 90-cm layers respectively.

An implicit assumption contained in the PROSPER model is that the resistance to flow of water in roots is directly related to the unsaturated conductivity of soils. The factor that relates root conductivity to soil conductivity (RTCON1 or RTCON2) has been assumed to equal 1×10^6, which has the effect of assuming negligible resistance to water flow inside the root system compared with flow resistance in the surrounding soil. As experimental results are developed, the assumption will probably change.

The aboveground resistance to water flow in the plant (RSTEM) was estimated as 5000 (days), following the work of Cowan (1965). The resistance to water vapor flow exhibited by litter has been estimated as 3×10^5 days. This value was developed by trial and error estimation, using measured and estimated litter evaporation rates as a guide.

Four input parameters are used to specify the assumed exponential relationship between surface resistance and surface potential for summer vegetation (TMS, PWPS, RESS, POWS). The minimum surface resistance (TMS) for leaves of mesophytic species are often found to be in the range of 1 to 5 sec cm^{-1} (Cowan and Milthorpe, 1968). The critical leaf water potential (PWPS), at which surface resistance becomes maximum has been determined for many species to be in the range of -13 to -27 bars (Ritchie and Hinckley, 1975). The cuticle resistance of leaves is usually taken to be the maximum surface resistance (RESS) and values in the range of 20 to 400 sec cm^{-1} are appropriate (Cowan and Milthorpe, 1968). The exponential relationship between resistance and potential obtained for field plants often has an almost on-off form and a value of POWS ≤ -0.5 is suitable. In any given model application, experimental data for the site should be used if possible. The equivalent parameters for the winter time (TMW, PWPW, RESW, POWW) have usually been chosen intuitively to represent slow evaporation of water from the bare branches and litter in the case of deciduous forests (e.g., 7, -10, 100, -0.5, respectively). The ratio between the heat loss and transpiration surfaces are 1 (for leaves with stomata on both sides), 1.5 (for pine needles with stomata on 2/3 of the surface), 2 (for leaves with stomata on one side), and 1 (for bare branches and litter). The summer (SIGS) and winter (SIGW) values should be chosen from the information given above to represent the appropriate seasonal vegetation conditions.

Soil heat exchange can reduce the amount of energy in the canopy during summer and increase the energy during winter. The annual mean heat exchange (GM) is usually zero and the amplitude (GV) is about 20 langleys per day in temperate latitudes (van Wijk and DeVries, 1963).

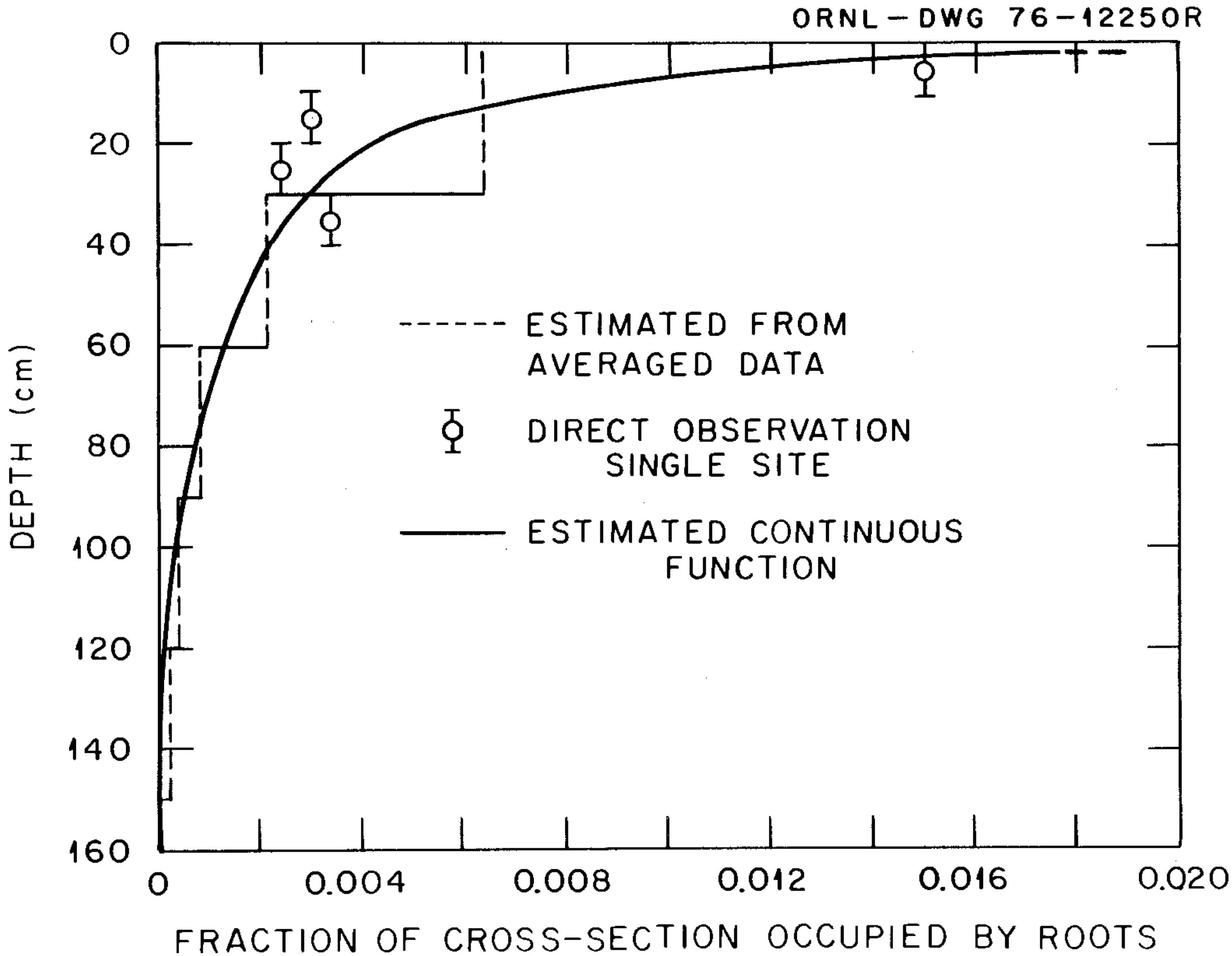

Fig. 22. Approximate relationship between soil depth and the fraction of root cross-section per unit soil cross-section area.

Table 12. A summary of parameters that characterize vegetation

---

- Type of vegetation (deciduous or coniferous)
- Resistances to water flow within roots, stems, and leaves
- Temporal patterns in albedo, leaf area index, interception storage, and heat exchange between soil and canopy
- Measures of vertical distribution of root density and cross-sectional area (per unit area of soil)
- Estimate of soil water pressure at the wilting point
- Estimated relationship between plant water potential and resistance to water flow or loss

---

Some sensitivity analyses of several landscape, soil, and plant parameters used in the PROSPER part of TEHM have shown that several parameters need to be carefully examined (Luxmoore et al., 1976a). Table 13, reproduced from the preceding report, indicates that the highly sensitive values include the summer leaf area index (ALMAX), the surface water potential beyond which surface resistance is at its maximum (PWPS), the root conductivity factor for the first root layer (RTCON1), and the characteristic resistance of litter to water flow (RLIT). Minimum stomatal resistance (TMS), stem resistance to water flow (RSTEM), the root density factor for the first soil layer [AT(1)], and the maximum interception storage (EPXMAX) are also sensitive in determining the monthly water balance. Values for ALMAX, PWPS, and TMS can be found for various field studies; however, RTCON1 and RSTEM are usually not well characterized. RLIT is best determined by adjusting its value until the annual or seasonal soil evaporation values are reasonable. EPXMAX can be found by matching measured or empirical functions of seasonal interception evaporation. Examining root data is useful for determining AT (1). These eight parameters are important in the PROSPER data; erroneous estimates will give erroneous simulation results.

The Channel Flow Module

The channel flow simulation component in the TEHM has been taken directly from the WHTM, and thus has been fully documented by Patterson et al. (1974) (Chapter V, pp. 77-91). The function of the channel flow portion of the model is to combine simulated runoff amounts from each portion or segment of a watershed in the proper time and space relationships, and to generate instantaneous flow estimates at specified points in the channel system.

As an aid to those who wish to use the TEHM for hydrograph generation, a brief description of the estimation of parameters that are appropriate for Walker Branch Watershed is included here. In addition, descriptions of the input formats have been reproduced from the WHTM documentation, and are included in the input descriptions that follow.

The channel system is parameterized by describing the configuration of reaches and the physical properties of each reach in the system. For Walker Branch Watershed, we have chosen to use a single reach to represent each of the two forks in the basin. The choice is partially dictated by the size of each channel reach. The minimum routing interval possible with the current model version is 3 min, and this time should be short relative to the travel time for water moving through the reach. Furthermore, because the time resolution of the input data is no better than hourly, and simulated channel inflows are uniform over 30-min simulated intervals, a more detailed channel system for simulation is unwarranted.

Table 13. Subjective indication of the sensitivity of PROSPER parameters to the monthly water balance, midday plant water status and daily evapotranspiration, and drainage rate

Parameter	Monthly Water balance	Daily rate		Midday	
		Evapotranspiration	Drainage	Water potential	Conductance
ALMAX	*****	*****	*****	*****	*****
PWPS	*****	****	*****	*****	****
RTCON1	*****	**	*****	***	****
PLIT	****	*	*	****	*
TMS	***	*****	****	****	*****
RSTEM	***	*****	****	****	*****
AT(1)	***	**	****	**	*
EPXMAX	***	*	*	0	0
ALBS	**	***	**	**	*
ARAT	*	*	**	*	*
POWS	*	**	*	**	***
INCL	*	**	**	**	***
AZIM	*	**	**	*	**
RESS	*	**	**	**	*
SDRAG	0	*	0	0	*
DL	*	0	**	*	*
RTCON2	*	0	*	0	0
FACTOR	*	0	**	0	0
AT(2)	0	0	*	0	0

[*****(high sensitivity) to * (low sensitivity); 0 (almost no sensitivity)].

The first input parameters required by the channel flow module are used to calculate a table of flow rate versus depth of flow. This table is used at the beginning of a storm when the model shifts from the assumption that inflow is equal to outflow to a detailed routing analysis. Data from the table are used to estimate an initial depth of flow in the reach (for the starting flow rate). The table must span the range of possible flow depths experienced in the reach, and provide sufficient information to allow accurate estimation of the depth for a given flow. For Walker Branch reaches, the mean depth will not exceed 2 ft in any reach under equilibrium-type conditions. Thus we have chosen to create a table containing 100 points of corresponding depth and flow at 0.02-ft increments in the range 0 to 2 ft.

Curlin and Nelson (1968) presented data on the length and upstream and downstream elevations for both forks of Walker Branch Watershed. From their data, Table 14 shown below was derived.

Table 14. Length and effective upstream and downstream elevations of the East and West Forks of Walker Branch Watershed

Fork	Length (ft)	Upstream elevation (ft)	Downstream elevation (ft)
East	3700	1010	880
West	2300	980	880

The channel geometry type is rectangular. It is approximated as a trapezoid with a bottom width of 4 ft, a top width of 6 ft and a bankfull depth of 2 ft. The floodplain is estimated to slope toward the incised channel at a rate of 1-ft drop for each 6-ft horizontal displacement.

The hydraulic roughness of the incised channel has been characterized by a Manning's coefficient of roughness (n) value of 0.2. This value is unusually high; however, it was estimated such that the observed relationship between stage and discharge in the reaches is preserved in the Manning equation relationship when the physical channel dimensions are used. The roughness of the floodplain is probably about double the value used for the natural channel, or about 0.4. This estimate is based upon the ratio of floodplain to natural channel roughness given by Chow (1959).

A summary of parameters that characterize the channel system is found in Table 15.

Table 15. A summary of parameters that characterize the channel system

- Geometry of each channel reach in the drainage system, including dominant shape, and dimensions of the average cross-section
- Configuration of reaches relative to one another, and contributing area for each
- Hydraulic properties of each reach and floodplain

OPERATION OF THE TEHM COMPUTER PROGRAM

Introduction

The data that describe watershed variables and the parameters that characterize specific basins are entered at the start of simulation of a given time interval. The input sequence progresses from precipitation data to climatic data and basin parameters, and finally to characterization of hydraulic properties of the stream channels draining the basin. Each of the three components may be used individually, but the latter two depend on output from preceding components. Both the precipitation data input and the data that characterize the stream channel network and hydraulic properties have been explained in detail by Patterson et al. (1975). Thus the sections describing those portions of the input data set have been abbreviated so that they include only those options actually used in the example application presented here. Users interested in other available options, such as time distribution of rainfall are referred to the earlier report.

Scaling Factors

The TEHM program, together with all input and output data associated with a one year simulation, is so large as to tax the storage capacity of many computers. For this reason, data are converted to integers and are packed into arrays, with more than one value stored in a single word to conserve space. Under most conditions, this need not concern the user; however there are occasions when the user must take action to remedy problems that arise when calculated values fall outside the range of normal expectation. Prior to storage, they are multiplied by an appropriate scaling factor to produce integer numbers, and when they are retrieved, they are divided by the same factor. However, because the numbers are stored in parts of words, if the scaled integer number is too large, information will be lost and an error will occur when data are retrieved and rescaled for use. There are checks built into the program to alert the user when this occurs, and an example of a warning message from such an error is shown on a monthly output summary later in this report.

There are three scaling factors which are built into the TEHM. They are:

RUNSCL: A scaling factor for calculated values of runoff rate from the land surface.

AERSCL: A scaling factor for calculated values of waterborne contaminant flux, and

SCALE: A scaling factor that has been used for storing total daily flow volumes as integer numbers.

The scaling factor RUNSCL is used to convert runoff rates generated during simulations to integers that are less than 32,767 and hence may be stored in two bytes or one half a standard integer word. One may therefore use a general knowledge of expected runoff rates to estimate the value of the scaling factor RUNSCL. For example, a flood frequency analysis of data for Walker Branch Watershed suggests that the peak flow rate for a 20-year return period flood would be about 170 cfs for the combined east and west forks (0.3765 sq. miles). Because runoff data are summed and stored for consecutive 30-min intervals, runoff rates that are scaled within the program have units of inches accumulated in each half hour. Flow rate may be converted from cubic feet per second to inches per half hour by dividing by the product of the basin area (square miles) and the conversion factor 1291.2. Thus, the expected 20-year return period peak flood flow rate corresponds to about 0.35 inches per half hour. RUNSCL can be estimated as the quotient of the maximum integer that can be stored and the expected runoff rate. Of course the actual instantaneous runoff rate will be higher than the foregoing estimate, because the flood peak is attenuated in the channel. One might expect channel input rates to be more than double the observed hydrograph peak rate. Under that assumption, a value of about 100,000 for RUNSCL would yield a scaled integer value of about 70,000 for the peak channel inflow rate for Walker Branch. It is thus possible that the value of RUNSCL would have to be reduced somewhat when periods that contain major storms are simulated to ensure that the scaled value is less than or equal to 32,767.

The value of RUNSCL also influences the minimum sensitivity of the scaled runoff record. Because the scaled value is stored as an integer, the minimum sensitivity of output is ± 1 unit of scaled flow, which corresponds to 1/RUNSCL inches per half hour runoff rate. For a given basin this may be converted to the flow rate (cfs) by multiplying by the product of the number of half hours per day, basin area in square miles, and the conversion factor 26.9 cfsd $(mi^2 \cdot in.)^{-1}$. Thus, when RUNSCL is 100,000, the sensitivity limit for flow is about ± 0.005 cfs for Walker Branch Watershed.

After a value for RUNSCL has been selected, it should be entered into the appropriate DATA statement in the BLOCK DATA subprogram of the TEHM if it differs significantly from the standard value of 100,000.

The scale parameter AERSCL has been used to convert the calculated flux of waterborne contaminant to an integer value for storage. However, in the version documented here, contaminant transport is not considered as a part of the hydrologic model. Thus it is not necessary to make adjustments to AERSCL.

The parameter SCALE was used in earlier versions of the model to prepare daily flow volume values for storage as integers in "packed" arrays. It is no longer used and need not be adjusted.

Precipitation Data Input

Formats

The first step in establishing precipitation data files for basin simulation is to specify basin identifiers and to indicate that precipitation data are to be entered. This input step is managed by the main control subroutine of the TEHM, which is subroutine OLDMAI. An abridged specification of the formats for data input is presented below.

Subroutine	Card* number	Columns	Description of input data
OLDMAI	1		FORMAT (7A4,14X,2I4)
		1-28	WATSHD The identifying name for the basin. The character string should begin in col. 1.
		46	GAGES The number of raingages for which data are to be entered. 1 ≤ GAGES ≤ 7
		50	REACHS The number of channel reaches that will be needed to characterize the basin. 1 ≤ REACHS ≤ 7
OLDMAI	2		FORMAT (20(I3,1X))
		1-3	STAN(1) An abbreviated identification number (right-justified) for a raingage. 1 ≤ STAN(1) ≤ 999
		5-7	STAN(2) An abbreviated identification number (right-justified) for a raingage. 1 ≤ STAN(2) ≤ 999
		etc.	etc.
OLDMAI	3		FORMAT (A4)
		1-4	LBL A label to specify the component of the TEHM that will be executed next. Options are PREC, LAND, CHAN, and DIST. "PREC" is used for calling precipitation data management programs when hourly data are available.

Once the PREC option has been selected, it is necessary to specify detailed descriptive information to identify the location, number, and types of raingage sites for which data are to be filed. The input sequence for the Walker Branch example, where weighted-average hourly precipitation data are used, is described below. The cards immediately follow those described above when the data are assembled for simulation.

*Card numbers refer to the example input sets at the end of each section.

Subroutine	Card number	Columns	Description of input data
PRECIP	4		FORMAT(8A4)
		1-32	ACT An alphameric array that describes the input that will follow. The option used here is the character string OPEN RAINGAGE INVENTORY FILE, which must be left-justified.
OPNSET	5		FORMAT(2I3,2X,7A4)
		1-3	SPACES The maximum number of raingages for which data will be filed.
		4-6	YRS The maximum number of water-years for which data will be filed.
		9-36	INNAME The name of the basin for which data are to be entered.
	6		FORMAT(3I5)
		1-5	NYR The total number of years for which data will be filed. (right-justified)
		6-10	NGAG The total number of raingages in the basin for which data will be filed.
		11-15	NSEG The total number of separate homogeneous basin segments that represent the whole watershed.
PRECIP	7		FORMAT(8A4)
		1-32	ACT An alphameric array that describes the input that will follow. INPUT RAINGAGE INVENTORY is always used after the option OPEN RAINGAGE INVENTORY FILE (see card 4).
OPNSET	8		FORMAT(A1,I2,I6,6A4,9X,I5,3(I2,1X), 2X,I3,2(1X,I2),3X,2A4)
		2-3	STANF The abbreviated identification number (right-justified) for the raingage that is characterized by data that follow.
		4-9	WB The Weather Bureau or other identification number that relates the station to a field site. Input value must be right-justified.
		10-33	NAME The identifying name for the raingage station.
		43-47	ELEV The m.s.l. elevation of the raingage (feet). Input must be right-justified.

Subroutine	Card number	Columns	Description of input data
		48-55	LAT The latitude of the raingage site as:
		48-49	degrees latitude, right-justified
		51-52	minutes latitude, right-justified
		54-55	seconds latitude, right-justified
		59-67	LONG The longitude of the raingage site as:
		59-61	degrees longitude, right-justified
		63-64	minutes longitude, right-justified
		66-67	seconds longitude, right-justified
		71-78	GTYPE The recording interval or gage type. The character string RECORDING is used for hourly data input.
OPNSET	9		FORMAT (same as card 8)
		1	IDOL The $ character signals that no further inventory information is to be entered. Thus column 1 is blank on cards that contain raingage information, and contains only the $ character on the card that immediately follows the last information card.
PRECIP	10		FORMAT(8A4)
		1-32	ACT An alphameric array that describes the data that will follow. The character string READ HOURLY PRECIPITATION DATA, which must begin in column 1, selects the subprogram to input hourly precipitation data.
RDHRLY	11		FORMAT(A2)
		1-2	The character string NO causes the program to omit printing detailed tables of hourly precipitation data, and only gives a summary of monthly precipitation totals. Any other characters will cause printing of all input data.
RDHRLY	12		FORMAT(A1,I2,7X,6A4)
		2-3	NUMBER The abbreviated identification number (right-justified) for the raingage where data that follow were collected.

Subroutine	Card number	Columns	Description of input data
		11-34	CDTYPE A character string that identifies the data input format. STANFORD MODEL FORMAT is used in the example presented here.
RDHRLY	13-180		FORMAT(A1,9X,3(I2,1X),I1,(2F5.2)
		2-10	These columns are not examined by the program, but it is convenient to use them for data site identification, which can reduce errors in card handling.
		11-12	YEAR The calendar year associated with data that follow.
		14-15	MONTH The month associated with data that follow.
		17-18	DAY The day associated with data that follow.
		20	CN An index that signifies whether the data that follow are for the first 12 hours of the day (CN=1) or the second 12 hours (CN=2).
		21-80	FRP Hourly precipitation totals in inches. When CN=1, the first data value (columns 21-25) is for the hour ending at 1AM. When no precipitation falls in the twelve hour AM or PM interval, the card may be omitted entirely.
RDHRLY	181		FORMAT(A1,etc.)
		1	DOLLAR The $ character in column 1 indicates that all precipitation data have been entered for the station in question.
RDHRLY	182		FORMAT (A1, etc.)
		1	DOLLAR The $ character in column 1 on this card indicates that all raingage data for this run have been entered, and RDHRLY is to be exited.
PRECIP	183		FORMAT (8A4)
		1-32	ACT An alphameric array that describes the data that will follow. The character string $$, beginning in column 1, signals that all precipitation data management functions have been completed.

OLDMAI	184		FORMAT (A4)
		1-4	LBL A label to specify the component of the TEHM that will be executed next. The character string ENDR signals that the precipitation component has been completed.

Example Listing of a Precipitation Data Set (Table 16)

The following four pages contain an example of a precipitation data set for Walker Branch Watershed. The card numbers shown on those pages correspond to the card numbers listed in the input format specifications given in the preceding section. One should note that precipitation data cards are used for only those twelve hour intervals where measurable precipitation occurred.

Table 16. Example listing of a precipitation data set

CARD NUMBER

```
WALKER  BRANCH WATERSHED PRECIP                    1   2
  1
PRECIPITATION - DEPOSITION DATA INPUT
OPEN RAINGAGE INVENTORY FILE FOR STORING DESCRIPTIVE DATA
  1  1  WALKER BRANCH WEIGHTED RAIN
    1    1    2
INPUT RAINGAGE INVENTORY FILE DATA
  1       6THIESSEN WEIGHTED WBW AV                 109035D58M00S N 84D17M00S WRECORDING
$
READ HOURLY PRECIPITATION DATA
NO
  1          STANFORD MODEL FORMAT
 0006        73 10  1 1 0.0  0.0  0.01 0.0  0.07 0.01 0.06 0.04 0.09 0.01 0.26 0.10
 0006        73 10  1 2 0.14 0.0  0.0  0.0  0.0  0.0  0.0  0.0  0.0  0.0  0.0  0.0
 0006        73 10 14 1 0.01 0.17 0.04 0.0  0.03 0.0  0.0  0.0  0.0  0.0  0.0  0.0
 0006        73 10 28 1 0.0  0.01 0.01 0.0  0.13 0.27 0.51 0.37 0.19 0.18 0.02 0.08
 0006        73 10 28 2 0.10 0.01 0.0  0.0  0.0  0.0  0.0  0.0  0.0  0.0  0.0  0.0
 0006        73 10 29 2 0.0  0.0  0.0  0.0  0.0  0.0  0.0  0.0  0.0  0.0  0.07 0.03
 0006        73 10 30 2 0.01 0.0  0.0  0.0  0.0  0.0  0.0  0.0  0.0  0.0  0.0  0.0
 0006        73 10 31 1 0.0  0.0  0.0  0.0  0.0  0.0  0.0  0.0  0.04 0.03 0.07 0.04
 0006        73 10 31 2 0.06 0.02 0.01 0.07 0.02 0.01 0.0  0.0  0.0  0.01 0.0  0.0
 0006        73 11  5 1 0.0  0.0  0.17 0.04 0.0  0.30 0.0  0.0  0.0  0.0  0.0  0.0
 0006        73 11  8 2 0.02 0.0  0.06 0.0  0.0  0.03 0.0  0.0  0.0  0.02 0.0  0.0
 0006        73 11 15 2 0.0  0.0  0.0  0.0  0.0  0.0  0.0  0.15 0.05 0.0  0.0  0.0
 0006        73 11 21 1 0.0  0.0  0.0  0.0  0.0  0.0  0.03 0.46 0.24 0.10 0.10 0.08
 0006        73 11 25 1 0.0  0.0  0.0  0.0  0.0  0.0  0.0  0.0  0.17 0.01 0.0  0.0
 0006        73 11 26 1 0.0  0.0  0.0  0.0  0.0  0.08 0.04 0.0  0.0  0.04 0.24 0.13
 0006        73 11 26 2 0.04 0.20 0.03 0.0  0.0  0.0  0.0  0.10 0.41 0.47 0.46 0.46
 0006        73 11 27 1 0.48 0.0  0.0  0.0  0.01 0.0  0.0  0.0  0.0  0.04 0.70 0.0
 0006        73 11 27 2 0.09 0.10 0.04 0.07 0.03 0.07 0.13 0.54 1.09 1.32 0.47 0.24
 0006        73 11 28 1 0.20 0.38 0.03 0.03 0.0  0.0  0.0  0.0  0.0  0.0  0.0  0.0
 0006        73 12  4 1 0.0  0.0  0.0  0.0  0.0  0.0  0.0  0.0  0.0  0.0  0.0  0.17
 0006        73 12  4 2 0.14 0.07 0.0  0.0  0.03 0.07 0.0  0.09 0.11 0.0  0.0  0.0
 0006        73 12 13 1 0.0  0.0  0.0  0.0  0.0  0.03 0.56 0.30 0.54 0.0  0.0  0.0
 0006        73 12 20 1 0.0  0.0  0.0  0.0  0.01 0.17 0.09 0.18 0.12 0.13 0.06 0.0
 0006        73 12 20 2 0.10 0.09 0.09 0.01 0.03 0.0  0.0  0.0  0.0  0.0  0.0  0.0
 0006        73 12 21 1 0.0  0.0  0.0  0.0  0.0  0.0  0.0  0.0  0.0  0.0  0.02 0.0
 0006        73 12 21 2 0.04 0.0  0.0  0.0  0.0  0.0  0.0  0.0  0.0  0.0  0.0  0.0
 0006        73 12 25 2 0.0  0.0  0.0  0.10 0.27 0.10 0.31 0.28 0.20 0.20 0.19 0.31
 0006        73 12 26 1 0.49 0.44 0.37 0.37 0.31 0.14 0.06 0.04 0.29 0.37 0.14 0.04
 0006        73 12 29 1 0.0  0.0  0.0  0.0  0.0  0.0  0.0  0.0  0.01 0.04 0.0  0.02
 0006        73 12 29 2 0.0  0.0  0.0  0.01 0.0  0.0  0.27 0.17 0.0  0.03 0.0  0.0
 0006        73 12 31 1 0.0  0.0  0.0  0.0  0.07 0.10 0.03 0.0  0.0  0.07 0.0  0.0
 0006        73 12 31 2 0.04 0.09 0.08 0.17 0.01 0.01 0.01 0.0  0.0  0.0  0.0  0.0
 0006        74  1  2 2 0.0  0.03 0.0  0.16 0.01 0.03 0.06 0.0  0.0  0.14 0.37 0.01
 0006        74  1  3 1 0.06 0.0  0.0  0.0  0.0  0.0  0.0  0.0  0.0  0.0  0.0  0.0
```

Table 16 (continued)

CARD NUMBER																	
47	0006	74	1	3	2	0.0	0.01	0.0	0.09	0.06	0.07	0.07	0.01	0.09	0.04	0.0	0.0
	0006	74	1	4	1	0.0	0.0	0.0	0.07	0.0	0.0	0.0	0.0	0.0	0.0	0.0	0.0
	0006	74	1	6	2	0.0	0.0	0.0	0.01	0.09	0.07	0.01	0.01	0.0	0.0	0.01	0.0
50	0006	74	1	8	2	0.0	0.0	0.0	0.0	0.0	0.0	0.0	0.0	0.0	0.0	0.09	0.21
	0006	74	1	9	1	0.06	0.0	0.03	0.23	0.53	0.14	0.03	0.01	0.06	0.02	0.01	0.0
	0006	74	1	10	2	0.14	0.36	0.20	0.21	0.14	0.10	0.0	0.23	0.30	0.20	0.04	0.0
	0006	74	1	11	1	0.0	0.41	0.13	0.11	0.10	0.10	0.29	0.0	0.10	0.0	0.0	0.0
	0006	74	1	14	1	0.0	0.0	0.0	0.03	0.0	0.0	0.0	0.0	0.01	0.0	0.06	0.03
	0006	74	1	14	2	0.0	0.0	0.10	0.03	0.06	0.0	0.01	0.0	0.0	0.0	0.0	0.0
	0006	74	1	15	1	0.0	0.0	0.0	0.0	0.0	0.0	0.0	0.0	0.0	0.01	0.0	0.0
	0006	74	1	16	1	0.0	0.0	0.0	0.0	0.0	0.0	0.0	0.0	0.0	0.01	0.0	0.0
	0006	74	1	20	2	0.0	0.0	0.04	0.0	0.03	0.0	0.0	0.01	0.0	0.0	0.0	0.0
	0006	74	1	23	1	0.0	0.0	0.0	0.0	0.0	0.0	0.0	0.02	0.11	0.09	0.01	0.10
60	0006	74	1	23	2	0.01	0.03	0.06	0.0	0.0	0.0	0.0	0.0	0.0	0.01	0.01	0.01
	0006	74	1	24	1	0.07	0.0	0.0	0.0	0.0	0.0	0.09	0.03	0.01	0.04	0.03	0.13
	0006	74	1	24	2	0.13	0.14	0.01	0.07	0.02	0.0	0.0	0.0	0.03	0.0	0.06	0.0
	0006	74	1	26	1	0.0	0.01	0.10	0.10	0.10	0.11	0.11	0.06	0.0	0.0	0.0	0.0
	0006	74	1	26	2	0.0	0.0	0.0	0.0	0.04	0.0	0.13	0.07	0.0	0.0	0.0	0.0
	0006	74	1	28	1	0.0	0.0	0.0	0.0	0.07	0.0	0.0	0.0	0.0	0.40	0.26	0.02
	0006	74	1	28	2	0.08	0.02	0.0	0.0	0.0	0.0	0.0	0.0	0.01	0.0	0.0	0.0
	0006	74	2	1	2	0.0	0.0	0.0	0.0	0.0	0.0	0.0	0.0	0.0	0.09	0.03	0.0
	0006	74	2	2	1	0.07	0.18	0.11	0.0	0.0	0.0	0.0	0.06	0.04	0.20	0.04	0.06
	0006	74	2	2	2	0.03	0.01	0.0	0.0	0.0	0.0	0.0	0.26	0.0	0.0	0.0	0.0
70	0006	74	2	3	1	0.0	0.0	0.0	0.0	0.03	0.07	0.0	0.01	0.0	0.0	0.0	0.0
	0006	74	2	6	1	0.0	0.0	0.0	0.0	0.0	0.0	0.0	0.0	0.07	0.01	0.02	0.08
	0006	74	2	6	2	0.03	0.13	0.04	0.0	0.0	0.0	0.0	0.0	0.0	0.01	0.0	0.0
	0006	74	2	7	1	0.0	0.0	0.0	0.0	0.0	0.0	0.0	0.0	0.0	0.0	0.0	0.01
	0006	74	2	8	1	0.0	0.01	0.0	0.04	0.0	0.02	0.0	0.0	0.0	0.0	0.0	0.0
	0006	74	2	13	2	0.0	0.0	0.0	0.0	0.0	0.0	0.0	0.0	0.02	0.0	0.0	0.0
	0006	74	2	14	1	0.21	0.0	0.26	0.31	0.14	0.0	0.0	0.10	0.0	0.0	0.0	0.0
	0006	74	2	15	2	0.0	0.0	0.0	0.0	0.0	0.0	0.0	0.0	0.0	0.0	0.0	0.01
	0006	74	2	16	1	0.04	0.10	0.10	0.10	0.21	0.29	0.23	0.11	0.0	0.04	0.02	0.01
	0006	74	2	16	2	0.01	0.0	0.0	0.0	0.0	0.0	0.0	0.0	0.0	0.0	0.0	0.0
80	0006	74	2	19	1	0.0	0.0	0.01	0.04	0.16	0.0	0.01	0.0	0.0	0.0	0.0	0.0
	0006	74	2	19	2	0.0	0.09	0.01	0.0	0.0	0.0	0.0	0.0	0.0	0.0	0.0	0.0
	0006	74	2	21	2	0.0	0.0	0.0	0.0	0.0	0.0	0.0	0.0	0.0	0.04	0.19	0.21
	0006	74	2	22	1	0.24	0.10	0.0	0.0	0.0	0.0	0.0	0.0	0.0	0.0	0.0	0.0
	0006	74	2	28	1	0.0	0.0	0.0	0.0	0.0	0.0	0.0	0.0	0.01	0.0	0.0	0.0
	0006	74	2	28	2	0.0	0.07	0.0	0.01	0.0	0.0	0.0	0.0	0.0	0.0	0.0	0.0
	0006	74	3	5	1	0.0	0.0	0.0	0.0	0.0	0.0	0.0	0.01	0.0	0.09	0.01	0.09
	0006	74	3	5	2	0.13	0.19	0.0	0.0	0.01	0.0	0.04	0.06	0.06	0.01	0.09	0.01
	0006	74	3	6	2	0.0	0.0	0.01	0.0	0.19	0.01	0.54	0.0	0.01	0.0	0.0	0.0
	0006	74	3	10	1	0.0	0.0	0.0	0.0	0.0	0.0	0.01	0.0	0.0	0.0	0.0	0.0
90	0006	74	3	10	2	0.0	0.01	0.0	0.0	0.0	0.0	0.0	0.0	0.0	0.0	0.0	0.0
91	0006	74	3	12	1	0.0	0.0	0.0	0.0	0.0	0.0	0.0	0.0	0.0	0.10	0.0	0.0
92	0006	74	3	12	2	0.11	0.0	0.0	0.0	0.0	0.0	0.0	0.0	0.0	0.0	0.0	0.0

Table 16 (continued)

CARD NUMBER																	
93	0006	74	3	16	1	0.0	0.0	0.0	0.0	0.09	0.03	0.07	0.11	0.0	0.0	0.0	0.0
	0006	74	3	19	1	0.0	0.0	0.0	0.0	0.0	0.0	0.0	0.0	0.0	0.12	0.21	0.34
	0006	74	3	19	2	0.10	0.0	0.24	0.03	0.0	0.0	0.0	0.06	0.76	0.13	0.17	0.0
	0006	74	3	20	1	0.04	0.0	0.0	0.0	0.0	0.0	0.0	0.0	0.0	0.0	0.0	0.0
	0006	74	3	21	1	0.18	0.39	0.19	0.71	0.77	0.04	0.0	0.0	0.0	0.0	0.0	0.0
	0006	74	3	27	2	0.0	0.0	0.01	0.0	0.10	0.0	0.0	0.0	0.04	0.01	0.0	0.0
	0006	74	3	28	1	0.03	0.0	0.0	0.0	0.0	0.0	0.0	0.0	0.04	0.0	0.0	0.0
	0006	74	3	29	1	0.0	0.0	0.0	0.0	0.0	0.04	0.03	0.14	0.23	0.27	0.03	0.0
101	0006	74	3	30	1	0.22	0.0	0.0	0.0	0.0	0.0	0.0	0.0	0.0	0.0	0.0	0.0
102	0006	74	4	1	2	0.0	0.0	0.0	0.0	0.0	0.0	0.0	0.0	0.0	0.0	0.0	0.23
	0006	74	4	2	1	0.43	0.0	0.0	0.0	0.0	0.0	0.0	0.0	0.0	0.0	0.0	0.0
	0006	74	4	3	2	0.01	0.45	0.03	0.0	0.0	0.01	0.0	0.0	0.06	0.01	0.0	0.0
	0006	74	4	4	1	0.0	0.30	0.17	0.03	0.01	0.0	0.0	0.0	0.0	0.0	0.0	0.0
	0006	74	4	8	1	0.0	0.0	0.0	0.0	0.0	0.16	0.02	0.0	0.0	0.0	0.0	0.03
	0006	74	4	8	2	0.46	0.01	0.10	0.0	0.0	0.0	0.0	0.0	0.0	0.0	0.0	0.0
	0006	74	4	12	1	0.0	0.0	0.0	0.0	0.0	0.0	0.0	0.0	0.0	0.0	0.0	0.10
	0006	74	4	12	2	0.04	0.0	0.0	0.01	0.0	0.0	0.0	0.0	0.09	0.11	0.09	0.09
110	0006	74	4	13	1	0.01	0.0	0.0	0.0	0.0	0.0	0.0	0.0	0.0	0.0	0.0	0.0
	0006	74	4	14	2	0.0	0.0	0.0	0.03	0.0	0.0	0.0	0.0	0.0	0.0	0.0	0.0
	0006	74	4	16	2	0.0	0.0	0.0	0.0	0.0	0.0	0.0	0.0	0.0	0.0	0.08	0.0
	0006	74	4	22	2	0.0	0.0	0.0	0.0	0.01	0.09	0.08	0.0	0.03	0.09	0.07	0.0
	0006	74	5	2	1	0.07	0.0	0.0	0.0	0.0	0.0	0.0	0.0	0.0	0.0	0.11	0.03
	0006	74	5	2	2	0.06	0.0	0.0	0.01	0.03	0.27	0.0	0.0	0.0	0.46	0.0	0.0
	0006	74	5	4	1	0.0	0.0	0.0	0.0	0.0	0.0	0.0	0.13	0.0	0.0	0.0	0.0
	0006	74	5	5	2	0.0	0.01	0.10	0.06	0.0	0.0	0.0	0.0	0.0	0.0	0.0	0.0
	0006	74	5	7	1	0.0	0.0	0.0	0.0	0.0	0.0	0.0	0.0	0.0	0.0	0.01	0.0
	0006	74	5	8	2	0.0	0.0	0.0	0.0	0.0	0.0	0.0	0.0	0.17	0.02	0.04	0.33
120	0006	74	5	9	2	0.0	0.0	0.0	0.0	0.0	0.0	0.0	0.0	0.0	0.0	0.0	0.01
	0006	74	5	10	1	0.01	0.0	0.0	0.0	0.0	0.0	0.0	0.0	0.0	0.0	0.0	0.0
	0006	74	5	11	2	0.0	0.0	0.0	0.0	0.06	0.0	0.0	0.17	0.04	0.06	0.03	0.07
	0006	74	5	12	1	0.27	0.30	0.13	0.10	0.20	0.26	0.0	0.0	0.0	0.0	0.0	0.0
	0006	74	5	15	1	0.0	0.0	0.0	0.0	0.0	0.0	0.0	0.0	0.0	0.0	0.0	0.09
	0006	74	5	15	2	0.20	0.13	0.0	0.0	0.04	0.0	0.0	0.0	0.0	0.0	0.0	0.0
	0006	74	5	19	2	0.0	0.0	0.35	0.0	0.0	0.01	0.0	0.0	0.0	0.0	0.0	0.0
	0006	74	5	21	1	0.0	0.0	0.0	0.0	0.0	0.0	0.0	0.06	0.01	0.0	0.0	0.0
	0006	74	5	22	2	0.0	0.0	0.0	0.22	0.01	0.06	0.03	0.10	0.07	0.03	0.06	0.11
	0006	74	5	23	1	0.31	0.29	0.19	0.01	0.03	0.04	0.0	0.0	0.0	0.0	0.0	0.0
130	0006	74	5	26	1	0.0	0.0	0.0	0.0	0.0	0.0	0.0	0.0	0.0	0.0	0.0	0.01
	0006	74	5	26	2	0.09	0.13	0.14	0.03	0.10	0.10	0.07	0.0	0.0	0.0	0.0	0.0
	0006	74	5	29	2	0.0	0.0	0.0	0.0	0.0	0.0	0.04	0.0	0.0	0.0	0.0	0.0
	0006	74	5	30	2	0.02	0.0	0.0	0.0	0.0	0.07	0.0	0.0	0.0	0.0	0.0	0.0
	0006	74	5	31	2	0.0	0.0	0.0	0.0	0.0	0.07	0.0	0.0	0.0	0.0	0.0	0.0
	0006	74	6	1	1	0.01	0.0	0.0	0.0	0.02	0.0	0.0	0.0	0.0	0.0	0.0	0.01
	0006	74	6	1	2	0.0	0.0	0.0	0.01	0.0	0.0	0.0	0.0	0.0	0.0	0.0	0.0
	0006	74	6	6	1	0.0	0.0	0.0	0.0	0.0	0.0	0.0	0.0	0.0	0.0	0.07	0.03
138	0006	74	6	6	2	0.10	0.58	0.01	0.0	0.0	0.0	0.0	0.0	0.0	0.0	0.0	0.0

Table 16 (continued)

CARD NUMBER																	
139	0006	74	6	12	1	0.0	0.0	0.06	0.04	0.06	0.0	0.0	0.0	0.0	0.01	0.0	0.0
140	0006	74	6	13	2	0.0	0.0	0.0	0.0	0.0	0.0	0.0	0.0	0.01	0.0	0.0	0.0
	0006	74	6	16	1	0.0	0.04	0.14	0.10	0.04	0.02	0.0	0.0	0.0	0.01	0.01	0.0
	0006	74	6	25	2	0.03	0.01	0.0	0.0	0.14	0.0	0.0	0.0	0.0	0.0	0.0	0.0
	0006	74	6	27	2	0.0	0.0	0.0	0.0	0.17	0.17	0.04	0.03	0.0	0.0	0.0	0.0
	0006	74	7	15	2	0.0	0.0	0.0	0.0	0.01	0.0	0.0	0.0	0.0	0.0	0.0	0.0
	0006	74	7	19	2	0.0	0.0	0.0	0.41	0.07	0.0	0.0	0.0	0.0	0.0	0.0	0.0
	0006	74	7	23	2	0.04	0.0	0.0	0.0	0.0	0.0	0.0	0.0	0.0	0.0	0.0	0.01
	0006	74	7	24	1	0.01	0.10	0.08	0.20	0.0	0.0	0.0	0.0	0.0	0.0	0.0	0.0
	0006	74	7	26	1	0.0	0.0	0.0	0.0	0.0	0.0	0.0	0.0	0.0	0.01	0.11	0.0
	0006	74	8	2	2	0.0	0.0	0.0	0.08	0.02	0.0	0.0	0.0	0.0	0.0	0.0	0.22
150	0006	74	8	3	2	0.04	0.06	0.0	0.0	0.0	0.0	0.0	0.0	0.0	0.0	0.0	0.0
	0006	74	8	8	1	0.0	0.0	0.0	0.0	0.0	0.0	0.0	0.26	0.0	0.07	0.0	0.06
	0006	74	8	8	2	0.20	0.0	0.0	0.0	0.0	0.0	0.0	0.06	0.0	0.0	0.0	0.0
	0006	74	8	11	2	0.0	0.0	0.0	0.0	0.0	0.26	0.72	0.07	0.0	0.0	0.0	0.0
	0006	74	8	12	1	0.0	0.0	0.0	0.0	0.0	0.0	0.0	0.0	0.0	0.01	0.0	0.0
	0006	74	8	12	2	0.02	0.0	0.0	0.0	0.0	0.0	0.0	0.0	0.0	0.0	0.0	0.0
	0006	74	8	16	1	0.0	0.0	0.0	0.0	0.0	0.0	0.0	0.0	0.02	0.57	0.26	0.08
	0006	74	8	21	2	0.0	0.0	0.0	0.21	0.26	0.0	0.0	0.0	0.0	0.0	0.0	0.0
	0006	74	8	22	1	0.0	0.0	0.0	0.0	0.0	0.09	0.12	0.03	0.06	0.13	0.0	0.0
	0006	74	8	23	2	0.0	0.0	0.0	0.0	0.07	0.02	0.0	0.0	0.0	0.0	0.0	0.0
160	0006	74	8	27	2	0.0	0.0	0.0	0.0	0.0	0.04	0.0	0.0	0.0	0.0	0.0	0.0
	0006	74	8	28	1	0.0	0.0	0.0	0.0	0.0	0.0	0.0	0.0	0.02	0.0	0.0	0.0
	0006	74	8	28	2	0.0	0.0	0.20	0.0	0.0	0.0	0.0	0.0	0.0	0.0	0.0	0.0
	0006	74	8	29	2	0.0	0.0	0.0	0.0	0.16	0.49	0.26	0.13	0.02	0.0	0.0	0.03
	0006	74	8	30	1	0.0	0.0	0.0	0.0	0.0	0.0	0.0	0.0	0.0	0.04	0.0	0.0
	0006	74	8	30	2	0.0	0.0	0.0	0.0	0.02	0.18	0.0	0.0	0.0	0.0	0.0	0.0
	0006	74	8	31	2	0.0	0.0	0.14	0.06	0.0	0.0	0.0	0.0	0.0	0.0	0.0	0.0
	0006	74	9	1	1	0.0	0.0	0.43	0.23	0.0	0.04	0.0	0.0	0.0	0.0	0.0	0.0
	0006	74	9	2	1	0.0	0.0	0.10	0.10	0.09	0.29	0.0	0.0	0.0	0.0	0.0	0.0
	0006	74	9	2	2	0.0	0.20	0.03	0.0	0.0	0.0	0.0	0.0	0.0	0.0	0.0	0.0
170	0006	74	9	3	1	0.0	0.0	0.0	0.0	0.04	0.0	0.0	0.0	0.0	0.0	0.0	0.0
	0006	74	9	6	1	0.0	0.0	0.0	0.06	0.0	0.01	0.19	0.10	0.04	0.06	0.08	0.06
	0006	74	9	7	1	0.04	0.0	0.0	0.0	0.0	0.0	0.0	0.0	0.0	0.0	0.0	0.0
	0006	74	9	8	2	0.01	0.0	0.0	0.01	0.06	0.0	0.0	0.0	0.0	0.0	0.0	0.0
	0006	74	9	9	2	0.0	0.0	0.06	0.01	0.0	0.0	0.0	0.0	0.0	0.0	0.0	0.0
	0006	74	9	10	1	0.0	0.0	0.0	0.0	0.0	0.0	0.0	0.0	0.0	0.0	0.04	0.0
	0006	74	9	10	2	0.0	0.02	0.0	0.0	0.0	0.0	0.0	0.0	0.0	0.0	0.0	0.0
	0006	74	9	20	2	0.0	0.0	0.0	0.0	0.0	0.0	0.0	0.0	0.0	0.0	0.0	0.06
	0006	74	9	21	1	0.01	0.24	0.04	0.0	0.0	0.0	0.0	0.0	0.09	0.27	0.0	0.0
	0006	74	9	27	2	0.0	0.09	0.10	0.07	0.0	0.0	0.0	0.0	0.0	0.0	0.0	0.0
180	0006	74	9	29	1	0.0	0.0	0.06	0.15	0.17	0.0	0.0	0.0	0.0	0.0	0.0	0.0
181	$																
182	$																
183	$$																
184	ENDRUN																

Climatic Data and Basin Parameter Input

After precipitation data have been entered and filed, terrestrial hydrology simulations are initiated by providing climatic data and basin parameters. The input sequence begins with a call to the main control subprogram of the TEHM, then proceeds to subprograms that organize specific variables and parameters and finally initiate basin simulation when input has been completed. The description of input requirements and formats that follows is quite detailed and includes descriptions of many options that are not illustrated in the example run. It is intended that this description totally replace the description of the LAND link of the WHTM in the user's manual (Patterson et al. 1975). Those familiar with that document will note that extensive changes have been made to the code, and are cautioned that it is necessary to use this guide to construct data sets for use with the TEHM. Simple rearrangements of existing WHTM data sets for the LAND link of the WHTM will cause errors that will prevent successful completion of TEHM runs.

Formats

The first few cards in the input sequence for the terrestrial component of the TEHM are virtually the same as those used in the precipitation data management component. They are used to identify the basin to be simulated, the time period to be considered, and to gain access to the data input and terrestrial hydrology simulation subprograms.

Subroutine	Card number	Columns	Description of input data
OLDMAI	1		FORMAT(7A4,14X,2I4)
		1-28	WATSHD The identifying name for the basin. The name should begin in column 1.
		46	GAGES The number of basin segments that will be simulated in this run. $1 \leq$ GAGES ≤ 7
		50	REACHS The number of channel reaches that will be needed to characterize the basin. $1 \leq$ REACHS ≤ 7.
OLDMAI	2		FORMAT(20(I3,1X))
		1-3	STAN(1) An abbreviated identification number (right-justified) for a raingage site where data will be used. $1 \leq$ STAN(1) ≤ 999.
		5-7	STAN(2) An abbreviated identification number (right-justified) for a second data site.
		etc.	etc.

Subroutine	Card number	Columns	Description of input data
OLDMAI	3		FORMAT(A4) LBL A label that specifies the component of the TEHM that will be executed next. LAND is the character string that is used to initiate the terrestrial hydrology simulations.
TIMEWD	4		FORMAT(6(I2,1X))
		1-2	TIMES(1) The starting month of the simulation period (right-justified). (January = 1)
		4-5	TIMES (2) The starting calendar year (last two digits) of the simulation period (right-justified).
		7-8	TIMES (3) The first month after the simulation period ends (right-justified).
		10-11	TIMES (4) The last two digits of the calendar year associated with the first month after the simulation period.
		13-17	Not used.
LAND	5		FORMAT(A1,I2,1X,I3,1X,I2,1X,I2)
		2-3	SEG The identifying number for the basin segment to be simulated (right-justified).
		5-7	STANFD The abbreviated identification number for the raingage associated with the segment to be simulated (right-justified).
		9-10	YR1 The beginning calendar year of the period that will be processed for the segment identified in columns 2-3 of this card, TIMES(2) $\leq$ YR1 $\leq$ TIMES(4).
		12-13	YR2 The ending calendar year of the period that will be processed; TIMES(2) $\leq$ YR2 $\leq$ TIMES(4).

The foregoing data specify the general characteristics of the simulation run for the terrestrial component of the TEHM.

The following materials document the detailed information that is supplied for each segment of the basin. Table 17 lists the choices available to the user for purposes of supplying data. Not all options will be used in any study because some are equivalent and others invoke subroutines that are useful only for special studies. For example, the climatic variables

Table 17. The choices available for supplying input data to the TEHM

NBZ	BZ	Description
1	AIR TEMP (DAILY MAX/MIN)	Read daily maximum and minimum air temperature values [°F] into array TEM.
2	DEW POINT (DAILY AVERAGE)	Read average daily dewpoint temperature values [°F] into array DEW.
3	SOLAR RADIATION (DAILY TOTAL)	Read total daily solar radiation values [Langleys] into array RAD.
4	WIND SPEED (DAILY AVERAGE)	Read average daily wind speed values [m.p.h.] into array WINDS.
5	SNOPAR	Read parameters to characterize the snowpack and invoke snow melt simulation.
6	LAND SURFACE	Read parameters to characterize the land surface properties.
7	PROSPER READ	Read parameters and data tables to characterize the soil-plant-atmosphere water flow system.
8	SUBSURFACE PARAMETERS	Read parameters to characterize subsurface soil hydrologic properties.
9	ROCHM**	** These options are documented by Luxmoore
10	RDCER**	*et al.*, 1976b. They are available in the
11	RDDRY**	TEHM, but are not included in this document.
12	DEW POINT - BIMONTHLY	Read bimonthly values of average dew point temperature [°F]; one value that is used for each of the first 15 days of the month and a second for the remainder.
13	SOLAR RADIATION - BIMONTHLY	Read values of daily total solar radiation [Langleys].
14	WIND SPEED-BIMONTHLY	Read values of average daily wind speed [m.p.h.].
15	LAKE EVAPORATION	Read characteristics of anemometer exposure and invoke Penman-type free water surface evaporation estimates (daily).
16	GO	Terminate input of segment parameters and characteristics and initiate simulation of terrestrial ecosystem hydrology. Input for successive segments begins with card 5 read by LAND (see the preceding page of the input descriptions).

of dew-point temperature, solar radiation, and wind speed may be supplied as individual daily values or an average daily value for bimonthly intervals. Snowpack simulation parameters are used only where snowfall is considered significant in relation to the total precipitation. The following list is a guide to the variables and parameters that must be supplied as a minimum for any segment.

Option(s)	Description
1	Daily maximum and minimum air temperature
2 or 12	Daily average dew point temperature
3 or 13	Daily solar radiation
4 or 14	Daily average wind speed
6	Parameters that characterize land surface properties
7	Parameters that characterize soil-plant-atmosphere water flow
8	Parameters that characterize subsurface soil properties

Climatic variables must be supplied at least once for a watershed for any given year. However, if several basin segments may be assumed to be exposed to the same climatic forcing variables, it is not necessary to duplicate input data. If any climatic variable is supplied as part of the input for a segment, it is used. Otherwise, the data from the preceding segment are carried over and used for subsequent segments. However, it must be noted that if multiple-year continuous simulations are used for segments, it is necessary to supply all climatic data for each segment. Furthermore, channel flow simulation output is saved for only the final year simulated. Thus complete basin studies that include hydrograph simulation must be done one year at a time.

The remainder of the terrestrial component documentation describes the detailed input requirements for any given segment, organized in the same sequence that was used in Table 17 to present the available options. The first card for any option is always the NBZ, BZ input switch as described below:

Subroutine	Card number[a]	Columns	Description of input data
GETSET	6		FORMAT(I2,1X,A4)
		1-2	<u>NBZ</u> A control switch variable used to describe data that will follow. Table 17 contains a complete listing of the options. The last switch in the sequence for a segment must be <u>16</u>. As soon as it is encountered, simulation begins.

[a] Card number is associated with the sample input listing at the end of this section.

Subroutine	Card number	Columns	Description of input data
GETSET	6	4-7	BZ The first four characters of the description of the data to follow.
		8-80	These columns may contain any information useful in identifying the data that follow.

The remaining pages of this chapter describe input specifications for each of the options described in Table 17:

OPTION: NBZ, BZ = 1 AIR TEMPERATURE (DAILY MAX/MIN)

Subroutine	Card number	Columns	Description of input data
GETSET	1.1		FORMAT(I1)
		1	DCS(13) An integer control switch: DCS(13) = 1 when temperature observations were made between the occurrence of the daily minimum and maximum air temperatures on a given date. DCS(13) = 2 when temperature observations were made after both the daily minimum and maximum temperatures had occurred for a given date. (see discussion of temperature data)
GETSET	1.2 to 1.37		FORMAT(A1,6X,2I2,I1,22I3)
	1.38	1	IX, any character but $ is ignored. The character $ signals that all daily maximum and minimum temperature data have been read.
	1.2 to 1.37	2-7	Not reserved.
		8-9	Y, a 2-digit integer, the calendar year of the input.
		10-11	M, a 2-digit integer, the month of the input.
		12	C, a single digit, = 1 for days 1 through 11, = 2 for days 12 through 22, = 3 for days 23 through 31.
		13-15	Daily maximum temperature value [°F].
		16-18	Daily minimum temperature value [°F].
		19-21	Daily maximum temperature value [°F].
		22-24	Daily minimum temperature value [°F].
		...	...

Subroutine	Card number	Columns	Description of input data
		73-75	Daily maximum temperature value [°F].
		76-78	Daily minimum temperature value [°F].

Note: These daily maximum and minimum temperature values must be right-adjusted in their fields. Any unneeded fields should be left blank.

NBZ, BZ = 2 DEW DAILY

Subroutine	Card number	Columns	Description of input data

For NBZ, BZ = 2 DEWPOINT, the next cards required are:

ENTRY DAYIN (alternate entry to SUBROUTINE BIMON)	2.1 to 2.37		FORMAT(A1,6X,2I2,I1,11F6.0)
	2.37	1	X, any character but $ is ignored. The character $ signals that all daily dew data have been read and control should return to SUBROUTINE LAND.
	2.1 to 2.36	8-9	Y, a 2-digit integer, the year of the input.
		10-11	M, a 2-digit integer, the month of the input.
		12	K, a single digit, = 1 for days 1 through 11, = 2 for days 12 through 22, = 3 for days 23 through 31.
		13-18	Mean daily dewpoint temperature value [°F].
		19-24	Mean daily dewpoint value [°F].
		...	...
		73-78	Mean daily dewpoint value [°F].

NBZ, BZ = 3 SOLAR RADIATION

For NBZ, BZ = 3 SOLAR RADIATION, the next cards required are:

ENTRY DAYIN (alternate entry to SUBROUTINE BIMON)	3.1 to 3.37		FORMAT(A1,6X,2I2,I1,11F6.0)
	3.37	1	X, any character but $ is ignored. The character $ signals that all daily radiation data have been read and control should return to SUBROUTINE LAND.

Subroutine	Card number	Columns	Description of input data
		2-7	Blank. May be used for station number and data-type codes.
	3.1 to 3.36	8-9	Y, a 2-digit integer, the year of the input.
		10-11	M, a 2-digit integer, the month of the input.
		12	K, a single digit, = 1 for days 1 through 11, = 2 for days 12 through 22, = 3 for days 23 through 31.
		13-18	Integrated total daily radiation value for first of 11 day group (Langleys/day].
		19-24	Integrated total daily radiation value for second of 11 day group (Langleys/day].
		...	...
		73-78	Integrated total daily radiation value for last of 11 day group [Langleys/day].

NBZ, BZ = 4 WIND SPEED

For NBZ, BZ = 4 WIND SPEED, the next cards required are:

ENTRY DAYIN	4.1 to 4.37		FORMAT(A1,6X,2I2,I1,11F6.0)
(alternate entry to SUBROUTINE BIMON)	4.37	1	X, any character but $ is ignored. The character $ signals that all daily wind data have been read and control should return to SUBROUTINE LAND.
	4.1 to 4.36	8-9	Y, a 2-digit integer, the year of the input.
		10-11	M, a 2-digit integer, the month of the input.
		12	K, a single digit, = 1 for days 1 through 11, = 2 for days 12 through 22, = 3 for days 23 through 31.
		13-18	Average wind speed value [m.p.h.].
		19-24	Average wind speed value [m.p.h.].
		...	...
		78-78	Average wind speed value [m.p.h.].

Subroutine	Card number	Columns	Description of input data

for NBZ, BZ = 5 SNOPAR, the next card required is:

Subroutine	Card number	Columns	Description of input data
GETSET	5.1 (not shown in example)		FORMAT(9F6.2,4F5.2,I1,1X,I1) at LAN 1480.
		1-16	FRADCN, radiation melt parameter that allows for variation in slope and exposure in the watershed segments (Crawford and Linsley, 1966, pp. 50, 61; Jacques and Huff, 1972, p. 14).
		7-12	FCNMLT, convection-condensation melt parameter [inches per °F] (Crawford and Linsley, 1966, pp. 50,61).
		13-18	FSCF, snow correction factor (Crawford and Linsley, 1966, pp. 61; Jacques and Huff, 1972, p. 15).
		19-24	FELDIF, elevation difference [in thousands of feet] between the base temperature station and any watershed segment (Crawford and Linsley, 1966, pp. 51, 61).
		25-30	FIDNS, index density of new snow (Crawford and Linsley, 1966, pp. 49,61).
		31-36	FFCI, fraction of watershed with forest cover.
		37-42	FDGM, daily ground melt input parameter [inches] (Crawford and Linsley, 1966, p. 61).
		43-48	FWC, water content of snow at saturation [fraction by weight] (Crawford and Linsley, 1966, pp. 49,61).
		49-54	FMPACK, water equivalent of snowpack for complete areal coverage [inches] (Crawford and Linsley, 1966, p. 51).
		55-59	LIQW, liquid water content of the snowpack [inches], and initial value (Jacques and Huff, 1972, p. 15).
		60-64	DEPTH, snow depth [inches], an initial value (Jacques and Huff, 1972, p.15).

NBZ, BZ = 6 LAND SURFACE PARAMETERS

For NBZ, BZ = 6 LAND SURFACE PARAMETERS the next cards required are:

Subroutine	Card number	Columns	Description of input data
	6.1		FORMAT(5F5.1)
		1-5	FK1; the ratio of average segment rainfall to observed rainfall at raingage.

Subroutine	Card Number	Columns	Description of input data
		6-10	FA; the fraction of impervious area with direct hydraulic connection to stream channel.
		11-15	FL; the average length of overland flow (m).
GETSET	6.1	16-20	FSS; the average slope of the overland flow plane (m/m).
		21-25	FNN; the hydraulic roughness factor (Manning's n) for the overland flow plane.
		26-30	; switch to print variable contributing area dynamics. Put 1 in column 30.
GETSET	6.2		FORMAT(3F10.4,5I1)
		1-10	EPXMAX, the maximum interception storage value for the June to September period (cm).
		11-20	EPXMIN, the maximum interception storage value for the December to March period (cm).
		21-30	RNON, a switch to invoke computation of net long-wave radiation (RNLONG) for use in energy balance/E.T. calculation. A value > 1.0 will call the RNLONG function.
		41	CMMO, a switch to invoke conversion of monthly variables to metric units prior to output. A value = 1 will give results in centimeters, a value = 0 or blank gives inches.
		42	CMYR, a switch to invoke conversion of annual summary variables to metric units prior to output. A value = 1 will give results in centimeters, a value = 0 or blank gives inches.
		43*	NAWPLT, a switch to invoke print-plot output of monthly variables over an annual cycle. A value of 0 (or blank) will omit all plots (default option). A value of 1 will generate plots, and requires that the user supplies additional information as described below.

* More detailed explanations of plotting options are presented in the Appendix.

Subroutine	Card number	Columns	Description of input data
		44*	NPRPLT, a switch to invoke print-plot output of PROSPER results. A value = 1 will call for plots of intermediate results, and requires additional information as described below.
		45*	NSPLTS, a switch to invoke the line printer or Calcomp plotter to give 4 day, hourly output of PROSPER results. A value of 0 (or blank) will omit the plots. A value of 1 will generate plots, and requires that the user supplies additional information as described below.
GETSET	P-1 not shown (optional)		FORMAT(I2,(3I2,6A4)) N.B. The following input is required <u>only</u> if NAWPLT = 1
		1-2	NPLTS, Number of plotted graphs desired. (0<NPLTS<10).
		3-4	NU1, The index number of the first variable to be plotted. The "Monthly Summary Variables" table relates index number to the related variable. (0<NU1<24).
		5-6	NU2, The index number of the second variable to be plotted. If only 1 variable is to be plotted, a value NU2 = 0 may be used. (0<NU2<24).
		7-8	NU3, The index number of the third variable to be plotted. (0<NU3<24).
		9-16	TITL (1), The title associated with index number NU1.
		17-24	TITL (2), The title associated with index number NU2.
		25-32	TITL (3), The title associated with index number NU3.
	P-2 not shown (optional)		FORMAT(3I2,6A4) If NPLTS > 1, the following information is required for each additional plot:

* More detailed explanations of plotting options are presented in the Appendix.

Subroutine	Card number	Columns	Description of input data
	P-2	1-2	NU1 (J), The index number of the first MONSUM variable to be plotted on graph J $(J \geq 2)$. $(0 < NU1(J) \leq 24)$.
		3-4	NU2 (J), The index number of the second MONSUM variable to be plotted on graph J. $(0 \leq NU2(J) \leq 24)$.
		5-6	NU3 (J), The index number of the third MONSUM variable to be plotted on graph J. $(0 \leq NU3(J) \leq 24)$.
		7-14	TITL (1, J), The title associated with NU1 (J).
		15-22	TITL (2,J), The title associated with NU2 (J).
		23-30	TITL (3, J), The title associated with NU3 (J).
	not shown (optional)		If NPRPLT = 1, print-plots are made for every 4th hour for up to 11 days. One card is required for each month with plots (Cards $\leq$ 12).
GETSET	P-3		FORMAT(I5,4I2), for first month
	not shown (optional)	1-5	NMPLT, Number months with plot requests $(1 \leq NMPLT \leq 12)$
		6-7	MONPLT, Month with a plot request $(1 \leq MONPLT \leq 12)$
		8-9	PORPLT, if =1, the first third of month is plotted; if =0 or blank, no plots are made.
		10-11	PORPLT, if = 2, the second third of month is plotted; if =0 or blank, no plots are made.
		12-13	PORPLT, if = 3, the last third of month is plotted; if =0 or blank, no plots are made.
	P-4 not shown (optional)		FORMAT(4I2), for additional month with plot requests.
		1-2	MONPLT, Month with plot request $(1 \leq MONPLT \leq 12)$
		3-4	PORPLT, if =1, the first third of month is plotted.
		5-6	PORPLT, if =2, the second third of month is plotted.
		7-8	PORPLT, if = 3, the last third of month is plotted.

Subroutine	Card number	Columns	Description of input data
	not shown (optional)		Additional cards, one per month with the same format as card P-4.
			If NSPLTS = 1, plots are made for every hour in a four day period of month specified (cards ≤ 12).
	P-5		FORMAT(I5,A4,(3I2))
	not shown (optional)	1-5	NMSPLT, Number of months with hourly plots (1≤NMSPLT≤12)
		6-9	MACHIN, Leave blank for line printer hourly plots. Insert MECH for Calcomp plots.
		10-11	MONSPL, Month with the plot request (1≤MONSPL≤12)
		12-13	NBEG, Beginning day for plotting (1≤NBEG≤26)
		14-15	NEND, Ending day for plotting in the month. Note, NEND = (NBEG + 3 + 4N), where N = 0, 1, 2 . . . 7 (5≤NEND≤last day of month)
GETSET	P-6		FORMAT(3I2) for additional month with plot requests.
	not shown (optional)	1-2	MONSPL, Month with plot request (1≤MONSPL≤12) but = above month
		3-4	NBEG, Beginning day for plotting (1≤NBEG≤26)
		5-6	NEND, Ending day for plotting in the month. Note, NEND ≠ (NBEG + 3 + 9N), where N = 0, 1, 2 . . . 7. (5≤NEND≤last day of month)
	not shown (optional)		Additional cards, one per month with the same format as card P-6.

NBZ, BZ = 7 READIN

For NBZ, BZ = 7 READIN, the next cards required are:

READIN	7.1		FORMAT(I1,3X,19A4)
		1	NERR; A switch to indicate when new properties for a basin segment are to be read (NERR≥1). If NERR<1, values are continued from the preceding segment.

Subroutine	Card number	Columns	Description of input data
READIN	7.1	5-80	CASEID; An alphameric descriptive title for the segment.
	7.2		FORMAT(8G10.3)
		1-10, 11-20...	DL(I), I=1,8; the thickness of each of the "PROSPR" soil layers (cm).
	7 3	1-10, 11-20...	THETA(I), I=1,8; the initial volumetric water content of each of the PROSPR soil layers (cm^3/cm^3)
	7.4	1-10	F; the volumetric water content at field capacity for the deepest PROSPR soil layer (cm^3/cm^3)
	7.5	1-10	PAIR; Average air pressure at the basin segment (bars)
		11-20	CPO; the specific heat of air (cal/g^{0}K)
		21-30	XL; Average leaf length (cm)
		31-40	V; Long-term daily average wind speed in the canopy (cm/sec)
		41-50	FOLTYP; the predominant type of foliage; 0.0 for flat leaves, 1.0 for needles
	7.6	1-10, 11-20	AT(I), I=1,2; the root cross-sectional area per unit area of soil for the two soil layers in the root-zone.
		21-30, 31-40	ARAT(I), I=1,2; the fraction of total root biomass in each root-zone layer.
		41-50	RTCON1; the root conductivity factor for root-zone layer 1 (a factor describing the ratio of root conductivity to soil conductivity).
		51-60	RTCON2; the root conductivity factor for root-zone layer 2.
		61-70	RSTEM; the resistance to water flow between the root and the leaf (days).
	7.7	1-10	ALMIN; the leaf area index during the December to March period (ALMIN>0.)
		11-20	ALMAX; the leaf area index during the June to September period (ALMAX>0.)
		21-30	GM; the annual mean energy flow from the ground to the evapotranspiration surface (langleys/day).
		31-40	GV; the peak variation in annual mean energy flow from the ground to the evapotranspiration surface (langleys/day).

Subroutine	Card number	Columns	Description of input data
READIN	7.8	1-10	RLIT; the characteristic resistance of litter to water flow (days).
		11-20	WP1; The soil water content at the wilting point (in layers 1 and 2). The suggested values are the same
		21-30	as the residual (immobile) water contents - unless actual wilting point conditions are expected in the simulation. If simulated water contents fall below WP1 and/or WP2, the soil water content in both root zone layers is instantaneously averaged to maintain numerical stability in subsequent calculations (cm^3/cm^3).
	7.9	1-10	T1; the Julian date (day) for the start of leaf-out.
		11-20	T2; the Julian date (day) for the end of leaf-out.
		21-30	T3; the Julian date (day) for the start of leaf-fall.
		31-40	T4; the Julian date (day) for the end of leaf-fall.
	7.10	1-10	TMS; the minimum surface resistance for the June to September period (sec/cm).
		11-20	TMW; the minimum surface resistance for the December to March period (sec/cm).
		21-30	SIGS; the ratio of the heat loss surface area to the vapor loss surface area during the June to September period (2 for flat leaves, 1.5 for needles).
		31-40	SIGW; the ratio of the heat loss surface area to the vapor loss surface area during the December to March period (1 for deciduous leaf-off; 1.5 for conifers).
		41-50	ALBS; the average albedo during the June to September period.
		51-60	ALBW; the average albedo during the December to March period.

Subroutine	Card number	Columns	Description of input data
READIN	7.11		FORMAT(2G10.3,2I5)
		1-10	SDRAG; the average ratio of wind speed in the canopy to that at the recording anemometer during the June to September period.
		11-20	WDRAG; the average ratio of wind speed in the canopy to that at the recording anemometer during the December to March period.
		21-25	NSL; the number of soil layers to be simulated using PROSPR.
		26-30	NS; the number of soil types with input data contained among the (NSL) PROSPR soil layers. NS≤NSL.
	7.12	1-10	PWPS; the surface water potential (absolute value) beyond which the surface resistance is at the maximum value for the June to September period (bars).
		11-20	PWPW; the surface water potential (absolute value) beyond which the surface resistance is at the maximum value for the December to March period (bars).
		21-30	RESS; the maximum surface resistance during the June to September period (sec/cm).
		31-40	RESW; the maximum surface resistance during the December to March period (sec/cm).
		41-50	POWS; the exponential power parameter that relates surface resistance and surface water potential during the June to September period.
		51-60	POWW; the exponential power parameter that relates surface resistance and surface water potential during the December to March period.
		51-65	[illegible]
ASPECT (called from READIN)	7.13		FORMAT(3F10.5)
		1-10	DEGINC; the inclination of the average segment slope above horizontal (degrees)
		11-20	AZIM; the azimuth of the average segment slope (number of degrees from North in a clockwise direction).
		21-30	DEGLAT; the latitude of the segment, positive for the northern hemisphere and negative for the southern hemisphere (degrees).

Subroutine	Card number	Columns	Description of input data
READIN	7.14		FORMAT(A4)
		1-4	LFORM, a switch to determine use of subroutine SOIL (insert TABLE) or subroutine FORLOK (insert FORM). Subroutine BENLOK (insert LIST)
(The following sequence is used when LFORM = 'FORM')			
	P-7 (not shown)	1-40	FORMAT(10A4) ST, ST1, ST2, ST3, ST4, ST5, ST6, ST7, ST8, ST9 describe location, soil type, horizon 1 (e.g., WALKER BRANCH FULLERTON SOIL A1 HORIZON).
	P-8 (not shown)	1-80	FORMAT(8G10.4) HYCOND(J,JJ), JJ = 1,8. List of up to eight parameters for hydraulic conductivity function. J = 1 for soil horizon 1. HYCOND (1,1) = 1 for equation (29) = 2 for equation (30) = 3 for equation (31) HYCOND (1,2) = saturated soil water content (cm^3/cm^3) HYCOND (1,3) to HYCOND(1,8) - empirical values determined by fitting function to experimental data. (see discussion of Root Zone Evaporation, Transpiration, and Drainage).
READIN	P-9 (not shown)	1-50	FORMAT(8G10.4) SMPPAR (J,JJ), JJ = 1,8. List of up to eight parameters for soil water potential function. J = 1 for soil horizon 1. SMPPAR(1,1) = 1 for equation (32) = 2 for equation (33) = 3 for equation (34) = 4 for equation (35) SMPPAR(1,2) = saturated soil water content(cm^3/cm^3) SMPPAR(1,3) to SMPPAR(1,8) - empirical values determined by fitting equation to experimental data.

Subroutine	Card number	Columns	Description of input data
	P-10 (not shown)		same as card P-7 for J=2
	P-11 (not shown)		same as card P-8 for J=2
	P-12 (not shown)		same as card P-9 for J=2
	P-13 (not shown)		Cards for J=3. The number of cards will be determined by J=NS, where NS is the number of soil horizons with input characteristics. NS is read prior to these data on card 7.11.

(The following sequence is used when LFORM = 'TABLE')

Subroutine	Card number	Columns	Description of input data
SOIL (called by READIN)	7.15		FORMAT(10A4)
		1-40	ST; identification information for the soil type characterized by following information.
	7.16		FORMAT(T1,I2,T11,I2,T21,F5.4,T31,F9.5, T41,F5.3)
		1-2	N; the number of data points to be input with corresponding water content (cm^3/cm^3) and desorption pressure (cm of water).
		11-12	NC; the number of incremented pore classes to be used when calculating conductivities for specific water contents and desorption pressures ($NC \leq 51$).
		21-25	TMAX; the maximum water content possible for the soil (i.e. total soil porosity (cm^3/cm^3).
		31-39	SCON; an experimentally obtained saturated hydraulic conductivity (cm/day)
		41-45	RESWAT; an estimate of the residual (immobile) water (cm^3/cm^3).
	7.17		FORMAT(T1,F6.2,T11,F5.3,T21,F7.6,T31, F4.1,T41,F5.1)
		1-6	SURTEN; the surface tension of soil water (dynes/cm).
		11-15	DENWAT; the density of soil water (gm/cm^3)
		21-27	VISWAT; the viscosity of soil water (gm/sec cm).

Subroutine	Card number	Columns	Description of input data
SOIL		31-34	TEMP; the average temperature of soil water (°C).
		41-45	GRAVTY; the gravitational constant (cm/sec^2).
	7.18		FORMAT(F4.2)
		1-4	EXPON; the factor that accounts for interaction of pore classes (see (Green and Corey, Soil Sci. Soc. Amer. Proc. 35:3-8). (Usually =2).
	7.19		FORMAT(20F4.3)
		1-4, 5-8,...	THETA(J), J=1,N; the (ascending) volumetric water content values that correspond with the desorption pressures that follow. THETA(1) must be the lowest water content (cm^3/cm^3).
	7.20		FORMAT(10F6.1)
		1-6, 7-12,...	DP(J), J=1,N; the desorption pressures (absolute values in descending order) that correspond to the preceding water content values (cm of water).
READIN	7.21-7.26 (depending on soil option chosen)		The preceding card input set is required for all (NS) soil types (see card 7.15).
	7.27	1-80	FILTID; the identification information for the cumulative infiltration data.
	7.28		FORMAT(3F10.5,I5)
		1-10	TSTEP; the time step used in simulating infiltration loss (TSTEP=15.0 minutes).
		11-20	TIMST; the initial equivalent time point on the cumulative infiltration curve (min.).
		21-30	CIFLAS; the initial cumulative infiltration value (corresponds to TIMST) (cm).
		31-35	NRAATS; the number of points to be included in the table of corresponding time and cumulative infiltration values.

Subroutine	Card number	Columns	Description of input data
READIN	7.29-7.30		FORMAT(16F5.2)
		1-5, 6-10,...	CIF(I), I=1, NRAATS; cumulative infiltration amounts corresponding to the (following) times since the start of water input (cm).
	7.31-7.32		FORMAT(16F5.0)
		1-5, 6-10,...	RTIM(I), I=1, NRAATS; elapsed time from beginning point for the cumulative infiltration curve (minutes).

NBZ, BZ = 8 SUBSURFACE PARAMETERS

For NBZ, BZ = 8 SUBSURFACE PARAMETERS, the next cards required are:

GETSET			FORMAT(10D8.0)
	8.1	1-8	AREA1; the minimum (fractional) size of source areas (suggested value = 0.01 if not known).
		9-16	CUT; the drainage rate (cm/day) from source areas when their maximum extent is reached.
		17-24	CUTL; the minimum drainage rate (cm/day) for source areas to contribute to streamflow.
		25-32	WUP; the maximum (fractional) size of source areas. AREA1≤WUP≤1.0
		33-40	RNTL; the number of soil-water transmission layers between the saturated zone and the region simulated by PROSPR. (≤5).
	8.2	1-8, 9-16,etc.	SBD(I) (for I=1, RNTL); the thickness of each soil-water transmission layer (cm).
	8.3	1-8, 9-16,etc.	SSG(I) (for I=1, RNTL); the initial volumetric water content of each soil-water transmission layer (cm^3/cm^3).
	8.4	1-8	PORE; the volumetric pore space for any transmission layer (cm^3/cm^3).
		9-16, 17-24	KSAT(1), SA(1) Parameters that characterize three segments of

Subroutine	Card number	Columns	Description of input data	
		25-32, 33-40	KSAT(2), SA(2)	the water content versus hydraulic conductivity
		41-48, 49-56	KSAT(3), SA(3)	relation for transmission layers. (K=KSAT*EXP(SA*(Pore-θ))).
		57-63	WCK1	WCK1 and
		65-72	WCK2	WCK2 are the two water content (θ) values where the three curves join, and the relations are given for increasing values of K and θ.
	8.5		FORMAT(D10.5,2F10.5)	
		1-10	KSGW; the constant that relates ground-water flow to storage (hour^{-1}).	
		11-20	SGW; the volume of water (per unit area) in ground water storage (cm).	
		21-30	K24L; the fraction of groundwater lost or gained by seepage across the watershed divide ($K24L \leq 1.0$).	

9 RDCHM (not shown)

This statement will cause subroutine RDCHM to be called and a minimum of 11 cards to be read for input data to the soil chemistry model, SCEHM. The SCEHM model documentation (Begovich and Jackson 1974) describes the model and data requirements. An appendix in Luxmoore et al., 1976b describes the current input data format requirements which have been changed from the original in developing a coupled model for solute dynamics in vegetation and litter.

10 RDCER (not shown)

This statement will cause subroutine RDCER to be called and a minimum of 20 cards to be read for input data to the forest biomass model called CERES. The CERES model documentation (Dixon et al., 1976) describes the input data and format requirements.

11 RDDRY

This statement will cause subroutine RDDRY to be called and a minimum of 8 cards to be read for the data input to the DRYADS and DIFMAS models of solute uptake and accumulation by vegetation and litter. The documentation of the models (Luxmoore et al.,1976b) describes the input data and formats.

NBZ, BZ = 12 DEWPOINT-BIMONTHLY

Subroutine	Card number	Columns	Description of input data

FOR NBZ, BZ = 12 DEWPOINT-BIMONTHLY, the next cards required are:

BIMON	12.1-12.2		FORMAT(A1,6X,2I2,I1,12F5.0)
	(not shown)	1	X; any character but $ is ignored. The $ character signals that all bimonthly average dewpoint temperature data have been input, and control will return to subroutine GETSET.
		2-7	blank; may be used for a data card identification code.
		8-9	Y; an integer representing the last 2 digits of the water year.
		10-11	M; a dummy variable, may be blank.
		12	K; a single digit: = 1 for months 1 through 6, = 2 for months 7 through 12.
		13-17	DATA; the average daily dew point temperature [°F] for days 1 through 15 of month 1 (January) or 7 (July), depending on the value of K.
		18-22	DATA; the average daily dew point temperature [°F] for days 16 through the end of month 1 (or 7).
		...	...
		68-72	DATA; the average daily dewpoint temperature [°F] for days 16 through the end of month 6 (or 12).
		73-80	may be blank or used for identification purposes.

NBZ, BZ = 13 RADIATION-BIMONTHLY

For NBZ, BZ - 13 RAD BIMONTHLY, the next cards required are:

BIMON	13.1-13.2		FORMAT(A1,6X,2I2,I1,12F5.0)
	(not shown)	1	X; any character but $ is ignored. The $ character signals that all bimonthly radiation data have been read and control should return to GETSET.
		2-7	blank; may be used for a card identification code.
		8-9	Y, an integer representing the last 2 digits of the water year.

Subroutine	Card number	Columns	Description of input data
		10-11	M, a 2-digit integer, not used by main entry BIMON.
		12	K, a single digit, = 1 for months 1 through 6, = 2 for months 7 through 12.
		13-17	Mean integrated total daily radiation value for days 1 through 15 [Langleys/day] of month 1 (or 7).
		18-22	Mean integrated total daily radiation value for days 16 through 31 [Langleys/day] of month 1 (or 7).
		...	...
		63-67	Mean integrated total daily radiation value for days 1 through 15. [Langleys/day] of month 6 (or 12).
		68-72	Mean integrated total daily radiation value for days 16 through 31 [Langleys/day] of month 6 (or 12).
		73-80	Blank.

FOR NBZ, BZ = 14 WINDS-BIMONTHLY, the next cards required are:

Subroutine	Card number	Columns	Description of input data
BIMON	14.1-14.2		FORMAT(A1,6X,2I2,I1,12F5.0)
	(not shown)	1	X; any character but $ is ignored. The character $ signals that all bimonthly average wind speed data have been entered, and control will return to subroutine GETSET.
		2-7	May be used for a data card identification code.
		8-9	Y; an integer that represents the last 2 digits of the water year.
		10-11	M; a dummy variable, may be blank.
		12	K; a single digit, = 1 for months 1 through 6. = 2 for months 7 through 12.
		13-17	DATA; the average daily wind speed [mph] for days 1 through 15 of month 1 (January) or 7 (July), depending upon the value of K.
		...	...
		68-72	DATA; the average daily wind speed [mph] for days 16 through the end of month 6 (or 12).
		73-80	may be blank or used for identification purposes.

Subroutine	Card number	Columns	Description of input data
for NBZ, BZ = 15 EVAPO			
EVAPO	15.1		FORMAT(2F10.4)
		1-10	ANHT, anemometer height [feet] above ground level at the recording site.
		11-20	ANX, exponent in power relationship used to adjust wind movement to the 2 ft level. The recommended range for ANX is 0.29 to 0.61, usually 0.30.
		21-80	Blank.

The final input card for any land segment is:

Subroutine	Card number	Columns	Description of input data
GETSET	6 (last for any segment)		FORMAT(I2,1X,A4)
		1-2	<u>NBZ</u> A control switch variable. The value 16 initiates simulation for the segment.
		4-7	<u>BZ</u> A descriptive character string. Any characters may be used so long as they are not monitor controls.

<u>Example listing of a data set for terrestrial segments</u> (Table 18)

The following six pages contain input data for simulating the hydrology of two terrestrial segments. The card numbers and input options shown on these pages correspond with specifications given in the preceding section. One should note that since the climatic data (air temperature, dew-point temperature, solar radiation, and wind speed) are the same for both segments, they are not repeated in the input list for the second segment. The effect is that they will be carried over from the first segment without change.

Table 18. Example listing of a data set for terrestrial segments

	CARD NUMBER	
GENERAL	1	WALKER BRANCH WATERSHED LAND LINK 2 2
	2	1 2
BASIN	3	LAND SURFACE HYDROLOGIC SIMULATION
SPECIFICATIONS	4	10 73 10 74 10 74 WBW SIMULATION INPUT
SEGMENT ID	5	1 1 73 74 EAST FORK
NBZ, BZ	6	1 AIR TEMP (DAILY MAX/MIN) DEG. F.
AIR TEMPERATURE	1.1	2 THIS VALUE INDICATES THAT BOTH MAX. & MIN. TEMP ARE RECORDED ON DATE OF OCCUR.
		T 73101 71 64 78 64 78 64 82 61 75 62 78 58 76 63 76 62 78 60 78 60 78 58
		T 73102 77 57 75 57 76 52 79 46 74 44 64 36 71 35 73 41 78 41 76 46 75 48
		T 73103 74 47 74 47 74 45 77 49 75 42 62 41 54 41 49 43 52 44 0 0 0 0
		T 73111 66 40 70 45 73 54 69 54 61 34 48 31 48 37 48 35 48 31 41 27 51 25
		T 73112 59 27 66 31 72 47 68 54 55 35 55 30 59 33 67 49 68 49 67 46 63 41
		T 73113 68 44 67 57 69 50 63 49 70 59 64 40 52 32 60 28 0 0 0 0 0 0
		T 73121 66 31 63 32 60 42 63 43 62 40 51 30 42 29 46 27 49 26 40 26 32 15
		T 73122 44 31 59 40 39 36 41 35 36 26 32 19 31 16 49 24 46 30 30 17 34 13
	1.10	T 73123 44 25 57 30 51 40 68 47 55 31 52 24 50 37 46 31 53 45 0 0 0 0
		T 74 11 29 44 30 37 37 45 34 41 35 40 40 47 30 47 29 46 45 55 54 64 36 60
		T 74 12 26 35 25 41 36 40 39 49 49 61 54 69 52 65 52 57 52 62 43 63 37 67
		T 74 13 44 56 42 47 43 60 52 66 45 66 45 59 37 59 34 62 37 67
		T 74 21 37 67 53 62 35 56 26 40 22 53 40 47 36 50 27 36 25 32 22 47 30 45
		T 74 22 27 60 36 60 51 59 39 55 43 53 31 54 28 55 39 56 34 51 30 63 36 55
		T 74 23 26 51 25 56 19 25 13 41 20 55 34 50 0 0 0 0 0 0
		T 74 31 49 67 50 67 52 69 56 71 52 68 51 63 53 77 51 79 46 79 54 73 54 70
		T 74 32 45 68 38 53 32 60 33 65 37 58 31 47 29 51 50 61 49 54 33 56 27 55
		T 74 33 31 66 33 53 30 54 44 63 42 59 52 69 51 69 43 64 39 70
	1.20	T 74 41 49 82 58 75 56 77 54 73 40 52 37 58 35 67 39 62 36 55 30 63 40 72
		T 74 42 54 66 56 72 60 79 44 60 34 64 40 58 33 66 39 73 45 76 51 75 58 66
		T 74 43 47 70 43 59 34 71 41 75 44 81 52 83 54 82 54 81 0 0
		T 74 51 63 75 56 71 61 81 59 66 44 61 42 71 40 65 40 73 54 75 58 69 57 82
		T 74 52 56 73 48 73 49 84 61 70 62 80 60 87 63 86 63 85 64 86 64 75 62 79
		T 74 53 58 79 53 82 50 77 51 60 46 70 46 78 60 82 62 81 61 85
		T 74 61 65 76 57 72 54 80 58 83 54 81 61 72 62 85 63 83 64 83 58 82 52 79
		T 74 62 57 79 52 80 54 83 58 79 50 77 46 73 45 79 54 84 64 87 67 88 70 89
		T 74 63 60 74 56 72 48 71 44 75 52 76 54 66 54 83 52 84 0 0
		T 74 71 60 86 60 89 62 90 64 86 66 82 66 85 67 84 67 87 65 89 65 88 66 89
	1.30	T 74 72 64 89 0 89 58 91 60 93 64 88 61 92 66 92 67 82 67 88 62 87 59 86
		T 74 73 68 74 68 88 65 87 70 80 69 89 64 88 64 88 57 87 56 87
		T 74 81 57 90 63 87 67 76 62 81 55 81 62 83 63 78 68 79 68 84 68 87 67 85
		T 74 82 65 77 64 85 67 88 67 87 68 82 66 88 64 85 62 85 60 85 60 80 61 82
		T 74 83 63 86 64 86 64 88 65 90 68 87 67 82 70 85 68 77 67 83
		T 74 91 67 84 67 78 58 69 56 67 52 76 59 71 61 75 64 74 64 80 64 79 63 85
		T 74 92 63 84 66 80 60 71 55 75 50 77 54 74 53 80 55 83 56 82 56 73 46 69
		T 74 93 41 64 46 60 50 66 58 75 60 68 62 80 46 70 39 74 0 0
	1.38	$

Table 18 (continued)

NBZ, BZ — 6 — CARD NUMBER

2 DEW POINT TEMPERATURE (DAILY AVG.) DEG. F.

Card number													
2.1	D	73101	63.5	63.5	64.0	61.5	59.5	58.5	60.0	61.0	60.0	60.0	58.0
	D	73102	55.0	58.0	55.0	49.5	43.5	31.5	38.5	42.5	46.0	46.5	49.0
	D	73103	50.0	49.0	47.5	50.5	47.0	47.5	36.0	40.5	44.0		
	D	73111	40.0	45.0	53.5	53.5	44.0	26.5	32.0	40.5	33.0	21.5	25.5
	D	73112	31.5	33.0	45.5	53.0	39.0	32.0	37.5	46.5	49.5	49.0	45.5
	D	73113	49.0	56.0	53.0	54.0	59.5	43.5	26.0	31.0	0.0		
	D	73121	35.5	37.0	41.5	48.0	43.0	28.0	26.0	27.0	27.5	22.5	13.5
	D	73122	23.0	38.0	30.0	32.5	25.0	14.5	16.5	23.0	34.0	17.5	17.0
	D	73123	26.0	32.5	41.5	47.5	32.5	28.0	38.0	32.5	45.0		
2.10	D	74 11	31.0	29.5	39.0	33.5	34.5	39.5	35.5	33.5	46.5	54.0	43.0
	D	74 12	23.0	21.5	31.5	41.5	51.5	51.5	51.0	50.0	51.0	44.5	41.0
	D	74 13	46.0	42.0	45.5	53.0	47.0	45.5	40.5	39.0	36.5		
	D	74 21	40.0	52.5	40.0	20.5	23.5	35.5	39.5	24.0	18.5	23.5	22.0
	D	74 22	23.0	37.0	48.5	38.5	33.0	23.5	29.5	37.5	30.5	38.5	36.5
	D	74 23	25.5	26.5	15.0	14.0	20.0	31.5	0.0	0.0	0.0		
	D	74 31	46.0	48.0	47.5	46.5	49.5	51.5	53.0	50.0	46.5	51.0	44.0
	D	74 32	45.0	25.5	23.5	32.5	35.0	23.5	27.5	44.0	46.5	36.5	24.5
	D	74 33	34.5	27.0	25.0	39.0	42.5	50.0	50.0	38.5	38.0		
	D	74 41	51.5	50.5	59.0	52.0	33.5	27.5	30.0	43.5	27.5	34.0	37.0
2.20	D	74 42	49.0	57.0	51.5	38.5	39.0	40.5	38.0	41.5	42.5	48.5	54.0
	D	74 43	40.0	31.5	32.0	38.0	47.0	52.0	51.5	56.5	0.0		
	D	74 51	56.0	59.5	57.5	51.5	46.5	39.5	36.0	47.5	54.0	58.5	61.5
	D	74 52	48.0	46.5	53.0	59.5	63.0	63.5	66.0	66.5	64.0	63.0	63.0
	D	74 53	59.0	57.0	50.0	51.5	53.0	51.0	61.5	65.0	63.5		
	D	74 61	64.5	58.0	55.5	58.5	58.0	62.0	64.5	65.5	65.5	60.5	54.0
	D	74 62	56.0	56.0	58.0	61.5	56.0	48.5	52.5	61.0	68.5	70.5	67.0
	D	74 63	59.5	55.0	53.5	50.0	57.0	57.5	57.0	57.5	0.0		
	D	74 71	63.5	64.5	68.0	67.0	68.0	67.0	69.5	68.5	67.0	69.0	68.0
	D	74 72	63.0	33.0	62.0	65.5	65.0	65.5	68.5	69.5	71.5	64.0	63.5
2.30	D	74 73	66.5	70.5	69.0	69.5	70.5	68.0	66.5	59.0	59.0		
	D	74 81	61.0	66.5	68.5	67.0	58.5	65.0	65.5	68.5	70.0	70.0	68.0
	D	74 82	66.0	65.0	69.0	70.0	69.5	67.5	68.0	65.0	62.5	62.0	64.5
	D	74 83	66.5	67.5	68.0	69.5	70.5	70.5	71.0	69.0	70.5		
	D	74 91	68.0	69.0	59.0	53.0	56.0	60.0	64.0	66.0	65.5	66.0	66.5
	D	74 92	67.5	69.5	61.5	59.0	56.0	59.0	57.5	60.5	62.5	59.0	48.5
	D	74 93	43.5	49.0	52.5	57.0	62.0	63.5	54.5	44.0	0.0		
2.37	$												

DEW POINT TEMPERATURE

Table 18 (continued)

NBZ, BZ	CARD NUMBER														
	6	3 SOLAR RADIATION (DAILY TOTAL) LANGLEYS													
SOLAR RADIATION	3.1	S	73101	107.8	348.7	279.0	415.9	310.7	384.5	374.8	354.7	385.3	379.9	392.8
		S	73102	462.0	326.2	476.5	479.4	429.0	481.6	448.5	443.1	429.5	430.4	408.1
		S	73103	382.9	365.7	376.0	364.0	401.2	51.6	317.8	42.2	39.4		
		S	73111	370.7	369.5	271.4	239.4	130.8	310.5	70.4	48.4	320.4	366.5	352.9
		S	73112	323.3	310.1	246.6	101.9	303.6	335.7	190.5	274.4	196.5	146.7	215.5
		S	73113	171.7	94.7	191.9	57.5	46.9	144.7	309.7	305.6	0.0		
		S	73121	287.1	269.3	153.3	43.5	102.0	263.7	206.5	165.2	271.3	116.4	226.4
		S	73122	84.8	168.4	66.2	53.4	30.5	272.7	127.8	210.8	23.3	267.8	242.0
		S	73123	104.8	210.8	31.8	92.1	267.9	265.9	25.2	186.8	23.7		
	3.10	S	74 11	49.6	35.5	30.2	62.3	40.0	32.7	185.4	116.7	48.0	23.3	117.6
		S	74 12	256.4	195.4	32.3	49.8	61.0	145.5	134.4	53.6	88.1	283.2	311.2
		S	74 13	50.0	59.3	189.9	125.0	315.7	73.4	238.8	325.0	305.0		
		S	74 21	345.3	68.4	100.6	247.8	359.7	30.8	94.5	91.5	263.5	294.1	404.2
		S	74 22	403.6	219.0	108.7	280.2	193.1	447.6	333.1	129.9	439.3	325.9	66.3
		S	74 23	442.3	332.5	309.9	495.0	481.4	71.6	0.0	0.0	0.0		
		S	74 31	354.3	264.5	291.3	397.6	82.1	117.6	427.0	422.0	444.5	341.6	201.6
		S	74 32	389.1	526.4	521.4	384.0	192.6	333.5	162.6	97.1	98.6	114.2	568.3
		S	74 33	466.4	498.0	496.9	335.4	152.6	348.8	398.2	488.9	577.6		
		S	74 41	498.0	540.5	209.3	163.3	391.2	639.8	582.9	246.4	582.1	622.3	529.3
	3.20	S	74 42	176.6	367.5	377.6	565.0	627.3	436.7	521.3	552.6	626.8	509.6	150.5
		S	74 43	653.5	535.0	669.9	672.8	637.8	605.0	630.6	528.0	0.0		
		S	74 51	538.0	183.1	582.1	227.1	133.4	463.0	686.0	516.0	424.2	250.4	407.2
		S	74 52	578.0	642.0	673.0	122.0	313.4	486.5	422.5	415.2	573.2	248.5	342.5
		S	74 53	581.3	530.1	671.9	108.2	567.1	646.3	445.4	314.7	425.7		
		S	74 61	212.5	493.8	699.7	586.0	482.5	159.6	453.7	429.2	499.3	541.4	564.4
		S	74 62	595.5	694.2	655.5	391.8	627.3	611.1	679.6	593.5	444.8	397.3	523.5
		S	74 63	261.4	552.9	445.8	718.6	414.1	267.4	631.7	626.9	0.0		
		S	74 71	586.9	644.8	512.2	563.1	425.0	500.3	329.7	458.0	393.3	511.0	498.2
		S	74 72	679.6	668.9	660.6	548.1	617.8	575.2	558.1	235.4	422.3	532.8	497.0
	3.30	S	74 73	123.5	484.3	493.7	255.2	607.5	571.2	484.9	647.3	639.5		
		S	74 81	595.0	397.7	181.2	332.1	602.1	400.7	200.1	191.5	334.7	431.2	363.8
		S	74 82	217.6	473.0	474.5	502.7	226.8	500.9	334.3	511.8	574.1	300.6	359.7
		S	74 83	408.0	440.4	459.1	451.4	263.0	296.3	306.0	117.2	284.1		
		S	74 91	351.2	266.7	208.3	352.2	460.3	262.0	249.8	215.4	331.7	264.0	389.2
		S	74 92	255.4	270.0	122.0	481.9	378.1	195.0	481.9	463.1	419.9	146.5	467.4
		S	74 93	462.6	177.2	224.3	375.4	98.0	354.0	436.3	470.4	0.0		
	3.37	$												

Table 18 (continued)

NBZ, NB	6 (CARD NUMBER)	4	WIND SPEED (DAILY AVERAGE) MPH										
WIND SPEED	4.1	W	73101	1.50	2.04	1.38	1.46	3.63	2.75	2.67	1.50	1.42	1.67	2.25
		W	73102	1.33	3.13	2.46	1.83	3.17	1.38	1.50	0.88	1.04	1.71	1.17
		W	73103	1.13	1.21	1.33	1.00	1.75	1.96	4.83	6.29	3.08		
		W	73111	4.42	6.21	2.46	1.33	4.17	2.88	1.92	1.67	5.33	6.46	2.33
		W	73112	1.58	1.92	3.33	6.25	3.50	2.79	3.00	1.71	2.83	4.17	1.29
		W	73113	1.63	4.33	7.08	3.13	3.08	9.42	3.71	3.42	0.0		
		W	73121	0.54	1.92	1.38	2.88	7.50	4.04	4.00	3.63	3.38	5.75	2.25
		W	73122	2.00	7.46	3.88	2.71	7.50	4.63	2.29	1.21	3.96	5.79	2.00
		W	73123	2.00	2.04	1.63	6.33	5.75	2.13	3.21	4.08	1.58		
	4.10	W	74 11	4.80	4.80	1.20	2.90	1.70	3.80	2.00	4.40	2.80	5.50	5.00
		W	74 12	4.60	3.80	3.80	3.70	4.80	2.40	3.00	3.60	2.10	3.50	2.30
		W	74 13	4.00	2.40	1.20	6.60	4.30	3.40	1.00	1.50	3.90		
		W	74 21	4.40	3.30	3.70	3.50	1.90	2.40	5.50	4.20	3.90	4.90	2.80
		W	74 22	4.40	3.80	2.10	3.00	5.60	2.60	1.10	6.40	2.50	2.40	12.70
		W	74 23	1.10	6.50	4.40	1.40	2.60	3.20	0.00	0.00	0.00		
		W	74 31	4.20	4.20	6.40	9.70	5.60	1.20	3.20	2.50	1.80	4.60	4.60
		W	74 32	6.90	7.20	4.10	4.60	6.30	4.60	1.30	2.90	2.30	4.00	2.30
		W	74 33	2.70	6.50	6.20	4.70	1.70	2.10	2.30	7.00	2.00		
		W	74 41	8.20	3.10	3.30	4.50	7.50	4.50	6.40	7.40	3.10	1.30	2.50
	4.20	W	74 42	4.30	3.70	6.70	4.00	2.50	3.50	1.00	1.10	3.50	4.70	5.20
		W	74 43	5.30	5.60	1.80	1.70	1.30	2.50	3.10	3.70	0.00		
		W	74 51	2.60	2.20	5.40	3.20	3.30	3.10	3.50	3.70	3.20	2.40	3.70
		W	74 52	4.10	1.60	4.20	3.20	2.30	3.10	2.30	2.40	2.30	2.10	3.00
		W	74 53	3.10	2.70	2.40	3.50	2.40	2.90	5.10	3.00	4.30		
		W	74 61	4.40	3.50	4.70	2.30	3.00	2.00	3.30	2.30	3.50	6.50	2.70
		W	74 62	2.60	2.40	1.80	4.30	5.20	2.10	3.30	4.50	3.80	5.30	7.60
		W	74 63	6.50	6.10	3.80	3.80	4.00	3.40	3.10	4.50	0.00		
		W	74 71	4.30	3.40	2.80	3.60	4.00	1.90	2.00	2.30	2.20	2.40	2.90
		W	74 72	4.90	2.90	3.30	3.00	5.50	4.10	3.90	4.80	2.80	3.80	3.80
	4.30	W	74 73	4.80	3.50	3.10	3.50	3.30	2.90	4.30	2.60	2.80		
		W	74 81	3.20	3.50	5.00	4.60	3.60	3.30	2.50	2.70	3.50	2.40	5.30
		W	74 82	3.60	3.60	4.20	2.90	2.80	4.30	3.30	4.30	4.80	3.20	3.00
		W	74 83	2.20	2.50	3.00	2.40	3.00	2.80	6.30	6.00	4.10		
		W	74 91	3.70	4.00	6.00	6.70	6.70	6.40	3.00	4.40	3.00	3.50	2.00
		W	74 92	2.20	2.70	3.00	2.40	3.50	0.80	1.90	1.10	1.80	3.80	4.40
		W	74 93	5.50	3.10	2.70	2.10	2.50	3.30	5.90	2.80	0.00		
	4.37	$												

Table 18 (continued)

	CARD NUMBER	
NBZ, BZ	6	6 LAND SURFACE PARAMETERS
SURFACE	6.1	1.0 0.03 25. 0.24 0.4
	6.2	0.129 0.072 11
NBZ, BZ	6	7 PROSPER READ
SOILS AND VEGETATION	7.1	1 EAST FORK WBW SOILS AND VEGETATION PARAMETERS
	7.2	40. 50. 60.
	7.3	.1991 .2492 .2466
	7.4	.308
	7.5	0.9853 .24 10. 100. 0.0
	7.6	.004 .0015 .90 .10 1.0E06 1.0E06 5000.
	7.7	0.001 6.3 0.0 20.
	7.8	3.0E05 0.159 0.221
	7.9	110. 151. 262. 290.
	7.10	1. 7. 2. 1. 0.22 0.16
	7.11	0.47 0.64 3 2
	7.12	20. 10. 50. 100. -0.5 -0.5
	7.13	13. 180. 36. 1.
	7.14	TABLE OF SOIL PROPERTIES IS USED TO CHARACTERIZE SOILS
	7.15	FULLERTON AVG. A2 SOILS - WALKER BRANCH
	7.16	9 50 0.341 1440. 0.0
	7.17	73.49 0.999 0.1138 15. 980.
	7.18	2.0
	7.19	159 182 202 216 238 267 305 334 341
	7.20	15000. 5000. 1000. 667. 333. 100. 25. 5. 0.
	7.21	FULLERTON AVG B22T SOILS - WALKER BRANCH
	7.22	9 50 0.364 720. 0.0
	7.23	73.49 0.999 0.1138 15. 980.
	7.24	2.0
	7.25	221 238 253 262 271 308 334 358 364
	7.26	15000. 5000. 1000. 667. 333. 100. 25. 5. 0.
	7.27	CUMULATIVE INFILTRATION RELATION FOR TCA METHOD
	7.28	15. 0. 0. 21
	7.29	0 25 50 75 100 200 400 600 800 1000 1200 1400 1600 1800 2000 2200
	7.30	2400 2600 2800 3000 6000
	7.31	0. 0.15 0.83 1.75 2.74 6.8215.0023.2931.5739.8648.1556.4464.7273.0181.3089.59
	7.32	97.87106.2114.4122.7247.0
NBZ, BZ	6	8 SUBSURFACE PARAMETERS
SUB-SURFACE	8.1	0.01 10. 1.3 0.7 2.
	8.2	180. 180.
	8.3	.277 .277
	8.4	.364 19290.1140.6705 138.936 79.0039 380.00 111.460 0.284 0.333
	8.5	0.03 0.12 0.30
NBZ, BZ	6	15 LAKE EVAPORATION
LAKE	15.1	100. 0.24
NBZ, BZ	5	16 GO

Table 18 (continued)

SEGMENT ID	CARD NUMBER	
SEGMENT ID	5	2 1 73 74 WEST FORK - WBW INPUT PARAMETERS AND STATE VARIABLES
NBZ, BZ	6	6 LAND SURFACE
SURFACE	6.1	1.0 0.03 25. 0.23 0.4
	6.2	0.129 0.072 11
NBZ, BZ	6	7 PROSPER READ
SOILS AND VEGETATION	7.1	1 WEST FORK WBW SOILS AND VEGETATION PARAMETERS
	7.2	50. 50. 50.
	7.3	.205 .194 .194
	7.4	.228
	7.5	0.9853 .24 10. 100. 0.0
	7.6	.004 .0015 .90 .10 1.0E06 1.0E06 5000.
	7.7	.001 6.3 0.0 20.
	7.8	3.0E05 .179 .176
	7.9	110. 151. 262. 290.
	7.10	1. 7. 2. 1. .22 .16
	7.11	.47 .64 3 2
	7.12	20. 10. 50. 100. -0.5 -0.5
	7.13	13. 150. 36. 1.
	7.14	A TABLE OF SOIL PROPERTIES IS USED TO CHARACTERIZE SOILS
	7.15	BODINE AVG. A21 SOIL -WBW
	7.16	9 50 0.373 1440. 0.
	7.17	73.49 0.999 0.1138 15. 980.
	7.18	2.0
	7.19	179 187 205 216 242 279 329 364 373
	7.20	15000. 5000. 1000. 667. 333. 100. 25. 5. 0.
	7.21	BODINE AVG. B2T SOIL -WBW
	7.22	9 50 0.291 1440. 0.
	7.23	73.49 0.999 0.1138 15. 980.
	7.24	2.0
	7.25	176 184 194 199 209 228 257 284 291
	7.26	15000. 5000. 1000. 667. 333. 100. 25. 5. 0.
	7.27	CUMULATIVE INFILTRATION RELATION FOR TCA METHOD
	7.28	15. 0. 0. 21
	7.29	0 25 50 75 100 200 400 600 800 1000 1200 1400 1600 1800 2000 2200
	7.30	2400 2600 2800 3000 6000
	7.31	0. 0.15 0.83 1.75 2.74 6.8215.0023.2931.5739.8648.1556.4464.7273.0181.3089.59
	7.32	97.87106.2114.4122.7247.0
NBZ, BZ	6	8 SUBSURFACE PARAMETERS
SUB-SURFACE	8.1	.01 12. 1.8 0.7 2.
	8.2	180. 180.
	8.3	.212 .212
	8.4	.2916536730.228.06886202.134142.1391 700.00104.5259 0.210 0.233
	8.5	0.03 0.12 -0.46
NBZ, BZ	6	16 GO
LBL	3	ENDRUN

Simulation of Open Channel Flow

Formats and Example

The channel flow component of the TEHM has been taken directly from the WHTM, and has been described in detail by Patterson et al., 1974. For sake of completeness, an abbreviated description of the options used for simulating flow in rectangular channel reaches is presented here. The following documentation describes the cards contained in the example data set used for Walker Branch Watershed simulations, which is shown at the end of this section (Table 19).

Subroutine	Card number	Columns	Description of input data
OLDMAI	1		FORMAT(7A4,14X,2I4)
		1-28	WATSHD The name of the watershed that will be simulated.
		46	GAGES The number of basin segments that have been used to simulate the terrestrial hydrology. $1 \leq GAGES \leq 7$.
		50	REACHS The number of channel reaches that will be used to represent the basin drainage system. $1 \leq REACHS \leq 7$.
OLDMAI	2		FORMAT(20(I3,1X))
		1-3	STAN(1) The abbreviated identification number associated with a raingage used in the preceding simulations (right-justified).
		5-7	STAN(2) The abbreviated identification number associated with a second raingage used in preceding simulations (right-justified).
		etc.	etc.
OLDMAI	3		FORMAT(A4)
		1-4	LBL The character string command that selects the channel simulation sub-programs. CHANNEL SIMULATION, beginning in column 1 is used. (Note: only the first four characters are read.)

Subroutine	Card number	Columns	Description of input data
CHANL	4		FORMAT(A4)
		1-4	The character string INITIALIZE CHANNEL SIMULATION, beginning in column 1, is used to indicate that channel properties will be included in the following input (as opposed to reading them from a file). Only the first four characters are read.
	5		FORMAT(I5,F5.2,I5)
		1-5	IHT The number of points in an interpolation table that relates stage and discharge for each reach (right-justified). $1 \le IHT \le 100$.
		6-10	INCR The change in flow depth between each value in the stage-discharge table (right-justified).
		11-15	NTFLO The number of hourly flow values in a moving average that is used to test for storm flow conditions (right-justified). Experience indicates that 6 is a reasonable value.

(The following 5-card sequence represents specification of the properties of the two reaches (two cards each) plus a termination of reach specifications card (number 10). The length of this section will depend upon the value of the parameter GAGES. The number of cards is equal to twice the value of GAGES plus one.)

Subroutine	Card number	Columns	Description of input data
INITCH	6		FORMAT(A1,I4,I5,A4,1X,I3,I2,14I1, 7F6.1,I4)
		2-5	RCH The integer identifying number for the reach that is characterized.
		6-10	LIKE The identifying number for a reach that has the same geometry and roughness as the reach currently being characterized. The values for parameters W1, W2, H, SFP, NCH, and NFP for reach RCH will be set equal to those for reach LIKE. (right-justified).
		11-14	TYP The alphameric descriptor for the type of reach geometry. RECT stands for a rectangular (or trapezoidal) reach.

Subroutine	Card number	Columns	Description of input data
		16-18	TRIBTO The identifying number for the reach that receives flow from reach RCH (right-justified). Note that the outflow point is represented by a dummy reach that is represented by the number REACHES + 1.
		19-20	INGAGE The number of basin segments that supply inflow to reach RCH.
		21-24	CHAN Up to seven pairs of segment and associated abbreviated raingage identifying numbers that specify the terrestrial simulation output files to be used as input for reach RCH. The number of pairs is specified by INGAGE.
		35-76	CAR Up to seven (real) numbers, each occupying 6 columns, that designate the basin segment areas (mi^2) that contribute to reach RCH. The area for segment 1 lies in columns 35-40, segment 2 area occupies columns 41-46, etc.
	7		FORMAT(F7.1,3X,F6.1,1X,F6.1,27X,6F5.1)
		1-7	LENGTH The length of reach RCH (feet).
		11-16	ELUP The mean sea level elevation of the upstream end of the channel bed in reach RCH (feet).
		18-23	ELDN The mean sea level elevation of the downstream end of the channel bed in reach RCH (feet).
		51-55	W1 The average width of the channel bed at zero flow (feet).
		56-60	W2 The average width of the stream channel at bankfull stage (feet).
		61-65	H The average depth of the natural channel at bankfull stage (feet).
		66-70	SFP The average lateral slope of the flood plain toward the channel (ft/ft).
		71-75	NCH The hydraulic roughness coefficient (Manning's n) for the channel ($ft^{1/6}$).
		76-80	NFP The hydraulic roughness coefficient (Manning's n) for the flood plain ($ft^{1/6}$).

Subroutine	Card number	Columns	Description of input data
INITCH	8		FORMAT(A1,I4,I5,A4,1X,I3,I2,14I1, 7F6.1,I4)
		2-5	RCH The identification number of the second reach to be characterized.
		6-10	LIKE The number 1 (for the example input set in Table 19) could be used to avoid re-specifying geometry and roughness parameters, since they are the same as for the first reach. However, we have chosen to re-enter the data for the input example.
		11-14	TYP See card 6.
		16-18	TRIBTO See card 6.
		19-20	INGAGE See card 6.
		21-24	CHAN See card 6.
		35-76	CAR See card 6.
INITCH	9		The format and variables are the same as those specified for card 7, and pertain to the second reach to be characterized.
INITCH	10		FORMAT(A1, etc.)
		1	DOLLAR The character $, when placed in column one, signals that input data are complete for each of the reaches to be considered in the simulation.
TIMEWD	11		FORMAT(6(I2,1X))
		1-2	TIMES(1) The starting month for which channel simulations are desired. This value need not correspond to the terrestrial simulation period (i.e., it may be shorter).
		4-5	TIMES(2) The calendar year corresponding to TIMES(1).
		7-8	TIMES(3) The month immediately following the end of the desired simulation period; TIMES(3)>TIMES(1).
		10-11	TIMES(4) The calendar year associated with TIMES(3); TIMES(4)$\geq$ TIMES(2).

Subroutine	Card number	Columns	Description of input data
FLOWIN	12,13		FORMAT(A1,I4,I6,I5,2I3,2X,2A4,4X, F8.0,I4)

(For each reach where detailed printed output is desired, a single card containing the variables listed below is included. The final card in the sequence always contains only a $ character in column 1).

Subroutine	Card number	Columns	Description of input data
		2-5	INPUT(1) The identifying number (RCH) for a reach where detailed printed output is desired.
		6-11	CHAN(RCH,IO) A flag that signals when observed flow data for reach RCH are to be included as input to the simulation. When columns 6-11 contain 0 or are blank, no recorded flows will be entered.
		12-16	CHAN (RCH,PRIN) A flag switch that causes flow values to be printed at hourly intervals (when = 1) if the hourly flow exceeds the value specified in columns 37-44 of this card.
		17-19	YR1 The first calendar year of the water year to be simulated (two digits, right-justified).
		20-22	YR2 The second calendar year of the water year to be simulated (two digits, right-justified).
		25-32	CHAN The eight character description for the reach outflow point that is to be simulated.
		37-44	RCHAN (RCH, QMIN) The minimum hourly flow rate for which printed results are desired.
		45-48	CHAN (RCH, HRFL) Identifying number that will trigger hourly flow output when non-zero.
INITCH	14		FORMAT(A1,etc.)
		1	DOLLAR The $ character signals that printer output specifications are complete for the channel component of the TEHM.
OLDMAI	15		FORMAT(A4)
		1-4	LBL The character string ENDRUN signals that the input data are complete for the channel component of the TEHM. Only the first four characters are read.

Table 19. Example input data set for channel flow simulation for Walker Branch Watershed

Card no.	
1	WALKER BRANCH WATERSHED 2 2
2	1
3	CHANNEL SIMULATION
4	INITIALIZE CHANNEL SIMULATION
5	100 .02 6
6	1 RECT 3 111 .2282
7	3700. 1010. 880. 4. 6. 2. .1667 0.2 0.4
8	2 RECT 3 121 .1483
9	2300 980. 880. 4. 6. 2. .1667 0.2 0.4
10	$
11	10 73 10 74
12	1 1 73 74 EAST FORK .05 1
13	2 1 73 74 WEST FORK .05 2
14	$
15	ENDRUN

SUMMARY OF SIMULATION RESULTS

Scope

It is not intended that a comprehensive evaluation of the performance of the TEHM be included here. Instead, the objective is a presentation of selected simulation results as a vehicle for discussion of how to extract information from printed output and as a qualitative guide to the general accuracy of simulation of individual hydrologic processes. We hope that the limited discussion that follows will alert users to possible pitfalls in interpreting results and help them to avoid common errors. The portions of simulation output that have been selected for discussion are Monthly and Annual summaries of the segment water balance; end of the year soil moisture storages; throughfall estimates; streamflow simulation results; and simulated soil moisture content.

Monthly and Annual Segment Water Balance Summary

Monthly summaries of each segment water budget and daily values of selected hydrologic state variables are printed at the end of simulation for each month. Figures 23 and 24 show an example of this output for the month of November, 1973, for the West Fork of Walker Branch Watershed. The first information presented summarizes available solar energy during each hour of the first day. The variable RAD is the amount of radiant energy observed on a horizontal surface during the entire day. The second and third variables (SOLAR and SOLNET) are values for potential clear sky radiation to a horizontal surface and net potential clear sky radiation to vegetation on the sloping segment, respectively. The latter term is corrected for albedo and radiation exchange with the ground surface. Finally a vector of twenty-four values of hourly net potential radiation to the segment canopy are tabulated for the first day of the month. The estimated observed radiation for any hour is the product of actual observed daily radiation (RAD) and the ratio of the hour to total net potential radiation (SUNHR/SOLNET).

The second summary of information for each month includes a tabulation of water flux terms (infiltration, direct runoff, drainage to deeper soils, evapotranspiration, lateral subsurface flow, and net flux from the second to third soil layer) as calculated by the PROSPER model for each day. In addition, the noon-time values of conductance and water potential for the evapotranspiration surface and the volumetric water contents for the first, second, and bottom soil layers represented in PROSPER are given.

It is noted that on day 330 of 1973 a message is embedded in the monthly summary in Fig. 23 that shows (in part IRSTOR = 32654, RU =

```
SIMULATION OF NOV. 1973 BEGINS FOR SEGMENT NO.   2. PRECIP FILE KEY =      6 890
RAD,SOLAR,SOLNET,ALBVG,GND          370.69995         479.17529          415.61011          0.15999997          -13.103127
SUNHR
      0.0                 0.0                 0.0                 0.0                 0.0                 0.0
       19.684387           34.737274           46.519821           54.610916           58.459305           57.802658
       52.685760           43.457352           30.746201           15.418699           1.4878340           0.0
      0.0                 0.0                 0.0                 0.0                 0.0                 0.0

DAY  INFILT    RUNOFF       DRAINAGE       ET             FLLAT      FLNET          SURF.CON     SURF.POT      THETA1      THETA2   THETAN
     (CM)      -----------------(CM PER DAY)---------------------------------       (CM/SEC)      (BAR)      -(CM PER CM)-
305  0.0       0.0          0.1608D 00 0.1166D-01 0.0             0.2177D 00    0.1526D-01 -.9074D 01    0.2493D 000.2158D 000.2170D 00
306  0.0       0.0          0.1609D 00 0.1393D-01 0.0             0.1311D 00    0.1514D-01 -.9092D 01    0.2469D 000.2149D 000.2168D 00
307  0.0       0.0          0.1454D 00 0.1420D-01 0.0             0.1069D 00    0.1297D-01 -.9435D 01    0.2451D 000.2140D 000.2160D 00
308  0.0       0.0          0.1288D 00 0.1310D-01 0.0             0.9008D-01    0.1400D-01 -.9265D 01    0.2438D 000.2131D 000.2152D 00
309  0.12D 01  0.1511D-02 0.1700D 00 0.5513D-02 0.0               0.3943D 00    0.3264D-01 -.7260D 01    0.2573D 000.2189D 000.2177D 00
310  0.0       0.1290D-02 0.2294D 00 0.7153D-02 0.0               0.2104D 00    0.2256D-01 -.8174D 01    0.2523D 000.2176D 000.2194D 00
311  0.0       0.0          0.2057D 00 0.7463D-02 0.0             0.1554D 00    0.3963D-01 -.6741D 01    0.2498D 000.2164D 000.2185D 00
312  0.19D 00  0.0          0.1791D 00 0.1312D-02 0.0             0.1453D 00    0.5767D-01 -.5607D 01    0.2479D 000.2154D 000.2175D 00
313  0.0       0.0          0.1708D 00 0.6133D-02 0.0             0.1548D 00    0.2792D-01 -.7657D 01    0.2483D 000.2155D 000.2173D 00
314  0.0       0.0          0.1578D 00 0.3708D-02 0.0             0.1206D 00    0.1292D 00 -.3244D 00    0.2464D 000.2146D 000.2166D 00
315  0.0       0.0          0.1415D 00 0.7222D-02 0.0             0.1041D 00    0.1862D-01 -.8623D 01    0.2449D 000.2138D 000.2158D 00
316  0.0       0.0          0.1258D 00 0.9194D-02 0.0             0.8872D-01    0.1500D-01 -.9112D 01    0.2436D 000.2130D 000.2151D 00
317  0.0       0.0          0.1132D 00 0.1050D-01 0.0             0.7728D-01    0.1301D-01 -.9428D 01    0.2425D 000.2123D 000.2144D 00
318  0.0       0.0          0.1019D 00 0.1428D-01 0.0             0.6851D-01    0.1430D-01 -.9219D 01    0.2414D 000.2117D 000.2137D 00
319  0.42D 00  0.0          0.9138D-01 0.1028D-01 0.0             0.6778D-01    0.2814D-01 -.7637D 01    0.2405D 000.2111D 000.2130D 00
320  0.0       0.0          0.9799D-01 0.8423D-02 0.0             0.1453D 00    0.2116D-01 -.8326D 01    0.2444D 000.2129D 000.2136D 00
321  0.0       0.0          0.1036D 00 0.8588D-02 0.0             0.9557D-01    0.1803D-01 -.8696D 01    0.2426D 000.2122D 000.2138D 00
322  0.0       0.0          0.9778D-01 0.8659D-02 0.0             0.7378D-01    0.2288D-01 -.8140D 01    0.2414D 000.2116D 000.2134D 00
323  0.0       0.0          0.8927D-01 0.1414D-01 0.0             0.6120D-01    0.1249D-01 -.9518D 01    0.2404D 000.2110D 000.2129D 00
324  0.0       0.0          0.8160D-01 0.1240D-01 0.0             0.5216D-01    0.1734D-01 -.8785D 01    0.2396D 000.2104D 000.2123D 00
325  0.24D 01  0.1996D-01 0.1774D 00 0.6100D-02 0.0               0.7149D 00    0.3482D-01 -.7091D 01    0.2690D 000.2230D 000.2167D 00
326  0.0       0.2197D-02 0.3550D 00 0.1234D-01 0.0               0.3117D 00    0.1698D-01 -.8833D 01    0.2583D 000.2207D 000.2227D 00
327  0.0       0.1411D-02 0.2939D 00 0.1289D-01 0.0               0.2173D 00    0.1695D-01 -.8837D 01    0.2548D 000.2190D 000.2211D 00
328  0.0       0.1039D-02 0.2428D 00 0.1047D-01 0.0               0.1780D 00    0.2915D-01 -.7549D 01    0.2521D 000.2176D 000.2197D 00
329  0.37D 00  0.1479D-02 0.2193D 00 0.8500D-02 0.0               0.2285D 00    0.2250D-01 -.8181D 01    0.2552D 000.2181D 000.2189D 00
330  0.66D 01  0.2057D 01 0.3752D 00 0.2773D-03 0.0               0.1037D 01    0.4091D-01 -.6653D 01    0.2700D 000.2229D 000.2204D 00
          IRSTOR=       32702, RU=   0.17E 00, IOSTOR=             0, SCI=   0.0      , IDX30= 1290,  TL=492DB52D
331  0.14D 02  0.8143D 01 0.3837D 01 0.0            0.0            0.4800D 01    0.3385D-01 -.7166D 01    0.2889D 000.2364D 000.2389D 00
332  0.16D 01  0.1617D 01 0.3739D 01 0.7658D-02 0.0               0.2727D 01    0.2882D-01 -.7577D 01    0.2748D 000.2320D 000.2382D 00
333  0.0       0.2984D-02 0.7522D 00 0.8429D-02 0.0               0.4687D 00    0.2037D-01 -.8415D 01    0.2664D 000.2250D 000.2277D 00
334  0.0       0.2190D-02 0.4586D 00 0.9137D-02 0.0               0.3339D 00    0.1741D-01 -.8776D 01    0.2613D 000.2223D 000.2244D 00

MONTHLY WATER BUDGET (CM)

TOTAL INFILTRATION, EVAPOTRANSPIRATION, RUNOFF, DRAINAGE, LATERAL FLOW, SOIL WATER CHANGE AND BALANCE (CM)
      26.32695       0.2636491        11.85111        13.20243        0.0              1.009759        0.1913802D-11
ROOT WATER UPTAKE (CM)   LAYER 1   0.1327309D-05 LAYER 2   0.1918270D-06
FILE KEY =        890
```

Fig. 23. An example of the summary of calculations made by PROSPER for each month (November 1973).

```
****THE FOLLOWING DATA ARE IN CENTIMETERS****

SNOWPACK BALANCE    SNOWFALL IN    INTERCEPTED IN    RAIN ON PACK    MELT RELEASED    SUBLIMATION    STORAGE CHANGE
 0.0                0.0            0.0               0.0             0.0              0.0            0.0

 INTERCEPTION BALANCE    INTERCEPTION INPUT    CANOPY EVAPORATION    PRIOR STORAGE      CURRENT STORAGE    LOSS TO PACK
   0.421069490E-05          1.07973385            1.13631153         0.56582030E-01     0.0                0.0

LOWER ZONE BALANCE    INFILTRATION    DRAINAGE OUT    TRANSPIRATION     SOIL EVAPORATION    PRIOR STORAGE    CURRENT STORAGE
 0.16677760E-01       26.3268          25.0367        0.1468538E-05     0.2636299           34.193848          35.203598

SOURCE AREA BALANCE    DRAINAGE IN    DRAINAGE OUT    PRIOR STORAGE    CURRENT STORAGE
 0.0                  26.3267975      11.834752
DEEP SOIL BALANCE      DRAINAGE IN    DRAINAGE GWS    DRAINAGE CHANL
-.404529506E-03       13.2019768        5.2710342       0.209374 36E-11
  PRIOR STOR1        PRIOR STOR2     CURRENT STOR1     CURRENT STOR2
74.700775          0.0               82.632111
GROUNDWATER BALANCE    GW DRAINAGE IN     BASE STREAMFLOW    TRANSPIRATION    PRIOR STORAGE     CURRENT STORAGE
 0.151315398E-03        5.1129045           5.1884012        0.0              0.5726556E-01     1.6163006
                        DEEP LOSSES
                       -1.6346836

INTERFLOW CHECK    LAND T-INTF    SOURCE A - INTF    DEEP SOIL INTF    BALANCE-INTF
                   11.47941780      11.479711533       0.000000000     -.29425882E-03

PA=0.970 RES= 0.0  RES1= 0.0    MONTHLY WATER BALANCE=-0.16130842E-01

BALANCE=  -0.161308E-01
                          **** RUNOFF COMPONENT SUMMARY ****

              IMPERVIOUS    SURFACE    SOURCE AREA 1    SOURCE AREA 2    BASE          TOTAL

CENTIMETERS   0.78979504    0.0        11.47971058      0.00000000       5.18840122    17.45774841

FRACTION      0.04524035    0.0        0.65757066       0.00000000       0.29719746    1.00000763
```

Fig. 24. An example of the summary of monthly water balance terms for a vertical column through a segment.

0.17, and IDX30 = 1290). This is the warning message that was discussed earlier in conjunction with scale factors. The value of IRSTOR represents the scaled runoff input for a 30-min period. Because RUNSCL is set at 100,000, this implies a runoff input rate of 0.32654 in. per half hour or 158.7 cfs for the whole Walker Branch Watershed. The value of RU represents the volume of runoff generated (inches) for the last 15 min of the half-hour period. The value of IDX30 indicates which 30-min period during the month is referenced. The value 1290 indicates that the 30-min period beginning at 9 p.m. on November 26 has a scaled runoff value that may exceed the storage capacity allocated for it. It is quite important to note that only one line of warning per month will be printed. Thus, even though the value of IRSTOR printed here will not exceed the allocated storage size, subsequent periods may include values that are too large, and one must seriously consider changing RUNSCL. It should be noted, however, that the value RUNSCL will not affect printed output results for the terrestrial portion of the model output. Although erroneous records will be written in the files that are accessed by the channel simulation portion of the TEHM, these errors are important only when an attempt is made to generate simulated hydrographs.

Figure 24 is a detailed tabulation of water balance terms for a vertical column of basin segment, divided into several components. The interception component includes canopy storage of water and water that evaporates directly from vegetation surfaces. The lower zone compartment includes all of the soil layers considered by the PROSPER model. However, storage values presented here are on a per unit area of pervious surface material, rather than a per unit watershed segment area. Thus, conversion of these values to a unit segment area basis requires multiplication by the fraction of pervious area in the segment.

The source area budget tabulates only the input and source area runoff term per unit pervious area. The storage compartment is the same as that given for lower zone storage, hence the sum of the source area drainage plus drainage to deep soils equals the drainage loss from the lower zone.

The deep soil compartment includes all soil-water transmission layers, and is reported on a per unit pervious area basis.

The groundwater component is reported on a per unit area of watershed basis. Thus the groundwater input term is the product of the deep soil drainage term and the fraction of pervious area.

Finally, the monthly summary concludes with a runoff component summary, which gives absolute and fractional amounts of runoff assigned to each of five possible flow components.

At the end of simulation for each water year, the annual summary table is printed for each segment. Figure 25 is an example, and

WALKER BRANCH WATERSHED LAN SEGMENT 2 GAGE 6 WATER YEAR 1973-74

SEGMENT RUNOFF SUMMARY

	OCT.	NOV.	DEC.	JAN.	FEB.	MAR.	APR.	MAY	JUN.	JUL.	AUG.	SEP.	ANNUAL	
IMPERV RUNOFF	0.24	0.79	0.68	0.66	0.34	0.53	0.23	0.46	0.11	0.06	0.37	0.22	4.69	CM.
SURFACE RUNOFF	0.0	0.0	0.0	0.0	0.0	0.0	0.0	0.0	0.0	0.0	0.0	0.0	0.0	CM.
SOURCE AREA1 RO	0.0	11.48	7.60	4.56	0.99	4.77	0.60	0.33	0.0	0.0	0.0	0.0	30.32	CM.
SOURCE AREA2 RO	0.00	0.00	0.00	0.00	0.00	0.00	0.00	0.00	0.00	0.00	0.00	0.00	0.00	CM.
BASE FLOW	2.87	5.19	21.79	27.66	17.42	15.75	15.41	6.25	4.65	1.85	0.98	0.76	120.57	CM.
TOTAL STREAMFLOW	3.11	17.46	30.07	32.89	18.75	21.04	16.23	7.03	4.76	1.91	1.35	0.98	155.58	CM.
UNMSRD SEEPAGE	-0.90	-1.63	-6.86	-8.72	-5.49	-4.96	-4.85	-1.97	-1.47	-0.58	-0.31	-0.24	-37.99	CM.
TOTAL OUTFLOW	2.20	15.82	23.20	24.17	13.26	16.08	11.38	5.06	3.30	1.33	1.04	0.74	117.60	CM.

SEGMENT PRECIP/ET SUMMARY

	OCT.	NOV.	DEC.	JAN.	FEB.	MAR.	APR.	MAY	JUN.	JUL.	AUG.	SEP.	ANNUAL	
TOTAL PRECIP	8.66	27.41	24.13	24.38	13.36	19.71	8.99	17.63	5.00	2.67	14.88	9.52	176.35	CM.
INTRCEP EVAP	0.63	1.14	1.26	2.36	2.06	2.05	1.33	2.37	1.32	0.66	2.47	2.35	19.99	CM.
PROSPR TRANSP	2.61	0.00	0.00	0.00	0.00	0.00	1.12	9.23	7.98	3.36	6.62	7.21	38.12	CM.
SOIL EVAPOR	0.39	0.26	0.13	0.18	0.16	0.35	0.54	0.48	0.25	0.02	0.20	0.31	3.28	CM.
G.W.TRANSP	0.0	0.0	0.0	0.0	0.0	0.0	0.0	0.0	0.0	0.0	0.0	0.0	0.0	CM.
SNOW EVAPOR	0.0	0.0	0.0	0.0	0.0	0.0	0.0	0.0	0.0	0.0	0.0	0.0	0.0	CM.
TOTAL ET	3.63	1.39	1.39	2.54	2.21	2.40	2.99	12.08	9.55	4.04	9.29	9.87	61.39	CM.
POTENTIAL ET	6.57	3.20	1.90	1.76	3.18	6.22	9.74	9.18	10.73	12.00	8.06	5.56	78.10	CM.

SEGMENT MOISTURE STATUS-BEGINNING OF THE MONTH VALUES

	OCT.	NOV.	DEC.	JAN.	FEB.	MAR.	APR.	MAY	JUN.	JUL.	AUG.	SEP.		
SNOWPACK TOTAL	0.0	0.0	0.0	0.0	0.0	0.0	0.0	0.0	0.0	0.0	0.0	0.0	0.0	CM.
INTERCEPTED STOR	0.0	0.06	0.0	0.04	0.0	0.0	0.0	0.0	0.07	0.0	0.0	0.05	0.0	CM.
DETENTION STOR	0.0	0.0	0.0	0.0	0.0	0.0	0.0	0.0	0.0	0.0	0.0	0.0	0.0	CM.
DEPRESSION STOR	0.0	0.0	0.0	0.0	0.0	0.0	0.0	0.0	0.0	0.0	0.0	0.0	0.0	CM.
UPPER SOILS	28.76	33.17	34.15	35.32	33.82	33.04	33.94	31.01	31.44	26.61	25.17	30.33	28.72	CM.
DEEP SOIL 1	37.02	36.10	39.85	39.48	39.26	38.55	38.83	37.54	37.79	36.06	35.49	35.18	35.71	CM.
DEEP SOIL 2	37.02	36.36	40.30	39.59	39.34	38.86	38.89	38.00	37.79	36.69	36.04	35.71	35.75	CM.
GROUNDWATER	0.12	0.06	1.62	1.01	0.68	0.54	0.54	0.26	0.20	0.09	0.04	0.02	0.03	CM.
TOTAL CONTENT	102.91	105.74	115.92	115.44	113.10	110.98	112.20	106.81	107.29	99.44	96.74	101.29	100.21	CM.

SEGMENT WATER BUDGET SUMMARY

	OCT.	NOV.	DEC.	JAN.	FEB.	MAR.	APR.	MAY	JUN.	JUL.	AUG.	SEP.	ANNUAL	
PRECIPITATION INPUT	8.66	27.41	24.13	24.38	13.36	19.71	8.99	17.63	5.00	2.67	14.88	9.52	176.35	CM.
EVAPORANSPIRATION LOSS	3.63	1.39	1.39	2.54	2.21	2.40	2.99	12.08	9.55	4.04	9.29	9.87	61.39	CM.
OUTFLOW TOTAL	2.20	15.82	23.20	24.17	13.26	16.08	11.38	5.06	3.30	1.33	1.04	0.74	117.60	CM.
CHANGE IN MOISTURE CONTENT	2.83	10.18	-0.48	-2.34	-2.12	1.22	-5.39	0.48	-7.85	-2.70	4.55	-1.08	-2.70	CM.
BALANCE	-0.00	-0.02	-0.01	-0.01	-0.00	-0.01	-0.00	-0.00	-0.00	-0.00	-0.00	-0.00	-0.06	CM.

Fig. 25. An example of the monthly and annual water budget tabulation for a segment.

shows the 1974 water year summary for the West Fork of Walker Branch Watershed.

The first section is a segment runoff summary, which tabulates the major components of streamflow. Storm runoff comprises impervious, surface, and source area runoff components. Surface runoff comes from pervious areas when throughfall rates exceed infiltration capacities. In the version of the model presented here, only one source area runoff component is considered. Baseflow includes any groundwater gains or losses associated with transfer between adjacent segments. For example, in October, 1973, the total base flow (0.77 cm) is the difference between baseflow generated within the segment and unmeasured seepage loss. Here, the seepage loss is negative, which implies a gain. Thus the baseflow generated within the segment is 0.53 cm, which combines with 0.24-cm gain to produce the total base flow of 0.77 cm. The total streamflow is the sum of all baseflow and stormflow. This quantity corresponds to measured streamflow at the segment outlet. The row labelled total outflow corresponds to the total runoff generated within the segment. Thus total outflow is the sum of total streamflow and unmeasured seepage loss. In the example, round-off errors account for the slight differences. When groundwater seepage between segments occurs, the total outflow summary can be useful for direct comparisons between basins.

The precipitation and evapotranspiration summary for each segment includes precipitation, interception loss, transpiration loss, soil (and litter) evaporation, and a total evapotranspiration term. All terms given in this portion of the annual summary are assumed to occur over the entire basin (pervious and impervious areas). The row titled "POTENTIAL ET" refers to free water surface evaporation, estimated as lake evaporation using equations presented by Lamoreux (1962). These values serve only as an index to evapotranspiration and may differ significantly from it.

The moisture status of the basin is described in the third portion of the summary. It is intended as an index to the total water content of a vertical column that extends from the canopy to bedrock in the watershed. Each number represents a beginning of the month value for a storage compartment. Because water stored in vegetation is ignored and the groundwater storage term is only relative, the total content is probably most indicative of overall storage of water in the unsaturated soil column.

The final portion of the annual summary for a segment is a simple budget calculation. The input is precipitation, losses include all forms of evapotranspiration and runoff (generated from within the segment), and the change in storage is the difference in the sum of all storage compartments over the month. The overall balance term is calculated as the difference between input and the sum of output and change in storage. The imbalances that occur in some months are the result of round-off errors that occur during integration of various flux terms.

End of the Year Soil Moisture Storages

Often, simulations are run one year at a time. When this occurs, it is desirable to start the succeeding year simulations with final moisture storage values from the previous year. Figure 26 is an example of the printed output that is generated for each segment to simplify development of the input data set for a succeeding year. The layer thickness and end of year simulated theta (volumetric water content) values for all soil layers are tabulated, together with the groundwater storage value. The theta values are calculated using absolute moisture contents that are expressed on a per unit pervious area basis. Thus the product of theta values and layer thicknesses must be multiplied by the fraction of pervious area to obtain actual water contents per unit watershed area.

Throughfall Estimates

The estimation of throughfall and interception loss was discussed earlier. Figure 7 and Table 1 are indicative of the accuracy expected when using the TEHM, and the reader is referred back to that discussion for further details.

Soil Moisture

The information presented in Fig. 27 illustrates the ability of the model to reproduce field observation of soil moisture in the uppermost soil layers. Although one can argue that the figure demonstrates adequate model performance, the most interesting feature is the standard deviation in observed soil moisture. The large range of moisture values for a given date is not indicative of analytical errors. It measures the large spatial variability in soil moisture at any point in time. If the model were completely accurate, the simulated results should pass through the mean value of observed soil moisture. With the evidence available, it is not possible to assess the quality of model prediction. In part, this is because not enough information was available to calculate an area weighted average soil moisture. One thing illustrated by these results is the need to incorporate a statistical representation of moisture state variables in the model.

Streamflow Simulation

Perhaps the most commonly used index to hydrologic model performance is the ability of the model to accurately reproduce hydrographs. However, most comparisons are based upon single storm events or total

THE END OF THE YEAR VALUES TO BE USED TO START NEXT YEAR SIMULATIONS FOLLOW:

FOR THIS SEGMENT THERE ARE 3 SOIL LAYERS SIMULATED BY PROSPER
THEY HAVE THE FOLLOWING PROPERTIES:

LAYER	WATER CONTENT (CM)	LAYER THICKNESS (CM)	THETA VALUE
1	10.191531	50.000000	0.203831
2	9.7056755	50.000000	0.194114
3	9.7140791	50.000000	0.194282

THE SOIL WATER TRANSMISSION LAYERS HAVE THE FOLLOWING PROPERTIES

LAYER	WATER CONTENT (CM)	LAYER THICKNESS (CM)	THETA VALUE
1	36.814936	180.00000	0.204527
2	36.860257	180.00000	0.204779

THE GROUNDWATER STORAGE VALUE IS 0.254156E-01 CM.

Fig. 26. An example of the printed summary of soil moisture storage values at the end of a year.

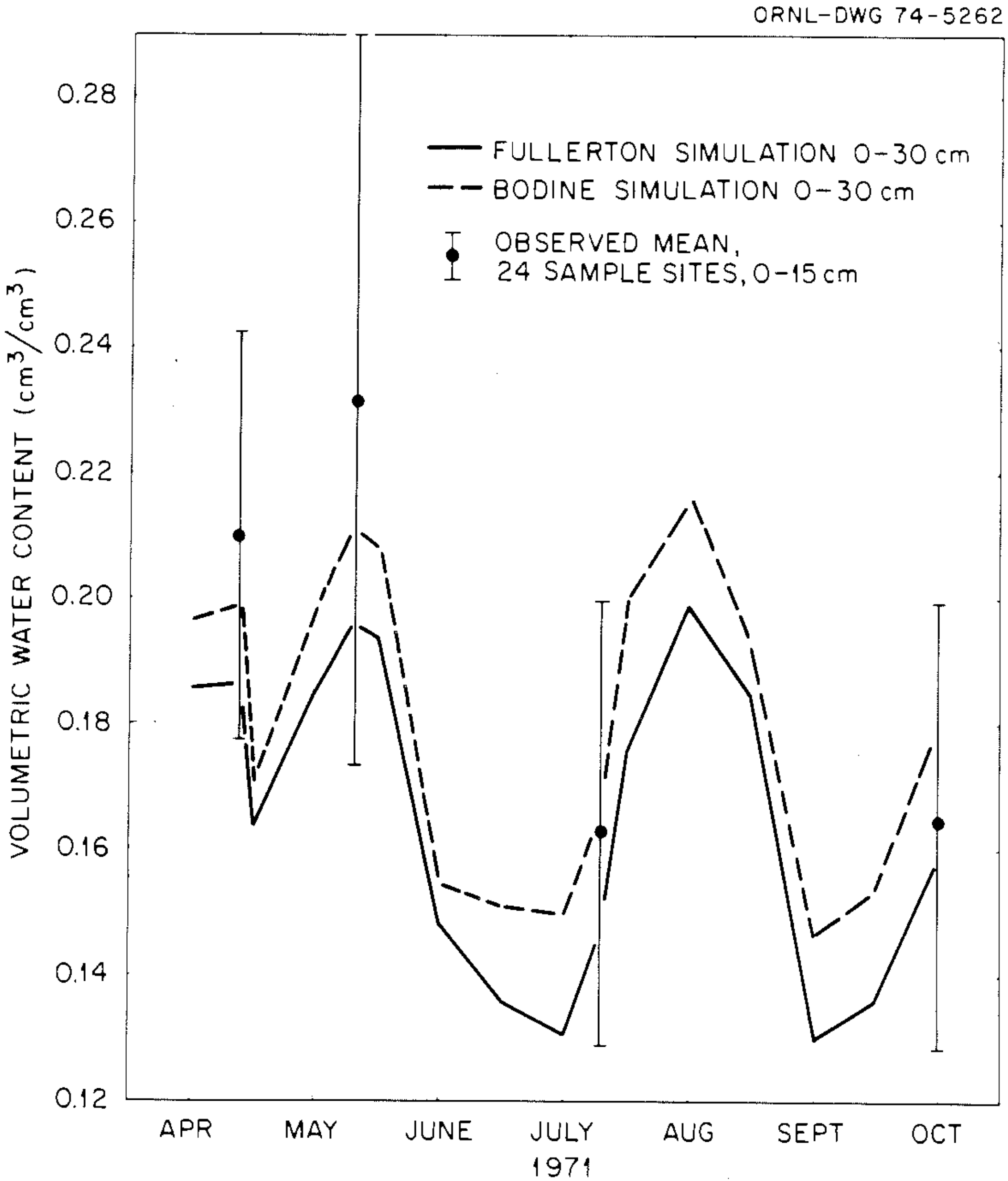

Fig. 27. Simulated and observed moisture content in surficial soils of Walker Branch Watershed.

flow volumes. We have chosen to present comparisons of simulated stormflow versus quickflow and simulated baseflow versus delayed flow, where quickflow and delayed flow are calculated from observed flow data using the method of Hewlett and Hibbert (1967). We used the hydrograph analysis package implemented at ORNL (Huff and Begovich, 1976) for determining monthly quick flow and delayed flow volumes. Figures 28, 29, and 30 show comparisons of simulated and "observed" storm flow, base flow, and total flow amounts for each month of the simulation period. It should be explained that the initial conditions for the period were taken from the simulation output for the preceeding three-year period. Furthermore, the vegetation parameters that had to be estimated by trial and error were determined using 1970 and 1971 data. Once they were set, they were not changed.

Of course there is no guarantee that the individual estimates of stormflow and baseflow are particularly accurate, or that the simulations compare well with observed data for the correct reasons. However, results for all years simulated to date are similar, and it is felt that these results represent a step forward in relating physical processes with flow components that are identified through traditional hydrograph analysis.

Future Plans

Most complex simulation models are never considered completed because there is usually more to learn about the processes they represent. The TEHM is no exception. The version of the model that has been documented here simply represents a point in the process of model evolution as our understanding grows and becomes more refined. However, we believe that the current version of the TEHM is useful for some applications, and more importantly that the model structure and data management capabilities provide a useful framework for others to use as a starting point for their work. For example, one interested in simulation of snowmelt processes could easily start with the TEHM structure and simply modify or replace the SNOMELT subroutine to suit his purposes. We intend to continue to develop the capabilities of the TEHM and to subject it to rigorous testing through future applications. Those others who choose to use the TEHM are encouraged to convey their successes, failures, and useful improvements to the authors.

ORNL DWG 76-17021

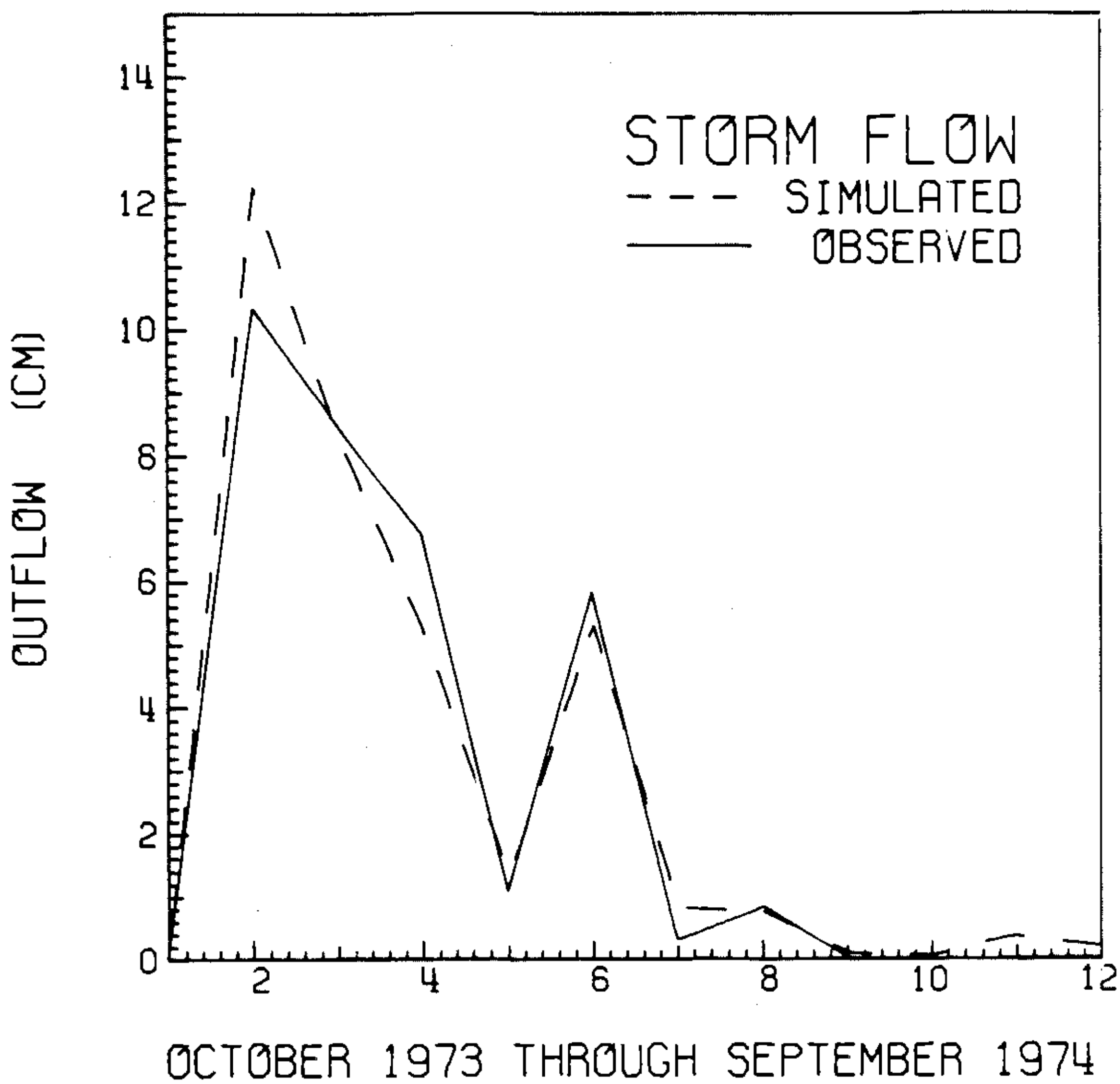

Fig. 28. Simulated and observed monthly storm flow for the West Fork of Walker Branch Watershed.

ORNL DWG 76-17022

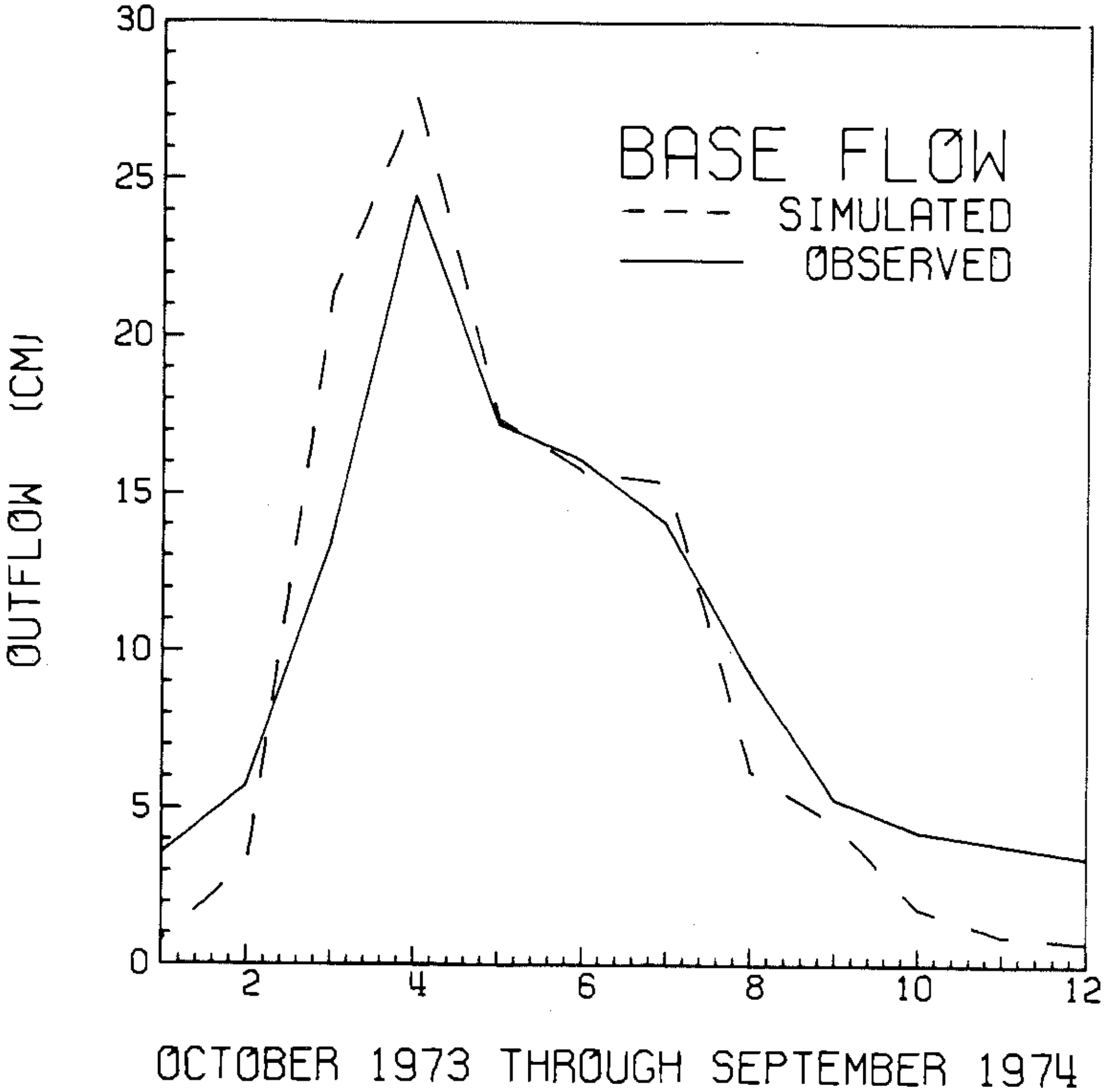

Fig. 29. Simulated and observed monthly base flow for the West Fork of Walker Branch Watershed.

ORNL DWG 76-17023

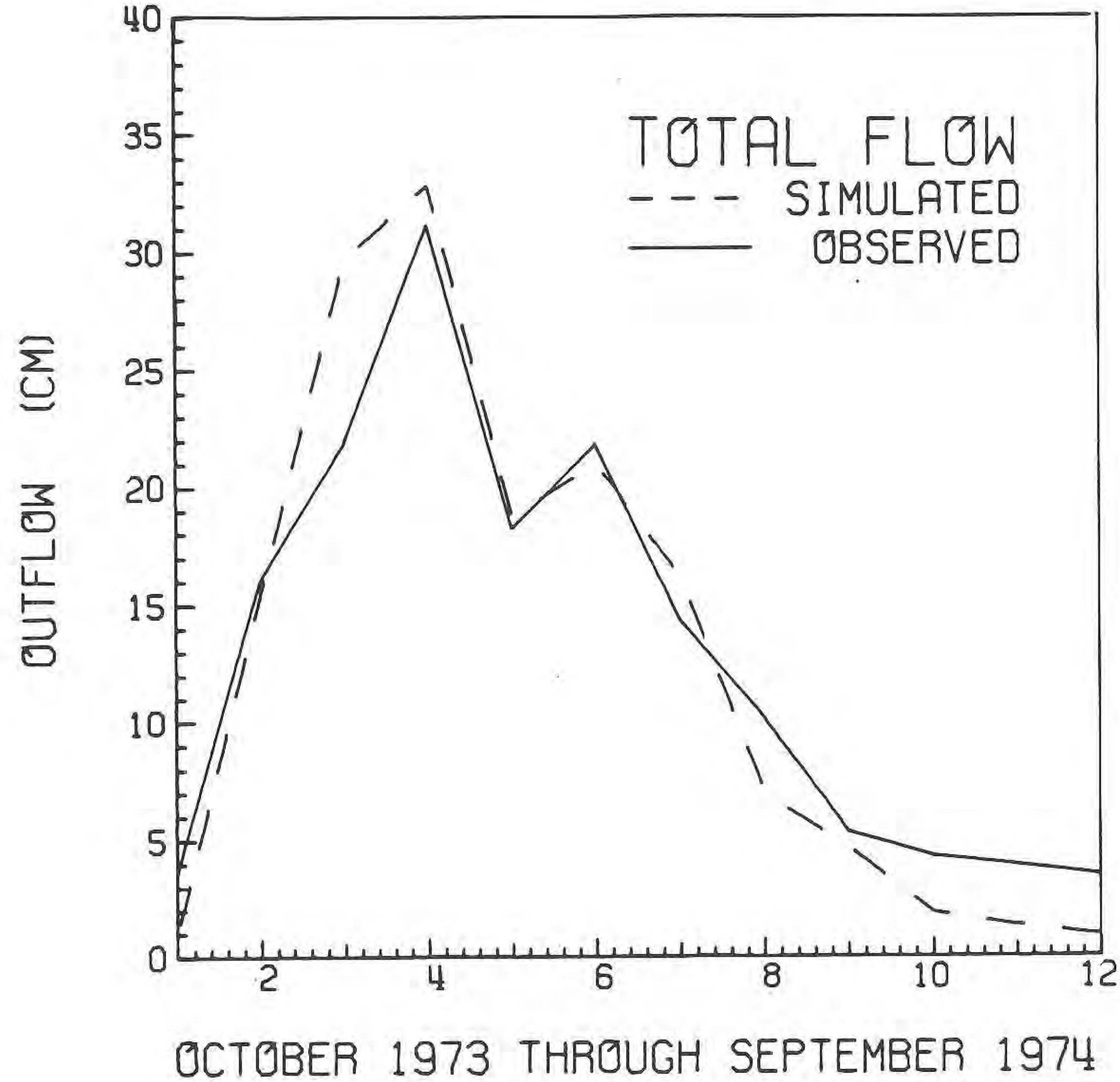

Fig. 30. Simulated and observed monthly total flow for the West Fork of Walker Branch Watershed.

BIBLIOGRAPHY

Begovich, C. L., and D. R. Jackson. 1975. Documentation and application of SCEHM: A model for soil chemical exchange of heavy metals. ORNL/NSF/EATC-16. Oak Ridge National Laboratory, Oak Ridge, Tennessee. 67 pp.

Betson, R. P., and J. B. Marius. 1969. Source areas of storm runoff. Water Resour. Res. 5(3):574-582.

Brunt, D. 1939. Physical and Dynamical Meteorology. The University Press, Cambridge, England. 428 pp.

Burgess, R. L., and R. V. O'Neill (eds.). 1975. Eastern Deciduous Forest Biome Progress Report (Sept. 1, 1973-August 31, 1974). EDFB/IBP-75/11. Oak Ridge National Laboratory, Oak Ridge, Tennessee. 252 pp.

Byers, H. R. 1959. General Meteorology (third edition). McGraw-Hill Book Company, Inc., New York. 514 pp.

Cheng, J. D., T. A. Black, and R. P. Willington. 1975. A technique for the field determination of the hydraulic conductivity of forest soils. Can. J. Soil Sci. 55:79-82.

Chow, V. T. 1959. Open-Channel Hydraulics. McGraw-Hill Book Company, Inc., New York. 680 pp.

Cowan, I. R. 1965. Transport of water in the soil-plant-atmosphere system. J. Appl. Ecol. 2:221-239.

Cowan, I. R., and F. L. Milthorpe. 1968. Plant factors influencing the water status of plant tissues. pp. 137-193. T. T. Kozlowski (ed.). Water Deficits and Plant Growth, Vol. 1. Academic Press, New York.

Crawford, N. H., and R. K. Linsley, Jr. 1966. Digital simulation in hydrology: Stanford watershed model IV. Department of Civil Engineering, Stanford University. Technical Report No. 39. 210 pp.

Curlin, J. W., and D. J. Nelson. 1968. Walker Branch Watershed Project: Objectives, facilities, and ecological characteristics. ORNL/TM-2271. Oak Ridge National Laboratory, Oak Ridge, Tennessee. 100 pp.

DeVries, D. A. 1955. pp. 277-304. In Solar Radiation at Wageningen. Meded. Landbouwhogeschool Wageningen 55(6).

Dickinson, W. T., and H. Whiteley. 1970. Watershed areas contributing to runoff. pp. 1.12-1.26. Symposium on Results of Research on Representative and Experimental Basins. Int. Assoc. of Sci. Hydrol. Publ. 96.

Dixon, K. R., R. J. Luxmoore, and C. L. Begovich. 1976. CERES - A model of forest stand biomass dynamics for predicting trace contaminant, nutrient, and water effects. ORNL/NSF/EATC-25. Oak Ridge National Laboratory Report, Oak Ridge, Tennessee.

Drummond, A. J. 1968. New value for the solar constant of radiation. Nature 218:259-261.

Dunne, T., and R. D. Black. 1970. Partial area contributions to storm runoff in a small New England watershed. Water Resour. Res. 6(5):1296-1311.

Engman, E. T., and A. S. Rogowski. 1974. A partial area model for storm flow synthesis. Water Resour. Res. 10(3):464-472.

Freeze, R. A. 1972. Role of subsurface flow in generating surface runoff. 1. Base flow contributions to channel flow. Water Resour. Res. 8(3):609-623.

Goldstein, R. A., J. B. Mankin, and R. J. Luxmoore. 1974. Documentation of PROSPER: A model of atmosphere-soil-plant water flow. EDFB/IBP-73/9. Oak Ridge National Laboratory, Oak Ridge, Tennessee. 75 pp.

Green, R. E., and R. J. Corey. 1971. Calculation of hydraulic conductivity: A further evaluation of some predictive methods. Soil Sci. Soc. Am. Proc. 35:3-8.

Grigal, D. F., and R. A. Goldstein. 1971. An integrated ordination-classification analysis of an intensively sampled oak-hickory forest. J. Ecol. 59:481-492.

Harris, W. F., R. A. Goldstein, and G. S. Henderson. 1973. Analysis of forest biomass pools; annual primary production, and turnover of biomass for a mixed deciduous forest watershed. pp. 41-64. H. Young (ed.), Proceedings of the Working Party on Forest Biomass of IUFRO. University of Maine Press, Orono.

Helvey, J. D., and J. H. Patric. 1965. Canopy and litter interception of rainfall by hardwoods of eastern United States. Water Resour. Res. 1(2):193-206.

Henderson, G. S. 1976. Personal communication. Environmental Sciences Division, Oak Ridge National Laboratory, Oak Ridge, Tennessee.

Henderson, G. S. and others. 1971. Walker Branch Watershed: A study of terrestrial and aquatic system interaction. pp. 30-48. ORNL-4759. Oak Ridge National Laboratory, Oak Ridge, Tennessee.

Hewlett, J. D. 1961a. Watershed management. pp. 61-66. Annual Report for 1961, Southeastern Forest Experiment Station, U. S. Forest Service.

Hewlett, J. D. 1961b. Soil moisture as a source of base flow from steep mountain watersheds. Southeastern Forest Experiment Station Paper 132. U.S. Dept. of Agriculture, Asheville, North Carolina. 11 pp.

Hewlett, J. D., and A. R. Hibbert. 1967. Factors affecting the response of small watersheds to precipitation in humid areas. pp. 275-290. In Int. Symp. Forest Hydrology, Pergamon Press, Oxford.

Huff, D. D. 1968. Simulation of the hydrologic transport of radioactive aerosols. Ph.D. Dissertation. Committee on Hydrology, Stanford University. 206 pp.

Huff, D. D., and C. L. Begovich. 1976. An evaluation of two hydrograph separation methods of potential use in regional water quality assessment. ORNL/TM-5258. Oak Ridge National Laboratory, Oak Ridge, Tennessee.

Ishaq, A. M. 1974. Application of remote sensing to the location of hydrologically active (source) areas. Ph.D. Dissertation, Dept. of Civil and Environmental Engineering, University of Wisconsin, Madison, Wisconsin. 223 pp.

Jacques, J. E., and D. D. Huff. 1972. Snow accumulation and melt simulation. U.S. IBP, Eastern Deciduous Forest Biome Memo Rept. No. 72-136, Univ. of Wisconsin-Madison, Inst. for Environ. Stud., Lake Wingra Study, 17 pp.

Kochenderfer, J. N. 1973. Root distribution under some forest types native to West Virginia. Ecology 54(2):445-448.

Kreith, F. 1965. Principles of Heat Transfer. International Textbook Co., Scranton, Pennsylvania. 620 pp.

Lamoreux, W. W. 1962. Modern evaporation formulae adapted to computer use. Monthly Weather Review, Vol. 90, No. 1:26-28.

Lee, M. T., and J. W. Delleur. 1972. Analysis of geomorphologic data and dynamic contributing area model for runoff estimation. Water Resources Research Center Tech. Rept. 24. Purdue University, Lafayette, Indiana. ca. 200 pp.

Lee, R. 1963. Evaluation of solar beam irradiation as a climatic parameter of mountain watersheds. Colorado State University Hydrology Papers, No. 2. Fort Collins, Colorado. 50 pp.

Linsley, R. K., Jr., M. A. Kohler, and J. L. Paulhus. 1958. Hydrology for Engineers. McGraw-Hill Book Co. New York. 340 pp.

Luxmoore, R. J. 1973. Application of the Green and Corey method for computing hydraulic conductivity in hydrologic modeling. EDFB/IBP-73/4. Oak Ridge National Laboratory, Oak Ridge, Tennessee. 22 pp.

Luxmoore, R. J., J. L. Stolzy, and J. T. Holdeman. 1976a. Some sensitivity analyses of an hourly soil-plant water relations model. ORNL/TM-5343. Oak Ridge National Laboratory, Oak Ridge, Tennessee.

Luxmoore, R. J., C. L. Begovich, and K. R. Dixon. 1976b. DRYADS and DIFMAS, FORTRAN Models for investigating solute uptake and incorporation into vegetation and litter. ORNL/NSF/EATC-26. Oak Ridge National Laboratory, Oak Ridge, Tennessee.

Marshall, T. J. 1958. A relation between permeability and size distribution of pores. J. Soil Sci. 9:1-8.

Mills, M. T., and M. Reeves. 1973. A multi-source atmospheric transport model for deposition of trace contaminants. ORNL/NSF/EATC-2. Oak Ridge National Laboratory, Oak Ridge, Tennessee. 77 pp.

Monteith, J. L. 1965. Evaporation and environment. p. 212. Fogg, G. E. (ed.), The State and Movement of Water in Living Organisms. Symposia on the Society for Experimental Biology, Number XIX. Academic Press Inc., New York. p. 212.

Murphy, C. R., and K. R. Knoerr. 1970. Modeling the energy balance processes of natural ecosystems. Final Research Report, 1969-1970. Grant 383-6102, School of Forestry, Duke University, Durham, North Carolina. 164 pp.

National Oceanic and Atmospheric Administration (NOAA). 1972. Daily, monthly, and annual climatological data for Oak Ridge, Tennessee, townsite and area stations. January 1951 through December 1971. Environmental Research Laboratories, Contribution File No. 61. Air Resources Atmospheric Turbulence and Diffusion Laboratory, Oak Ridge, Tennessee. 557 pp.

Nestor, C. W., Jr., K. C. Chandler, N. B. Grove, and J. D. McDowell. 1974. User's Manual for the graphics package ORGRAPH. ORNL-4596. Oak Ridge National Laboratory, Oak Ridge, Tennessee. 118 pp.

Patterson, M. R., J. K. Munro, D. E. Fields, R. D. Ellison, A. A. Brooks, and D. D. Huff. 1974. A user's manual for the FORTRAN IV version of the Wisconsin Hydrologic Transport Model. ORNL/NSF/EATC-7. Oak Ridge National Laboratory, Oak Ridge, Tennessee. 252 pp.

Peters, L. N., D. F. Grigal, J. W. Curlin, and W. J. Selvidge. 1970. Walker Branch Watershed Project: Chemical, physical, and morphological properties of the soils of Walker Branch Watershed. ORNL/TM-2968. Oak Ridge National Laboratory, Oak Ridge, Tennessee. 96 pp.

Reeves, M., and J. O. Duguid. 1975. Water movement through saturated-unsaturated porous media: A finite-element Galerkin model. ORNL-4927. Oak Ridge National Laboratory, Oak Ridge, Tennessee. 236 pp.

Reeves, M., and E. E. Miller. 1975. Estimating infiltration for erratic rainfall. Water Resour. Res. 11(1):102-110.

Ritchie, G. A., and T. M. Hinckley. 1975. The pressure chamber as an instrument for ecological research. Adv. Ecol. Res. 9:166-254.

Shinn, J. H. 1969. Analysis of wind data from a South Carolina coastal forest. Tech. Rept. ECOM-6036, U.S. Army Electronics Command, Atmospheric Science Laboratory, Fort Huachuca, Arizona. 23 pp.

Stiffler, W. D. 1957. The soil moisture regime under native hardwoods at five elevations in the southern Appalachians. M. F. Thesis, University of Michigan School of Natural Resources, Ann Arbor. 93 pp.

Swift, L. W., Jr., W. T. Swank, J. B. Mankin, R. J. Luxmoore, and R. A. Goldstein. 1975. Simulation of evapotranspiration and drainage from mature and clear-cut deciduous forests and young pine plantation. Water Resour. Res. 11(5):667-673.

U.S. Naval Observatory. 1945. Tables of Sunrise, Sunset and Twilight, Supplement to the American Ephemeris. 1946. Washington, D. C.

van Wijk, W. R., and D. A. DeVries. 1963. Periodic temperature variation in a homogeneous soil. W. R. van Wijk (ed.). Physics of Plant Environment. John Wiley and Sons, Inc., New York. 382 pp.

van Wijk, W. R., and D. W. Scholte Ubing. 1963. Radiation. W. R. van Wijk (ed.). Physics of Plant Environment. John Wiley and Sons, Inc., New York. 382 pp.

Westley, G. W., and J. A. Watts (eds.). 1970. The Computing Technology Center Numerical Analysis Library. CTC-39. Union Carbide Corporation Nuclear Division Computing Technology Center, Oak Ridge, Tennessee. 462 pp.

Weyman, D. R. 1973. Measurements of the downslope flow of water in a soil. J. Hydrol. 20:267-288.

APPENDIX

Conversion of Relative Humidity to Dew Point Temperature

The basis for the conversion of relative humidity to dew point temperature is the use of an equation adapted from the work of Lamoreux (1962). An approximation to saturation vapor pressure as a function of air temperature is:

$$e_s = (2.1706 \times 10^8)\ e^{(-7482.6/(Ta+398.36))} \quad , \qquad (1)$$

where

e_s = saturation vapor pressure (mb),
e = base of natural logarithm, and
Ta = air temperature (°F).

We use maximum air temperature and minimum relative humidity, which we assume to occur simultaneously, to estimate dew point temperature. The dew point temperature is assumed constant for a day. One may rearrange Eq. (1) to yield

$$T_{dew} = \{7.4826 \times 10^3/\ln\,[2.1706 \times 10^8/(RH \times e_s/100)]\} - 398.36 \quad ,(2)$$

where

T_{dew} = dew point temperature °F,
ln = natural logarithm,
RH = relative humidity (%), and
e_s = saturation vapor pressure (mb).

Thus, we calculate dew point temperature by the following steps:

(1) Compute saturation vapor pressure with Eq. (1) and the daytime maximum temperature.
(2) Compute dew point temperature with Eq. (2) and the daytime minimum relative humidity. The calculated saturation vapor pressure (step 1) is also used.

The calculation method described above can lead to an estimated dew point temperature that exceeds the minimum daytime temperature. Although this implies supersaturation of the atmosphere, internal tests in the watershed simulation model select the higher of the ambient air or dew point temperatures to estimate actual vapor pressure. The code that implements the basic dew point temperature calculation is included in the following pages.

Program Structure, Input and Output

The program is arranged to read up to one full year of daily maximum and minimum air temperature and daily relative humidity values, then compute the corresponding daily dew point temperatures and output them in a format that can be used directly by the comprehensive watershed simulation model.

An example data set is shown in Fig. 1. Each component of the input data set is described below:

Component	Format	Description of Information
1	(3X,A2,A4)	DDCC20 is a code that describes the data to be generated. The first letter refers to the variable considered (D = dew point, A = air temperature, H = humidity, etc.). The second letter refers to frequency of observation (H = hourly, D = daily, M = monthly). The third letter refers to site (C = Coweeta, H = Hubbard Brook, I = Iron Fork, D = Davidson River, etc.). The fourth letter refers to station type (R = raingage, C = climatic, W = weir). The final two digits refer to the station ID number. The example represents dew point temperature on a daily basis at Coweeta climatic station 20.
2	(I2,1X,A4)	The variables are a switch and identifier that control program execution sequence. The switch options are: 1 = read temperature data; 2 = read humidity data; 3 = calculate dew point temperature and generate output. In the example, temperature data are to be read.
3	(A1,A2,A4, 2I2,I1,22I3)	This is standard input format for daily maximum and minimum temperature data. The first character is a control to signal the end of data input. When it is a $, the program cycles back to read a new switch and identifier. The next two variables contain the data code. They are not used here. The next 3 variables are the year, month, and card number. The latter value may be 1, 2, or 3, depending on whether data for the first, second, or third eleven-day period will follow. The

Component	Format	Description of Information
3	(A1,A2,A4, 2I2, I1,22I3)	22 remaining values are daily maximum and minimum temperatures in degrees Fahrenheit for the days specified. For example, the first card contains daily maximum and minimum air temperature for climatic station 20 at Coweeta for the first 11 days of May 1973. Note the $ on the last card of the temperature data set.
4	(I2,1X,A4)	The 2 RLHU indicates that relative humidity data will be read next. (See component 2 for more information).
5	(A1,A2,A4, 2I2,I1,11F6.0)	This is the standard input format for most daily climatic data. The first card shows the input for relative humidities (%) at Coweeta climatic station 20 for the first 11 days of May 1973. (See component 3 for more information).
6	(I2,1X,A4)	The 3 TDEW indicates that dew point temperature is to be computed. (See component 2).
7	(5(1X,I2),1X, F6.2)	The first four numbers are the month and year starting and ending values, respectively. They may be equal if only one month is to be considered. The fifth number is related to climatic data observation time. A value of 1 means that the observation time falls between the daily minimum and maximum temperature (e.g., 8 AM). This means the maximum reported for a given date actually occurred the day before. A value of 2 means data actually correspond to the date shown. The final number is only used if a 1 was used to indicate observation time. In that case, the last number refers to the actual maximum temperature on the last date where dew point is to be calculated. In the example, only May 1973 is considered, and no adjustment of temperature values is needed.

The results obtained when the example input set was used are shown in Fig. 2. One may verify the accuracy of the results for any given date by using standard tables of saturation vapor pressure and temperature. In practice, the output would be generated on punched cards, or stored in a data file for direct access by the watershed simulation model.

Reference:

Lamoreaux, W. W. 1962. Modern evaporation formulae adapted to computer use. Monthly Weather Review, Vol. 90, No. 1: 26-28.

FIGURE 1. AN EXAMPLE INPUT DATA SET FCR THE DEW-POINT PROGRAM

```
   DDCC20
  1 TAIR
ADCC20 73 51  74 51 68 59 69 52 63 45 68 40 78 42 67 52 61 59 75 52 82 48 78 53
ADCC20 73 52  73 49 65 46 71 43 76 45 70 40 73 45 69 38 69 45 72 52 78 48 83 49
ADCC20 73 53  60 59 72 55 80 52 79 54 71 62 78 61 78 56 77 51 78 51
$
  2 RLHU
HDCC20 73 51   39.0   60.0   46.0   30.0   28.0   35.0   55.0   84.0   41.0   31.0   51.0
HDCC20 73 52   42.0   34.0   41.0   33.0   33.0   33.0   33.0   51.0   47.0   38.0   35.0
HDCC20 73 53   51.0   59.0   37.0   61.0   95.0   51.0   46.0   40.0   39.0
$
  3 TDEW
   5 73   5 73   2

//
```

HASP-II JOB STATISTICS -- 20 CARDS READ -- 0 LINES PRINTED -- 0 CARDS PUNCHED --

```
       1   TAIR
       2   RLHU
       3   TDEW
CDCC20 73 51 47.50 53.61 47.38 31.12 33.72 42.00 50.32 56.14 49.73 48.00 53.00
CDCC20 73 52 48.58 35.50 43.00 44.85 39.61 42.23 33.00 45.00 50.69 48.00 49.00
CDCC20 73 53 59.00 55.00 51.41 54.00 62.00 58.42 55.56 50.85 51.00
```

```
      BLOCK DATA
      INTEGER*2 NSDCL
      COMMON/D/LASTDA(2,12),NSDCL
      DATA LASTDA/2*31,29,28,2*31,2*30,2*31,2*30,4*31,2*30,2*31,2*30,
     +2*31/,NSDCL/'$'/
      END


      FUNCTION LASDAY(IY,IM)
      INTEGER*2 NSDCL
      COMMON/D/LASTDA(2,12),NSDCL
      LASDAY = LASTDA((MOD(IY,4)+5)/3,IM)
      RETURN
      END


C     THIS PROGRAM CONVERTS AIR TEMPERATURE AND RELATIVE HUMIDITY INTO
C     THE CORRESPONDING DEW POINT TEMPERATURE. CODED BY D.D.HUFF MAY 75.
      INTEGER*2 A1,NSDCL,ZONE,IX
      INTEGER*4 A2,G,Y,C,ZZ,YR1,YR2,YEAR,DATMP,YRTMP,BZ
      DIMENSION TEM(2,12,31),REL(11),RH(12,31),TDEW(12,31),MAMI(22)
      COMMON/D/LASTDA(2,12),NSDCL
C
      READ(5,1000) A1,A2
 1000 FORMAT (3X,A2,A4)
      DO 500 JK=1,2
  200 READ(5,100) NBZ,EZ
  100 FORMAT(I2,1X,A4)
      WRITE(6,101) NBZ,EZ
  101 FORMAT (5X,I2,2X,A4)
      GO TO (1,2,3), NBZ
C
C     NBZ=1 FOR DAILY TEMPERATURE (MAX AND MIN) INPUT.
C     NBZ=2 FOR DAILY RELATIVE HUMIDITY INPUT.
C     NBZ=3 TO START DEW POINT CALCULATIONS.
      STOP 123
    1 READ 1004,IX,ZONE,G,Y,M,C,MAMI
C     MAMI IS A 22 ELEMENT ARRAY THAT HOLDS 11 DAILY TEMPERATURE VALUES.
 1004 FORMAT(A1,A2,A4,2I2,I1,22I3)
      IF(IX.EQ.NSDCL) GO TO 200
C     NSDOL = $ SIGNALS END OF INPUT SET.
      LAST = 11*C
      IF (C.EQ.3) LAST=LASDAY(Y,M)
      ZZ = 11*(C-1) +1
      DO 1012 L=ZZ,LAST
      LL = 2*(MOD((L-1),11)+1)
      TEM(1,M,L) = MAMI(LL-1)
 1012 TEM(2,M,L) = MAMI(LL)
C
C     TEM(1,M,L) = MAX DAILY TEMPERATURE FOR MONTH=M,DAY=L
C     TEM(2,M,L) = MIN DAILY TEMPERATURE FOR MONTH=M,DAY=L
C
      GO TO 1
C     END TEMPERATURE INPUT
C
C     READ THE RELATIVE HUMIDITY VALUES
    2 READ(5,102) IX,ZONE,G,Y,M,C,REL
C     REL IS THE 11 ELEMENT DAILY RELATIVE HUMIDITY ARRAY
  102 FORMAT(A1,A2,A4,2I2,I1,11F6.0)
      IF (IX.EQ.NSDCL) GO TO 200
      LAST = 11*C
      IF (C.EQ.3) LAST= LASDAY(Y,M)
      ZZ = 11*(C-1)+1
      DO 103 L=ZZ,LAST
      LL = MOD((L-1),11)+1
  103 RH(M,L) = REL(LL)
C     RH(M,L) IS THE RELATIVE HUMIDITY ON MONTH=M,DAY=L.
      GO TO 2
```

```
C - - - - - - - - - - - - - - - - - - - - - - - - - - - - - - - - - - - - - - -
C       THE FOLLOWING SECTION COMPUTES DEW POINT TEMPERATURE.
C
      3 READ(5,300) M1,YR1,M2,YR2,NOBS,TMP
    300 FORMAT(5(1X,I2),1X,F6.2)
        IF (NOBS.NE.1) GO TO 307
        MN = M2 +1
        TEM(1,MN,1) = TMP
    307 CONTINUE
C       NOTE THE CODE ONLY ACCEPTS ONE YEAR (12 MONTHS) OF DATA
C       M1,YR1 ARE STARTING MONTH AND YEAR
C       M2,YR2 ARE ENDING MONTH AND YEAR.(M1.GE.M2 AND YR1.GE.YR2)
        IF(M2.LT.M1) M2 = M2 + 12
        DO 301 N=M1,M2
        YEAR = YR1
        MONTH = N
        IF (N.LE.12) GO TO 303
        YEAR = YR2
        MONTH = N-12
    303 LAST = LASDAY(YEAR,MONTH)
        DO 304 J=1,LAST
        DATMP = J
        MOTMP = MONTH
C       DETERMINE DAILY MAXIMUM TEMPERATURE ASSOCIATED WITH NOBS
C       NOBS = 1 WHEN OBSERVATION TIME LIES BETWEEN DAILY MIN AND MAX
C       NOBS = 2 WHEN MIN AND MAX READINGS ARE FOR DATE REPORTED
        IF(NOBS-1) 2141,214,213
   2141 STOP 3000
C       WHEN NOBS NE 1 OR 2, PROGRAM STOPS
    214 IF (J.NE.LAST) GO TO 215
        MOTMP = MONTH + 1
        IF (MOTMP.GT.12) MOTMP = 1
        DATMP = 1
        GO TO 213
    215 CONTINUE
        DATMP = J + 1
    213 TA = TEM(1,MOTMP,DATMP)
        TMIN = TEM(2,MONTH,J)
        ES = 2.1706E+08*EXP(-7482.6/(TA+398.36))
C       ES IS THE SATURATED VAPOR PRESSURE (MB) FOR TA.
        TDU = 7.4826E+03/ALOG(2.1706E+08/(RH(MONTH,J)*ES/100)) - 398.36
    304 TDEW(MONTH,J) = TDU
C - - - - - - - - - - - - - - END OF MONTH CALCULATIONS FOLLOW - - - - - -
        DO 306 K = 1,3
        NN = 11*(K-1)+1
        LL = NN+10
        IF (K.EQ.3) LL = LAST
        WRITE(6,305) A1,A2,YEAR,MONTH,K,(TDEW(MONTH,JJ),JJ=NN,LL)
        WRITE(7,503) A1,A2,YEAR,MONTH,K,(TDEW(MONTH,JJ),JJ=NN,LL)
    305 FORMAT(1X,A2,A4,1X,2I2,I1,11F6.2)
    503 FORMAT(A2,A4,1X,2I2,I1,11F6.2)
    306 CONTINUE
    301 CONTINUE
  500   CONTINUE
        STOP
        END
//
```

Available Plotting Options

Written as a supplement to TEHM, two plotting options are available to the user. The first option, generates annual water year print plots with data at monthly intervals. The second option does printer or Calcomp plots for the PROSPER part of TEHM. If CERES or CERES-DRYADS-DIFMAS, are being executed, plots will be generated for variables in CERES or CERES and DRYADS. All subroutines for these options are site dependent and use ORGRAPH (Nestor, 1974). The routines are described below.

Annual Water Year Plotting

A subroutine named AWYPLT has been written to allow generation of print-plots during TEHM simulation runs. The objective is to provide a tool for evaluating monthly simulation results over an annual cycle. Up to three variables may be plotted simultaneously for any segment, and up to ten separate plots may be generated in a run of any segment.

The variables that may be displayed are included in the array MONSUM. The user has the option to call for print plots, and may opt for no plots by default. A description of the mechanism for specifying desired plots is given under card 6.2 Subroutine GETSET.

Soil-Plant-Water Relation Plots

The detailed hourly information on soil-plant-water relations can be examined in print plots or in Calcomp plots. Plots can be made for any third of any month (NPRPLT = 1) with a data point every four hours or for any multiple of a four-day period (NSPLTS = 1) with hourly data points. CERES and DRYADS printer plots are generated if NPRPLT equals one and if those models are included in the simulation run. The variables plotted are shown in Table 20. The input cards required are also listed under card 6.2 for Subroutine GETSET.

Table 20. Variables plotted in PROSPER, CERES, AND DRYADS

PROSPER	CERES	DRYADS
Surface conductance (cm/sec)	Hourly photosynthesis (g CO_2/cm^2leaf/hr)	Leaf uptake (mg/m^2/hr)
Surface potential (bars)	CO_2 chloroplast	Gas uptake (mg/m^2/hr)
Volumetric water content (cm^3/cm^3)	Leaf storage (g/m^2)	Leaf to stem phloem flux (mg/m^2/hr)
Evapotranspiration (cm/hr)	Leaf sugar (g/m^2)	Roots to stem xylem flux (mg/m^2/hr)
Drainage (cm/hr)	Leaf to stem translocation	Root solute uptake (mg/m^2/hr)
Flux from root zone (cm/hr)	Stem to fruit translocation	Leaf litter mineralization (mg/m^2/hr)
Infiltration (cm/hr)	Stem to root translocation	Leaf element pool (mg/m^2)
	Stem sugar (g/m^2)	Stem element pool (mg/m^2)
	Stem storage (g/m^2)	Root element pool (mg/m^2)
	Root sugar (g/m^2)	Litter element pool (mg/m^2)
	Root storage (g/m^2)	Total plant solute demand
	Fruit sugar (g/m^{α})	
	Fruit storage (g/m^2)	

EDFB/IBP-76/8
ORNL/NSF/EATC-27

INTERNAL DISTRIBUTION

1-100. S. I. Auerbach
101-105. C. L. Begovich
106. A. A. Brooks
107. R. L. Burgess
108-117. E. D. Copenhaver
118. F. L. Culler
119. R. C. Dahlman
120. J. O. Duguid
121. N. T. Edwards
122. J. W. Elwood
123. C. W. Francis
124. W. Fulkerson
125. T. Grizzard
126. W. F. Harris
127. G. S. Henderson
128. J. T. Holdeman
129-143. D. D. Huff
144. P. L. Johnson
145. W. C. Johnson
146. S. V. Kaye
147. N. M. Larson
148. S. E. Lindberg
149-164. R. J. Luxmoore
165-169. J. B. Mankin
170. R. D. McCullock
171. J. K. Munro
172. B. D. Murphy
173. J. S. Olson
174. R. J. Olson
175. R. V. O'Neill
176. M. R. Patterson
177. H. Postma
178. R. J. Raridon
179. M. Reeves
180. D. E. Reichle
181. C. R. Richmond
182. H. H. Shugart
183. R. H. Strand
184. E. G. Struxness
185. N. E. Tarr
186. R. R. Turner
187. R. I. Van Hook
188-190. J. A. Watts
191. J. P. Witherspoon
192-193. Central Research Library
194-195. CSD Library, 4500N
196. Document Reference Section/Y-12
197-198. Laboratory Records
199. Laboratory Records-RC
200. ORNL Patent Office

EXTERNAL DISTRIBUTION

201. Research and Technical Support Division, ERDA-ORO
202. Jay Bloomfield, Research Scientist, New York State, Department of Environmental Conservation, 50 Wolf Road, Albany, NY 12233
203. D. S. Ballentine, Division of Biomedical and Environmental Research, ERDA, Washington, DC 20545
204. R. P. Betson, Head, Hydrologic Research and Analysis Staff, TVA, 410 Evans Building, Knoxville, TN 37902
205. Andrew W. Breidenbach, Director, National Environmental Research Center, Environmental Protection Agency, Cincinnati, OH 45268
206. Richard Carrigan, Division of Advanced Environmental Research and Technology, National Science Foundation, 1800 G Street NW, Washington, DC 20550
207. D. C. Coleman, Natural Resource Ecology Laboratory, Colorado State University, Ft. Collins, CO 80521

208. J. C. Corey, E. I. Depont de Nemours, Savannah River Laboratory, Aiken, SC 29801
209. N. H. Crawford, Hydrocomp, 1502 Page Mill Road, Palo Alto, CA 94304
210. Kermit Cromack, Department of Forest Management, Oregon State University, Corvallis, OR 97331
211. James W. Curlin, Environmental Policy Division, Congressional Research Service, Library of Congress, Washington, DC 20540
212. J. M. Davison, Soil Science Department, University of Florida, Gainesville, FL 32611
213. C. W. Edington, Assoc. Dir. for Res. and Devel., Div. of Biomedical and Environ. Research, ERDA, Washington, DC 20545
214. H. L. Falkenberry, Power Research Staff, Tennessee Valley Authority, Chattanooga, TN 37401
215. C. A. Federer, N. E. Forest Expt. Sta., P. O. Box 640, Durham, NH 03824
216. P. M. Fleming, Division of Land Use Research, CSIRO, P. O. Box 109, Canberra City ACT, 2601, Australia
217. Farley Fisher, Environmental Protection Agency, Office of Toxic Substances, 401 M Street, SW, Washington, DC 20460
218. R. Franklin, Division of Biomedical and Environ. Research, ERDA, Washington, DC 20545
219. W. R. Gardner, Soil Science Department, University of Wisconsin, Madison, WI 53715
220. F. A. Gifford, NOAA-Air Resources Turbulence Diffusion Lab., P. O. Box 3, Oak Ridge, TN 37830
221. D. F. Grigal, Soil Science Dept., Univ. of Minnesota, St. Paul, MN 55101
222. J. D. Hewlett, School of Forest Resources, Univ. of Georgia, Athens, GA 30602
223. H. R. Hickey, Jr., Division of Environmental Planning, TVA, Chattanooga, TN 37401
224. T. C. Hutchinson, Institute for Environmental Studies, University of Toronto, Ontario, Canada
225. L. Douglas James, Water Resources Institute, University of Kentucky, Lexington, KY 40506
226. D. W. Johnson, College of Forest Resources, University of Washington, AR-10, Seattle, WA 98195
227. J. J. Jurinak, Utah State University, Logan, UT 84322
228. W. A. Jury, Department of Soil Science and Agricultural Engineering, University of California, Riverside, CA 92507
229. J. A. Kadlec, Department of Wildlife Sciences, Utah State University, Logan, UT 84321
230. R. H. Kadlec, College of Engineering, The University of Michigan, Ann Arbor, MI 48109
231. H. Kornberg, Electrical Power Research Institute, P. O. Box 10412, Palo Alto, CA 94303
232. Ray Lassiter, Southeast Environmental Research Laboratory, Water Quality Research, Environmental Protection Agency, Ahtens, GA 30601

233. J. V. Lagerwerff, Agricultural Research Center, Building 0007, Room 301, Beltsville, MD 20705
234. W. L. Lindsay, Professor, Department of Agronomy, Colorado State University, Ft. Collins, CO 80521
235. J. L. Liverman, Director, Division of Biomedical and Environmental Research, U.S. Energy Research and Development Administration, Washington, DC 20545
236. Ulrik Lohm, Swedish Coniferous Forest Project, Box 7008, S-75607, Uppsala, Sweden
237. Paul Lommen, Ecology Center UMC-52, Utah State University, Logan, UT 84322
238. William Lower, Environmental Trace Substances Research Center, University of Missouri-Columbia, Rural Route 3, Columbia, MO 65201
239. Alan M. Lumb, Georgia Institute of Technology, Civil Engineering Department, 225 N. Avenue, Atlanta, GA 30332
240. Leland J. McCabe, Chief, Criteria Development Branch, Water Supply Research Laboratory, Environmental Protection Agency, National Environmental Research Center, Cincinnati, OH 45286
241. M. T. Mills, Geophysics Corporation of America, Technology Division, Burlington Road, Bedford, MA 01730
242. A. M. Moore, Biology Dept., Western Carolina Univ., Cullowhee, NC 28723
243. C. H. Mortimer, Center for Great Lakes Studies, University of Wisconsin, Milwaukee, WI 53201
244. Armond Georges Nassongne, Information Technology Division, Scientific and Technical Information and Information Management, Commission of the European Communities, Aldringen, Luxembourg
245. Bengt Nihlgard, Ecology Building, Helgonavag 5, S-233, 63 Lund, Sweden
246. A. L. Page, Department of Soil Science and Agricultural Engineering, University of California, Riverside, CA 92507
247. A. J. Peck, Division of Land Resources Management, CSIRO, Private Bag, P. O. Wembley, Western Australia, Australia 6401
248. D. H. Pilgrim, School of Civil Engineering, The University of New South Wales, P. O. Box 1, Kensington, New South Wales, Australia 2033
249. T. Rogerson, U.S. Forest Service, P. O. Box AA, Fayetteville, AR 72701
250. Gary L. Rolfe, 396 Fevier, University of Illinois, Urbana, IL 61801
251. Milton E. Rose, Mathematical and Computer Sciences Program, Molecular Sciences and Energy Research, Division of Physical Research, U.S. Energy Research and Development Administration, Washington, DC 20545
252. R. J. Ruane, Div. of Environmental Planning, TVA, Chattanooga, TN 37401
253. Walter Sanders, III, Southeast Water Quality Laboratory, Water Quality Office, Environmental Protection Agency, Athens, GA 30601

254. Glen Schweitzar, Director, Office of Toxic Substances-OCF, Environmental Protection Agency, 401 M Street SW, Washington, DC 20460
255. M. J. Shaffer, U.S. Bureau of Reclamation, Water Quality Office, Denver Federal Center, P. O. Box 25007, Denver, CO 80225
256. D. H. Slade, Meteorologist, Div. of Biomedical and Environmental Research, ERDA, Washington, DC 20545
257. Ivan Smith, Midwest Research Institute, 425 Volker Boulevard, Kansas City, MO 64110
258. Phillip Sollins, College of Forest Resources, University of Washington, AR-10, Seattle, WA 98195
259. T. D. Steele, U.S. Geological Survey, WRD, Denver Federal Center, Bldg. 53, Lakewood, CO 80225
260. Marvin Stephenson, Division of Advanced Research and Technology, National Science Foundation, 1800 G Street, Washington, DC 20550
261. L. H. Stolzy, Department of Soil Science and Agricultural Engineering, University of California, Riverside, CA 92502
262. E. L. Stone, Department of Agronomy, Cornell University, Ithaca, NY 14850
263. L. W. Swift, Jr., Coweeta Hydrologic Laboratory, P. O. Box 601, Franklin, NC 29734
264. K. K. Tanji, Department of Water Science and Engineering, University of California, Davis CA 95616
265. C. H. Thompson, Chief, Hazardous Materials Branch, Division of Oil and Hazardous Materials, Office of Water Programs, Environmental Protection Agency, Washington, DC 20460
266. C. A. Troendle, Timber and Watershed Laboratory, Parsons, WV 26286
267. D. E. Walling, Dept. of Geography, Armor Bldg., Rennes Drive, Exeter, England EX4 4RJ
268. J. E. Watkin, Environmental Secretariat, Division of Biology, National Research Council of Canada, Ottawa, Ontario, KLA OR6, Canada
269. R. L. Watters, Bio-Transport and Effects Program, Div. of Biomedical and Environmental Research, ERDA, Washington, DC 20545
270. Bobby G. Wixson, Professor of Environmental Health, Department of Civil Engineering, University of Missouri, Rolla, 115 Engineering Research Building, Rolla, MO 65401
271. G. M. Woodwell, The Ecosystems Center, Marine Biological Laboratory, Woods Hole, MA 02543

272-298. Technical Information Center, Oak Ridge, TN 37830

299-359. Given EDFB/IBP distribution.